NTNU – Trondheim
Norwegian University of
Science and Technology

Experimental testing and development of CO2 compressors

Eksperimentell utprøving og utvikling av CO2 kompressorer

Anders Ask

Product Design and Manufacturing
Submission date: June 2012
Supervisor: Petter Nekså, EPT
Co-supervisor: Armin Hafner, SINTEF

Norwegian University of Science and Technology
Department of Energy and Process Engineering

NTNU
Norwegian University
of Science and Technology

Department of Energy
and Process Engineering

EPT-M-2012-16

MASTER THESIS

for

Anders ASK

Spring 2012

Experimental testing and development of CO_2 compressors

Eksperimentell utprøving og utvikling av CO_2 kompressorer

Background and objective

Research on novel industrial refrigeration systems using natural refrigerants: To release the potential of refrigeration systems based on natural refrigerants, novel components ensuring high performance and maintainability are required. On a path to a sustainable energy future, energy systems applying natural working fluids represent a sustainable solution in many regions on earth. Availability of energy- and cost efficient compressors and heat exchangers for natural working fluids like carbon dioxide, ammonia and hydrocarbons can change the refrigeration world completely.

A test facility able to test CO_2 compressors with a shaft capacity in the range of 100 kW has been built and will be installed at the SINTEF-NTNU laboratory premises. In parallel a high efficient CO_2 compressor has been developed. The compressor should be tested and a detailed evaluation of the results should be performed. Since the test rig also is new, adjustment and development of the measuring and data acquisition, as well as processing of the data, will have to be performed.

The following tasks are to be considered:

1. Literature survey on experimental investigation of compressors, with emphasis on CO_2 as refrigerant
2. Adaption of the measurement equipment and data logging systems of the new compressor test facility
3. Perform initial tests and develop the uncertainty analysis of the measurement results
4. Plan and perform an experimental program for the new CO_2 compressor
5. Report and evaluate experimental results, including a detailed loss analysis
6. Summary of the findings and draft version of a scientific paper which describes the test facility
7. Proposal for further work

-- " --

Within 14 days of receiving the written text on the master thesis, the candidate shall submit a research plan for his project to the department.

When the thesis is evaluated, emphasis is put on processing of the results, and that they are presented in tabular and/or graphic form in a clear manner, and that they are analyzed carefully.

The thesis should be formulated as a research report with summary both in English and Norwegian, conclusion, literature references, table of contents etc. During the preparation of the text, the candidate should make an effort to produce a well-structured and easily readable report. In order to ease the evaluation of the thesis, it is important that the cross-references are correct. In the making of the report, strong emphasis should be placed on both a thorough discussion of the results and an orderly presentation.

The candidate is requested to initiate and keep close contact with his/her academic supervisor(s) throughout the working period. The candidate must follow the rules and regulations of NTNU as well as passive directions given by the Department of Energy and Process Engineering.

Risk assessment of the candidate's work shall be carried out according to the department's procedures. The risk assessment must be documented and included as part of the final report. Events related to the candidate's work adversely affecting the health, safety or security, must be documented and included as part of the final report.

Pursuant to "Regulations concerning the supplementary provisions to the technology study program/Master of Science" at NTNU §20, the Department reserves the permission to utilize all the results and data for teaching and research purposes as well as in future publications.

The final report is to be submitted digitally in DAIM. An executive summary of the thesis including title, student's name, supervisor's name, year, department name, and NTNU's logo and name, shall be submitted to the department as a separate pdf file. Based on an agreement with the supervisor, the final report and other material and documents may be given to the supervisor in digital format.

Department of Energy and Process Engineering, 16. January 2012

Olav Bolland
Department Head

Professor II Petter Nekså
Academic Supervisor

Research Advisors:
Senior Research Scientist Armin Hafner

ABSTRACT

CO_2 is a natural refrigerant and is well suitable in many cooling applications. It has been used within the refrigeration industry from the 1900s, but got replaced as the synthetic refrigerants got introduced. In 1990 these fluids were proved damaging to the ozone layer and got replaced by a new series of synthetic fluids, which later have shown to be harmful to the global climate and therefore bound with restrictions from the governments. In the early 1990s at Norwegian University of Science and Technology(NTNU), professor Gustav Lorentzen introduced the transcritical refrigeration process and reintroduced CO_2 as a refrigerant with favourable properties.
Now the use of CO_2 in heat pump applications is wide spread, and competitive alternatives within most markets are presented. However, there are still areas of improvement, and at the laboratories of SINTEF and NTNU a rig is being installed meant to do experiments on high effect CO_2 cooling systems, with a cooling capacity of 400kW and a compressor capacity of el 100kW. Currently the rig is placed in Lustenau Austria at Obrist Engineerings facility where a 100kW high efficient semi hermetic 6 cylinder single stage piston compressor is being tested. This compressor is a new development and a result of a cooperation between SINTEF and Obrist Engineering. The background for this development was the lack of single stage compressors able to deliver flow rates in the range of 10 to 90m^3/h.

For experiment purposes the losses in the reciprocating cycle were evaluated, where the overall isentropic efficiency is most defining for the energy efficiency, and also the defining value for the entirety of all losses in the compressor unit.

The test campaign was conducted in different test series, where the test points were set by Obrist Engineering with background in a cooling application on a fishing vessel. 3 series were set, where a fixed pressure ratio of 65/30 bar, 110/30 bar and 80/20 bar was tested in experiments with varying motor speed from 800 - 3800 rpm and a constant superheat at 10K. As the executions showed, some of the test points were not able to be tested, because of lack of power supply in the local power grid, and the maximum input power was set to 94kW.
Test results revealed a relatively high overall efficiency with values at 73.5% for a pressure ratio of 65/30 bar. Also for the two other pressure ratios the efficiency showed to be satisfying in comparison with on the shelf compressors commercially available to day. However, the test campaign revealed a high volumetric loss in high pressure ranges, which partly can be substantiated with a relatively high clearance volume due to the shear size of the cylinder. In addition, $P_{indicated}$ for low speeds versus high speeds shows a possible too small valve area at discharge for the highest speeds.

SAMMENDRAG

CO_2 er et naturlig kuldemedium og er godt egnet i mange kjøleapplikasjoner. Det har blitt brukt innen kjøleindustrien siden tidligt på 1900tallet, men ble erstattet etter som de syntetiske kuldemedier ble innført. På 1990tallet ble disse væskene bevist skadelig for ozonlaget og erstattet av en ny serie syntetiske væsker, som senere har vist seg å være skadelig for det globale klimaet og dermed bundet med restriksjoner fra myndighetene. I begynnelsen av 1990 ved Norsk teknisk-naturvitenskapelige universitet (NTNU), introduserte professor Gustav Lorentzen den transkritiske kjøle prosessen og gjeninnførte CO_2 som et naturlig kuldemedium med gunstige egenskaper.

Nå har bruk av CO_2 i varmepumpeanlegg hatt en stor økning, og konkurransedyktige alternativer innenfor de fleste markeder er tilgjenglige. Men det er fortsatt områder med forbedringspotenisale, og på laboratoriene til SINTEF og NTNU blir en rig etter hvert installert, ment for å gjøre eksperimenter på høy kapasitets CO_2 kjølesystemer med en kjølekapasitet på 400 kW og en kompressor kapasitet på 100kW. Foreløpig er riggen plassert i Lustenau Østerrike ved Obrist engineerings anlegg hvor en 100kW høy effektiv semi hermetisk 6 sylindret ett trinns -stempelkompressor på 380cc blir testet. Denne kompressoren nyutvikling og et resultat av et samarbeid mellom SINTEF og Obrist Engineering. Bakgrunnen for denne utviklingen var mangelen på enkle ettrinns kompressorer med mulighet for å levere i området fra 10 til 90 m^3/h.

For å evaluere kompessorens ytelse ble virkningsgradene for volumetrisk- og isentropisk- virkningsgrad evaluert.

Forsøkene ble gjennomført i ulike testserier, satt av Obrist Engineering med bakgrunn i en kjølendesyklus på et fiskefartøy. 3 Serier ble satt, med trykkforholdene 65/30 bar, 110/30 bar og 80/20 bar som alle ble kjørt med varierende motorhastigheter fra 800-3800 rpm og en konstant overoppheting på 10K. Som forsøkene etter hvert viste, ble noen av testpunktene ikke gjennomført grunnet for liten strømtilførsel fra det lokale strømnettet i Lustenau Østerriket.

Testresultater for øvrig viste en relativt høy total virkningsgrad med verdier på 73,5% for et trykkforhold på 65/30 bar. Også for de to andre trykkforholdene viste effektiviteten seg å være tilfredsstillende i forhold til kompressorer som er kommersielt tilgjengelige i dag. Imidlertid avslørte testene et høyt volumetrisk tap i høye trykkområder, som delvis kan underbygges med et relativt høyt klaringsvolum som naturlig kommer den store sylinderstørrelsen i kompressoren. I tillegg viser $P_{indikert}$ for lave hastigheter versus høye hastigheter en mulighet for at utløpsventilen er for liten.

PREFACE

This work has been performed at the Department of Energy and Process Engineering at the Norwegian University of Science and Technology(NTNU) in Trondheim Norway.

Main supervisor has been Chief Scientist Petter Neksaa, and Senior Research Scientist Armin Hafner at SINTEF department of Energy Research.

The study has been a part of the MSc education in Mechanical Engineering at NTNU spring 2012. The subject of study has been given by SINTEF as a part of work within research project CREATIV, which is financially supported by the Research Council of Norway and several other industry partners.

I would like to thank all those who have helped me with my project, and especially Obrist Engineering in Lustenau Austria whom has been more than helpful with my work and has welcomed me into their facilities in Lustenau for two occasions. Extra thanks go to Roman Laesser who did a great job with the execution of the experiments and gave me lots of test data to work with. Also thank you to my german friend, Titus Langhof, who was a great travel buddy on the last trip to Austria.

Anders Ask, June 14, 2012

CONTENTS

I INTRODUCTION 1

1 BACKGROUND 3

1.1 Scope of work . . . 3

1.1.1 Structure . . . 4

1.2 Introduction . . . 5

1.3 Thermodynamic properties . . . 8

II NOVEL DEVELOPMENT OF A SEMIHERMETIC R-744 COMPRESSOR 11

2 COMPRESSOR LOSS AND DESCRIPTION 13

2.1 Fundamentals . . . 13

2.2 Compressor build-up . . . 19

2.3 Energy loss analysis . . . 19

2.4 Motor and VSD loss . . . 20

2.5 Lubrication system . . . 22

2.6 Valve loss . . . 24

2.7 Volumetric loss . . . 28

2.8 Internal Heat Exchange . . . 31

3 THE TEST RIG 35

3.1 Description of the test plant . . . 35

3.2 Description of the refrigeration circuit . . . 38

3.3 Uncertainty . . . 40

3.4 Experimental setup . . . 40

4 EXPERIMENTAL RESULTS 43

4.1 The Isentropic Efficiency . . . 43

4.2 Volumetric Efficiency . . . 45

4.2.1 Indicator diagram . . . 48

4.2.2 Temperature variation . . . 52

4.3 Frequency converter . . . 52

5 DISCUSSION 55

5.1 Isentropic efficiency . . . 55

5.2 Volumetric efficiency . . . 57

5.2.1 Valve loss . . . 57

5.2.2 Oil Circulation Rate . . . 59

5.2.3 Improvement in the oil separation . . . 59

5.3 Frequency Converter . . . 62

6 CONCLUSION 63

6.1 Overall efficiency . . . 63

6.2 Volumetric efficiency . . . 63

6.3 Oil circulation . . . 63

6.4 Frequency converter . . . 64

7 FURTHER WORK 65

III APPENDIX 67

A TEST RESULTS AND UNCERTAINTIES 69

B HIGH EFFICIENT 100KW R-744 COMPRESSOR 81

B.1 Abstract 81

B.2 Introduction 81

B.3 Description of the test plant 82

B.3.1 Compressor build-up 84

B.3.2 Description of the refrigeration circuit 84

B.4 Results and discussion 85

B.5 Conclusion 89

C UNCERTAINTY 91

C.0.1 Fixed error 91

C.0.2 Random error 91

C.0.3 Experimental use 93

C.1 Measurements of actual quantities 93

D RISK ANALYSIS 97

BIBLIOGRAPHY 103

LIST OF FIGURES

Figure 1	logp-h diagram showing different cycles in refrigeration	9
Figure 2	Shematic drawing of the compressor driving mechanism, and the discharge and suction valve in the cylinder	14
Figure 3	Position, velocity and acceleration of a moving piston inside a cylinder at a compression cycles	15
Figure 4	P-v diagram of the Carnot compression cycle, and a sketch of the compression work in an ideal adiabatic gas compression cycles	17
Figure 5	The compressor - motor - VSD arrangement showing four levels	20
Figure 6	Typical efficiencies for high-efficient motors and VSD as a function of % nominal speed, *ASHRAE Journal, December 1999*	21
Figure 7	The sketched oil flow for lubricant in the compressor unit. Constant lines indicates the main gas flow, whilst the black dashed lines indicates the oil flow	23
Figure 8	The oil droplet separation unit in the suction gas	24
Figure 9	The pressure volume diagram shows a compression cycles as ideal and non ideal, with TDC (top dead center) and BDC (bottom dead center)	25
Figure 10	The Valve lift displayed as a function of the crank angle, where a typical actual opening in a plate valve is shown	27
Figure 11	Effect of different pressure ratios on the volumetric efficiency of a given cylinder	29
Figure 12	Picture a) and b) are pictures of the used piston rings, and c) is the ends used on the permanent piston ring in picture b)	30
Figure 13	Temperature and pressure variation in a complete compression cycle	32
Figure 14	The container at Obrists facilities	36
Figure 15	Principal drawing of the test rig facility incorporating the pipe work, vessels, heat exchanger and supporting system	37
Figure 16	Drawing of the refrigeration cycles in log p-h chart	39
Figure 17	Isentropic efficiency with variation in rpm with a constant superheat at 10K	44
Figure 18	Volumetric efficiency at varying rpm	46
Figure 19	The oil circulation rate for 3 different pressure ratios	47
Figure 20	Compariosn of volumetric and isentropic efficiencies.	48
Figure 21	Measured indicator diagrams for the different cycles	49

Figure 22 Measured suction- and discharge chamber pressures versus crank angle at varying motor speed and pressure ratios 50
Figure 23 Variation in the discharge temperature at different pressure ratios for variation in motor speed 52
Figure 24 Efficiency for the danfoss frequency converter for variation in the motor load 53
Figure 25 Comparison of efficiencies with 2 different on the shelf compressors available on the marked today, running at 1500 rpm with discharge pressure of 80 bar and 10K superheat 56
Figure 26 Plot of indicator diagram in the same figures for 3 different pressure ratios 58
Figure 27 Draft sketch of the first proposal for improvement of the oil droplets removal in the suction gas 60
Figure 28 Draft sketch of the second proposal for improvement of the oil droplets removal in the suction gas 61
Figure 30 Principal drawing of the test rig facility incorporating the pipe work, vessels, heat exchanger and supporting system 83
Figure 31 Compariosn of volumetric and isentropic efficiencies. . . . 86
Figure 32 Plot of indicator diagram in the same figures for 3 different pressure ratios 88
Figure 33 Comparison of efficiencies with 2 different on the shelf compressors available on the marked today, running at 1500 rpm with discharge pressure of 80 bar and 10K superheat 89
Figure 34 *Gaussian distribution* 92

LIST OF TABLES

Table 1 — T_c-critical temperature; P_c-critical pressure; ODP-ozone depletion potential; GWP-Global warming potential. Data from UNEP . . . 10
Table 2 — Compressor data . . . 19
Table 3 — The installed transducers in the full test rig . . . 40
Table 4 — Test program matrixes for the R-744 compressor, planed by Obrist Engineering . . . 41
Table 5 — The calculated isentropic efficiency with calculated uncertainties as the percentage value of deviation . . . 45
Table 6 — The calculated volumetric efficiency with calculated uncertainties as the percentage value of deviation . . . 47
Table 8 — Uncertainty in the results with 3 different pressure ratios . 69
Table 9 — Compressor data . . . 84
Table 10 — The installed transducers in the full test rig . . . 85

NOMENCLATURE

A	area m^2
cp	speseific heat J/kgK
h	enthalpy J/kg
K	kelvin
l	length of arm m
m	mass kg
p	pressure bar
Q	heat J
q	specific heat J/kg
r	radius m
s	entropy J/kgK
T	temperature °C
V	volume m^3
v	specific volume m^3/kg
W	work J/s (watt)

Greek

δ deviation -also used as subscript

β degrees

η efficiency

ρ density kg/m^3

ω 1/s

Subscripts

1	inlet pressure, suction

2	outlet pressure, discharge
c	cold
comp	compressor
disch	discharge
el	electric
H	hot
is	isentropic
loss	energy lost to the environment
motor	the elctrical motor
m	motor
net	netto
oil	motor oil, lubricant
s	isntropic
shaft	compressor shaft
suct	suction, inlet compressor
v	volumetric
vol	volumetric
wall	cylinder wall

ACRONYMS

NTNU	Norwegian University of Technology and Science
R-744	Carbondioxcide
OE	Obrist Engineering
GWP	Global Warming impact
COP	Coefficient of Performance
ODP	Ozone Depletion Potential

RPM Revolutions per Minute

TDC Top Dead Center

BDC Bottom dead center

VSD Variable Speed Drive

Uncertainty

cd total uncertainty

h enthalpy J/kg

u standard uncertainty

Rev Revolutions per minute (RPM)

V Volume m^3

v degrees of freedom

Greek

δ deviation

σ standard deviation

Subscripts

inlet inlet pressure, suction

fixed Fixed uncertainty

outlet outlet pressure, discharge

random Random uncertainty

Part I

INTRODUCTION

1 BACKGROUND

1.1 SCOPE OF WORK

This thesis is a part of cooperation between several institutions and a consortium compromising 20 international industry and research partners. The partners in industry cover high intensive power consumers and several areas of applications i. e.metallurgy, pulp and paper, fishery, food production and supermarkets. Providing the research and development are among other SINTEF involved, and the goal is to develop new environmental friendly energy efficient solutions for the future in energy demanding industries. The cooperation is called Creativ, and this thesis is a product of this cooperation. [16]

Development of a high capacity compressor for CO_2 is definitely a project where the purpose is to improve the energy efficiency in the cooling industry, and in this work the main goal were to plan and execute initial tests for a compressor developed by SINETF and Obrist Engineering. Also a literature survey on what kinds of measurements were needed to quantify efficiencies such as volumetric- and isentropic efficiency was necessary in this thesis.

A natural sub objective was a literature survey on why CO_2 is energy saving, and why it is used as a natural refrigerant. Also earlier developments in the refrigeration industry regarding natural refrigerants and CO_2 was done.

For planning a test campaign for a piston compressor a good overview of what has been done earlier and what is custom in such experiments was necessary. Both regarding uncertainty in results and what kind of results which were needed. It was not the intention in in this thesis to do any simulations on a working compressor in any way. The compressor was made in advance, and all analyses for design purposes were done by SINETF and Obrist Engineering before it was built.

In the planning the most important part was to establish a tool for calculation of desired values from the test data. Most commonly used, and best tool, was a excel spread sheet, where all formulas were plotted in before the execution of the compressor experiments.

The initial plan was to bring the test facility to Trondheim and NTNUs labs early in the spring and plan experiments and conduct a thorough test campaign there. This was however not possible and all the experiments had to be done in Austria Lustenau. Which in turn made the planning of an experimental program and experimentation less thorough, and it was mainly up to Obrist Engineering and their team to determine both the test program and the execution of the experiments. On that basis the planning and execution of the experiments were amputated compared to the initial plan for this thesis. All test results in this work are based on the conducted experiments done in Lustenau Austria 21 - 24 may 2012.

1.1.1 *Structure*

PART I GIVES AN introduction into the refrigeration and compressor technology, both with a historically aspect as well as challenges met today as the CO_2 reintroduced as a working refrigerant in the refrigeration industry. In addition the fundamentals of the thermodynamics in refrigeration are introduced.

PART II IS WHERE experimental set-up, results, discussion and conclusion are described. An analysis of losses in a working reciprocating compressors is described in Chapter 2, both with reference to the current compressor, and also on a general plane. The main objective with this chapter is to point out questions needed to be asked in a experimental evaluation of a piston compressor in order to quantify losses and performance. The experimental set-up is explained in Chapter 3. Results, discussion and conclusion follows thereafter.

PART III IS THE APPENDIX and consists of the uncertainty calculations as well as the results for the different compressor set points and a full cycle for the test rig. Also a safety analyses for the trip to Austria is attached. In addition there is a draft for a paper in Appendix B.

1.2 INTRODUCTION

The refrigeration and heat pump industry started as early as 1830, and the use of suitable refrigerants have since then been under development to be as efficient and safe as possible. At first it was normal to use whatever worked, and among many others, CO_2 was widely used in refrigeration industry in the beginning. There were a wide range of substances in use, and the selection criteria for a good refrigerant was its ability to be used in practical systems, regardless of its toxicity, flammability and harm to environment. As the development against commercial use got important, new and safer refrigerants became necessary and synthetic substances like CFCs (Chloro-Fluro-Carbon) and HCFC (Hydro-Chloro-Fluro-Carbon) got introduced in 1930s. They were named the miracle substances because they met all the criteria a good refrigerant should have. Because these substances were so stable, they later showed to be harmful for the environment, and from 1994 a worldwide phase out was agreed on to restore the ozone layer. Since then the use of HFC (Hydro-Fluoro-Carbon) has been introduced. These refrigerants however, have shown to have a massive impact on the global warming, and since 1999 the HFCs has been listed in the Koyoto Protocol as substances contributing to global warming [3]

.

From early times there have been applications for pressure increase by applying external mechanical work. Already in the middle ages there was hand operated bellow used in metal blacksmiths, and to days piston compressors can be considered derived from the design of an Otto von Guerickes air vacuum pump and the spectacular test with the Magdeburg hemispheres in 1656. The first industrial manufactured single stage compressors were used for pumping air in iron foundries in mining, and the pressures ranged from 3 - 7 bar. As the process industry developed, two stage compressors with higher load and pressures were put to use in liquefaction of technical gases in the end of 19th century. The industrial growth continued to increase, and as the car industry developed with piston machines, also the production of piston compressors for commercial use was initiated. And as the use of piston compressors for generating compressed air in energy supply and as part of refrigeration, the mass production of piston compressors started. Due to lack of suitable oils in high temperatures, steam engines without cylinder lubrication where developed and non-lubricated piston compressors appeared on the marked in the 1930s which were very popular in breweries where odorless and oil free air was a requirement. Nowadays there has been a big development in the marked for reciprocating compressors, and among others self-adjusting sealing elements and more wear resistant ring materials have contributed to the use of non-lubricated piston compressors in several process applications for pressures up to 30MPa.

A large portion of piston compressors, both in numbers and in installed power, are today used in the refrigeration industry. An electrical motor is the power supply for the compressor, and due to leakage of greenhouse refrigerants a common design is where both the compressor and motor are fitted in to one item. This gives the possibility for a fully welded unit, and is the most used design for smaller piston compressors used in the refrigeration industry (for example for household refrigerators). One distinguish between this and a semi hermetic solution where the housing is bolted with static seals, which is used for larger compressors used in the commercial industry. This is mostly because of better cooling possibilities in the motor part, it is easier to maintain with the possibility for replacing parts or motor, in addition, it is easier to control the speed of the compressor.

In today's industry the impact on the environment need to be as little as possible, both because of reputation and the economic governmental restrictions, and since it was discovered that the synthetic fluids have a substantial impact on the environment the study of finding natural excising fluids to use in refrigeration has attracted big attention. The main difficulties with CO_2 as a non-synthetic refrigerant, is the need for high pressures and low temperature cycles, which also were the main reasons for replacing it in the early 1900s. Since then the engineering industry has made huge steps and CO_2 has been rediscovered as a useful refrigerant. A pioneer in the area was the founder of the Department of Refrigeration and Air Conditioning at the Norwegian university of science and technology (NTNU), Professor Gustav Lorentzen. In late eighties and early 90s, he investigated the possibilities of reintroducing CO_2 as refrigerant and his studies at NTNUs labs and published works have showed that CO_2 is a good replacement for HFCs and CFCs in many uses within heat pump engineering. This is mainly because of the process which he was studying, where he found the cooling capacity and COP could easily be controlled by increasing the high side pressure to above the critical. The cycle was called a transcritical cycle, in which the heat is rejected by gas cooling in the critical zone and not by condensing in a mixed phase and heat is extracted as vapor liquid. From his work professor Lorentzen was awarded a patent on the transcritical cycle with an arrangement where the high side pressure was altered automatically.[7]
Professor Lorentzens legacy is alive within the walls of SINTEF and NTNU still today, and since his retirement substantial work has been conducted on the same labs and the institution he started. Several studies on different applications based on the transcritical cycle and CO_2 as refrigerant has been done. A study of using R-744 to heat tap water has successfully resulted in a commercial application developed by the Japanese company Ecocute, and to day Japan is experiencing a significant reduction in emission of CO_2 to the atmosphere[11], based on the research from SINTEF and NTNU. Also in the mobile air conditioning industry the use of R-744 as refrigerant have been successful. Today this technology is a good environmental friendly alternative in among other car industry[13]. However, new markets for using R-744 are considerable and further research on novel solutions are needed.

An area of great interest, where the use of refrigeration application is substantial on a world basis, is the use of a single CO_2 plant in high efficient cooling applications typically used in supermarkets and for cooling of cold storage halls. As much as 15% of the electricity production worldwide is used in heat-pumping systems for refrigeration, air conditioning and heat pumps[16][**?**], and the numbers are not likely to decrease in the future. The most used refrigerants in developed countries are synthetic fluids like HCFC-22, this is mostly because the technology is the cheapest and compressors are available on local markets. However, in Norway and Denmark most of the new centralized systems are being built with CO_2 as working fluid at low temperature levels. Also countries like Germany an UK the use of non-HFC systems are being built.[1] A typical system here is using a CO_2 cascade system where CO_2 is the refrigerant of the low temperature circuit. It is also possible to use a direct system using only CO_2 in subcritical / transcritical, depending on the ambient temperature, and has shown to be efficient and cost effective in greater parts of Europe[11]. Today however, there are no compressors on the market to deliver the necessary load, at typically 10-90 m^3/h [8], needed at high pressures to run an high effect industrial R-744 system, and systems are therefore built with an arrangement with several operating compressors. A development of a single high efficient compressor will therefore most likely improve the efficiency of systems running CO_2 as the only refrigerant, as well as making the system cost less expensive.[1]

1.3 THERMODYNAMIC PROPERTIES

In the rest of this thesis the refrigeration name R-744 will be used

As for the refrigeration science CO_2 is given the name R-744, where R stands for refrigerant, the given class 7 refers to a class of non-organic and 44 is from the molecular weight.

R-744 is not like any other known refrigeration fluids, and in many ways it can be considered thermodynamically preferable compared with other refrigerants. It has a critical temperature at 31.1°C which is considerably lower than other commonly used fluids In addition, the critical pressure at 71.8 bar is much higher than the synthetic fluids. At ambient temperatures exceeding the critical point at 31.1°C a subcritical cycle will not be possible and the process will reject heat in the critical region in a gas cooler with a pressure at typically above 80 bar. In a regular system using R-134a with the same ambient conditions the heat rejection would occur in a condenser with typically maximum pressures at less than 15 bar[7]. Consequentially the volumetric capacity of R-744 is higher and the cross sectional flow of the fluid is smaller and the equipment redesigned for R-744 is more compact than what is used in regular systems. For a compressor the displacement for R-744 will be 80% - 90% smaller than what is necessary for R-134a. And because of smaller pressure ratios, there are also favorable possibilities for making more efficient compressors for R-744 applications than what is available today for synthetic fluids.[11][13] The heat transfer is also better, both because of the high density and the fact that R-744 has a smaller surface tension and less pressure drop than other known refrigerants.[12]

With a triple point at -56.6°C and 5.17 bar it implies that also at sub-critical conditions a R-744 system will be running at a higher pressure than conventionally used refrigerants. It also implies that it is not necessary to run at negative pressures in extreme cooling applications, which makes it, together with the high density and low surface tension, particularly suitable for freezer systems where it is working with a significant higher COP than any other alternative.[1] In a cooling application it has to work in a cascade system along with a synthetic fluid. A transcritical cycle is possible, but at high efficient applications there are today (2012) not compressors on the marked to handle the high pressures needed. [1]

Professor Lorentzen investigated the cycle where heat is rejected in the critical area by gas cooling. In this phase the enthalpy is not linear with pressure, and therefore the high side pressure is automatically controlled, fluctuating with the necessary cooling effect of the plant to maintain a maximum COP at all time. [7] Figure 1 shows a transcritical cycle (points 1-2-3-4) in a refrigeration process with a maximum pressure at 90 bar and an outlet temperature at 40°C in the gas cooler. The gradient for the isotherm at 40°C is increasing when the high

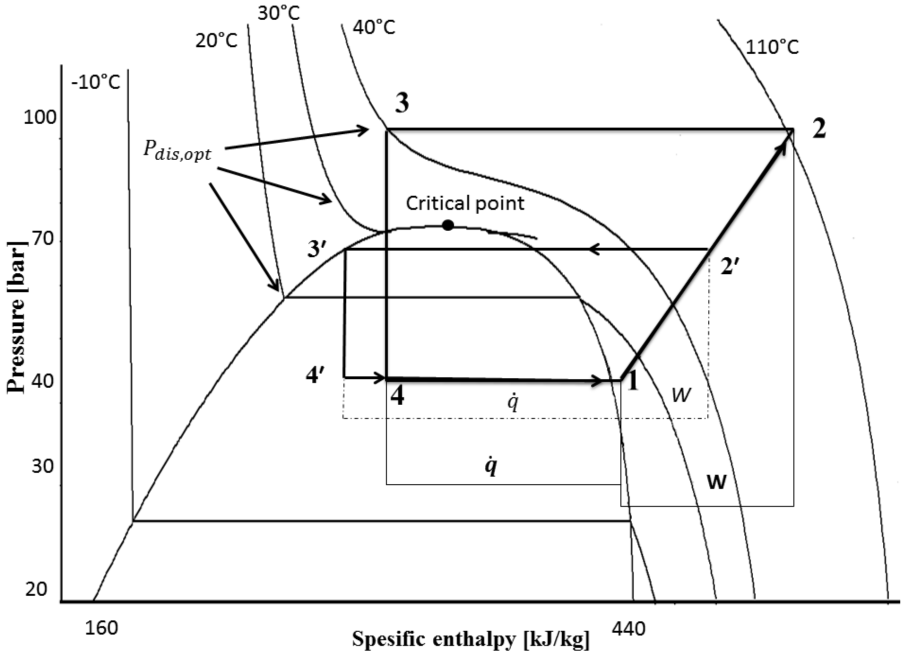

Figure 1: logp-h diagram R-744, transcritical cycle (1-2-3-4),subcritical cycle (1-2´-3´-4´), specific compressor work(w), specific cooling capasity (q), optimal discharge pressure($P_{dis,opt}$)

side pressure is increasing, thus the work will increase more than the heat out, and the total performance of the system will drop. At one point($P_{dis_{opt}}$) the high side pressure will have an ideal set point in order to have a maximum COP of the system, and this is why it is crucial to control the high side pressure in a transcritical cycle. Also as the temperature out of the gas-cooler changes, the pressure needs to be altered. Further it is noticed from figure 1 that in a subcritical process (1-2´-3´-4´), the condensing takes place below 30°C and a successful heat rejection cannot be done with temperatures above this temperature. In comparison with synthetic made fluids, R-744 has a lesser impact on the global warming, and from table 1 the global warming impact (GWP) numbers are listed as impact on the global warming measured in CO_2 equivalents. Here R-744 has a GWP at 1, and the release of 1 kg R-417A would be equivalent to releasing 2300 kg of CO_2. R-744 is also a waste product in combustion processes, and not made in addition to other releases, which in fact will make the use of R-744 a neutral refrigerant in perspective of a natural CO_2 cycle.

As for refrigeration and in search of a replacement for synthetic made fluids, R-744 is a good option. It has advantageous properties regarding thermodynamic features, and also several aspects as[7]:

	Physical data			Environmental data	
Refrigerant number	Molecular mass [kg/kmol]	T_c [°C]	P_c [bar]	ODP	GWP
R-744	44,01	31,1	70,3	0,000	1
HCFC-22	86,47	96,1	49,36	0,040	1790
HCFC-134a	102,03	101,1	40,6	0,000	1370
R-407C	86,20	86,0	46,2	0,000	1700
R-417A	106,75	86,1	46,1	0,000	2300
R-410A	72,58	71,4	48,6	0,000	2100
R717	17,03	133,3	112,8	0,000	-

Table 1: T_c-critical temperature; P_c-critical pressure; ODP-ozone depletion potential; GWP-Global warming potential. Data from UNEP [1]

1. Global Warming Potential (GWP) is set to one since the gas is recovered from waste gas. R-744 is applied as reference substance.
2. Ozone Depleting Potential (ODP) is set to zero.
3. Non flammable and non explosive.
4. Nontoxic and non-irritating decomposition products.
5. Excellent thermodynamic properties.
6. The price is a fraction of today's available refrigerants.
7. R-744 components might be smaller and lighter compared to e.g. R-22 caused by a high density.

Using R-744 as working fluid has shown to be successful in many applications, and is used in commercial refrigeration applications with success. However there are challenges to overcome. In particular in higher ambient temperatures, where the COP of a R-744 system has shown to be slightly lower than for a traditional system using synthetic fluids. Mainly because of the high energy consumption in the compression needed to overcome the big pressure differences in the cycle. In a cascade system it will however improve the total COP by reject heat in heat exchanging with a system running a synthetic fluid. The big pressures needed to handle the highest pressures in a safe application for commercial use, call for a robust system both in equipment and couplings, which in turn is more expensive to produce. The main challenges are therefore to produce a low cost system which can match today's commercially used systems in both price and performance. In industrial high effect systems these challenges are met with higher efficiency in the compression and smart solutions, i.e. expanders and ejectors [11].

Part II

NOVEL DEVELOPMENT OF A SEMIHERMETIC R-744 COMPRESSOR

2 COMPRESSOR LOSS AND DESCRIPTION

This chapter will be used to discuss different kinds of losses in a general compressor, and see them in comparison to the newly developed SINTEF / Obrist compressor. One of the main characteristics with a piston compression are that it is possible to evaluate all points in the compression cycles, and match them up with the design of the application. Hence the foundation will be general losses caused by known physics, but experiences and explanations of the specific compressor will be compared.

2.1 FUNDAMENTALS

A compression cycle in a piston compressor is rather straight forward and easy to adapt from i.e. a bicycle pump analogy where a piston is moving up and down from top in a closed cylinder. In a single acting compressor, air or gas is compressed into a smaller space as the piston moves forward in the cylinder, thus raising its pressure. At opposite movement new fluid is sucked in to the cylinder chamber ready to be compressed. From *Amontons Law* it is known that pressure will increases at higher temperatures inside a fixed volume of gas, and further from *Boyles Law* it is known that temperature will increase as the pressure increase in a fixed control volume [5]. These two factors are elements in natural limitation of design operations in all compressor types and compression units.

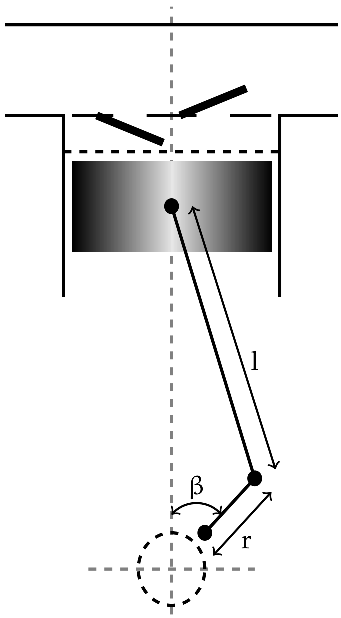

Figure 2: Shematic drawing of the compressor driving mechanism, and the discharge and suction valve in the cylinder

Figure 2 shows a single acting compressor with connections, cylinder walls and suction and discharge valves. The piston is connected to the shaft which is driven by a motor, and both inlet and outlet flow is controlled by a valve opening at a given pressure difference between cylinder and system pressure. Both the performance of the valves and the speed of the piston is a crucial factor in losses, and therefore also important in design purposes. The speed and acceleration of the piston will wary throughout the suction and compression cycles, but the mean velocity however, is straight forward to adapt from the speed of the shaft (RPM) connected to the motor and the stroke length (distance from top dead position to the bottom dead position of the cylinder). However, the velocity is not constant through the stroke, which influences the losses in the compressor.

From figure 2 a general equation for the stroke length, H, can be derived: Using the cosine law with respect to the angle β yields

$$l^2 = h^2 + r^2 - 2hr\cos(\beta)$$

The relationship $\sin^2\beta + \cos^2\beta = 0$ was used, and the equation for the position of the piston is

$$\begin{aligned} l^2 - r^2 &= H^2 - 2rH\cos(\beta) + r^2\left[(\cos^2\beta + \sin^2\beta) - 1\right] \\ l^2 - r^2 + r^2 - r^2\sin^2\beta &= H^2 - 2rH\cos\beta + r^2\cos^2\beta \\ l^2 - r^2\sin\beta &= (H - r\cos\beta)^2 \end{aligned} \tag{1}$$

Piston placement, velocity and acceleration with respect to crank angle β

$$H = r\cos\beta + \sqrt{l^2 - r^2\sin^2\beta} \tag{2}$$

$$\frac{dH}{d\beta} = -r\sin\beta - \frac{r^2\sin\beta\cos\beta}{\sqrt{l^2 - r^2\sin^2\beta}} \tag{3}$$

$$\frac{d^2H}{d\beta^2} = -r\cos\beta - \frac{r^2(\cos^2\beta - \sin^2\beta)}{\sqrt{l^2 - r^2\sin^2\beta}} - \frac{-r^4\sin^2\beta\cos^2\beta}{(\sqrt{l^2 - r^2\sin^2\beta})^3} \tag{4}$$

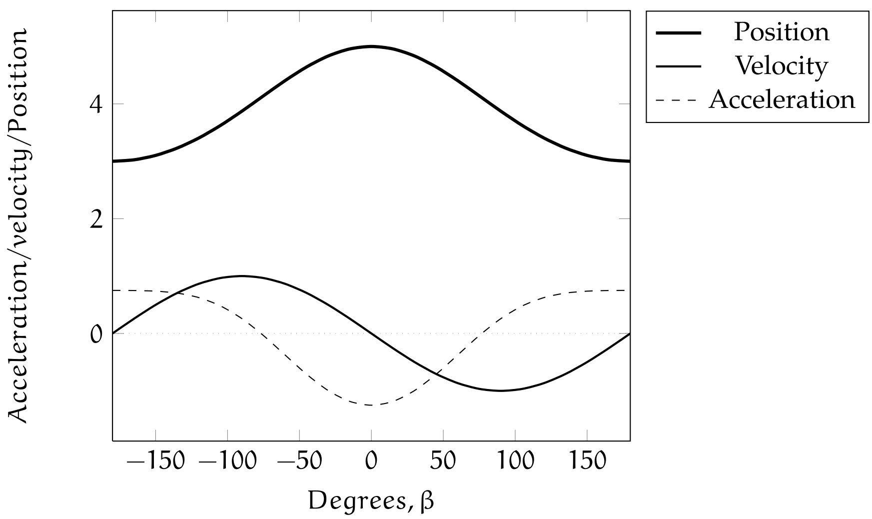

Figure 3: Position, velocity and acceleration of a moving piston inside a cylinder at a compression cycles

Figure 3 displays the velocity and acceleration with respect to piston placement in the cylinder, and it is evident that the piston has great changes in the velocity through the stroke, and at top an bottom, there is a small stop at the top and bottom position($\beta = 0, 180$) .
The valves are automatic spring-loaded and open only when a proper differential pressure across the valve exists. Inlet valves open when the pressure inside the cylinder is slightly below the intake pressure, and the discharge valve opens when the pressure inside the cylinder is slightly above the discharge pressure (system pressure). Both the suction and discharge valves are the same basic design and only differ with the location in relation to the working chamber. The piston is not, at top dead center (TDC), in contact with the valves, hence there is a small gap between the cylinder and piston containing pressurized gas causing compressed gas to further be expanded at the suction stroke influencing negative on the total efficiency. The minimum clearance obtainable will wary from 4% - 16% of the total stroke length in most reciprocating compressors [5]

The sealing between the piston and against the non-moving cylinder wall in lubricated reciprocating compressors is done by piston rings touching the cylinder wall lubricated by a film of lubrication oil. The rings are made from special types of cast iron or different types of polymers (i.e flour polymer,PITFE or high temperature polymers,PEEK). Lubrication oil is contained in a reservoir in the base of the crankcase where oil, from parts open to the crankcase, drain down by gravity. Main bearings however, is often fed from a fully pressurized lubrication system, where a positive displacement pump draws oil from the reservoir and delivers it under pressure to a circulation system. The oil is forced through drilled passages in the main bearing saddles, crankshaft and the connection rod. Under operation, all surfaces are separated by a layer of oil film which normally prevents metal to metal contact, wear and reduces friction in the compressor.

The compression cycles follows the same steps as a piston engine used in vehicles namely the Carnot cycles, only in a reversed order. Left side of figure 4 shows the cycles with 4 steps in a p-ν diagram, where the $W_{net,in}$ is the work needed to compress the fluid. Figure 4 to the right is a sketch in the same diagram showing the adiabatic process in an ideal compression, where the entropy is constant. The work needed is the sketched area below the adiabatic line, and given from equation

$$W = \int dp dV \tag{5}$$

And will show to be useful in experimental results when there is possibilities to measure both pressure and volume in the compression cycle.

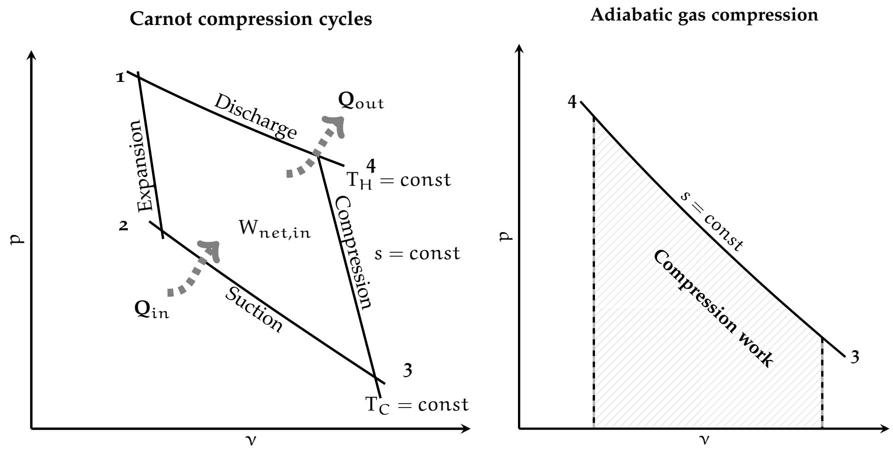

Figure 4: P-v diagram of the Carnot compression cycle, and a sketch of the compression work in an ideal adiabatic gas compression cycles

- **Reversible Adiabatic expansion**(process 1-2, temperature drops from T_H to T_C) cylinder head is at top dead center(TDC) and the discharge valve closes causing a negative pressure inside the cylinder and an adiabatic expansion as the piston is moving to the bottom dead center(BDC).

- **Reversible Isothermal Expansion**(process 2-3, T_C=constant) the negative pressure inside the cylinder causes the inlet valve to open and gas expands isothermally while receiving energy $Q_i n$ from the inlet gas.

- **Reversible Adiabatic Compression** (process 3-4, temperature rises from T_C-T_H), the inlet valve is closing and the piston has reached the bottom dead point (BDC) and is returning to the cylinder head compressing the gas adiabatically until its temperature is T_H and the pressure is just below the system pressure causing the discharge valve to open.

- **Reversible Isothermal Compression**(process 4-1, T_H=constant), the discharge valve opens and the piston is compressing gas while energy $Q_o ut$ is discharged to the hot reservoir by mass transfer. [10] [6]

In such a process, the second law of thermodynamics gives restrictions to the process efficiency when it states that the process cannot operate outside the boundaries of T_C and T_H. The total work of the process is given from the area below the lines, and $W_{net,in}$ is the work needed from the compressor. In comparison with the work done by the electrical motor it is normal to use the isentropic efficiency, here it is custom to assume constant entropy and following equation for isentropic work per unit of mass flowing through the compressor can be derived:

$$\left(-\frac{\dot{W}_{net,out}}{\dot{m}}\right) = h(p_{disch}, T_{disch}) - h(p_{suct}, T_{suct}) \tag{6}$$

The inlet conditions are fixed and the process depends on the enthalpy at the exit, h_2. From the expression 6 it shows that the magnitude of work needed will decrease as h_2 decreases. Therefore the minimum allowable work corresponds to the minimum allowable specific enthalpy at the compressor exit, which in theory is when the entropy is constant. Therefore the minimum allowable work per unit of mass possible is given by:

$$\left(-\frac{\dot{W}_{net,out}}{\dot{m}}\right)_s = h(p_{disch}, s_{suct}) - h(p_{suct}, T_{suct}) \tag{7}$$

In an actual process the temperature will increase because of increased pressure, and $h_2 > h_{2s}$. An isentropic compressor efficiency can then be defined by:

$$\eta_{is} = \frac{(-\dot{W}_{net,in}/\dot{m})_s}{(-\dot{W}_{net,in}/\dot{m})} = \frac{\dot{m} dh_{is}}{W_{el}} \tag{8}$$

	dh	Difference in enthalpy from suction to discharge
Where	s	entropy
	W_{el}	Electrical power to the system

There are several reasons for avoiding droplets and vapour through the inlet valves, and that it will in all cases lead to a severe breakdown of the compressor. Some of the reasons are that the density of liquid droplets will cause rapid wear on the valves and cylinder because of incompressibility, and cause the protecting oil film to vanish. Also as the temperature increases and the droplets condense, the heat they absorb will cause local cooling of the metal and the valves will eventually break. Finally a huge amount of liquid will have a hard time getting in to the cylinder as the passages are small, which will cause a rapid tear on the construction. As a sum of this an compressor for the refrigeration industry is not designed for liquid of any kind in the cycles, and the inlet flow is kept in the superheated area with good margin. A consequence of this heated fluid is a increase in the specific suction volume, thus decreasing the mass flow rate. These factors strongly affect the performance of a compressor and a refrigeration system as a whole. Even if the increase in specific suction volume causes an increase in volumetric efficiency, the increase in power consumption because of decrease in mass flow causes the total efficiency to drop. Also in a refrigeration plant the effects have a negative impact on the total COP linear to the decrease in mass flow rate.[15] Experimental results have shown a 17 % negative influence on the total efficiency at pressure ratio 6.7 on a compact reciprocating compressor[12], and in a semi hermetic reciprocating compressor, where the inlet gas is used to cool down the motor, the influence on increased superheat has shown to be substantial. [15]

2.2 COMPRESSOR BUILD-UP

Mass produced compressors are made from a standardized selection to keep the cost down, and the SINTEF/Obrist compressor has the same basic details: The housing is made from cast iron which cowers on both ends witch are reinforced with ribs on the inside. The housing has ribs on the outside for better cooling, and is also mounted with 6 cylinders bolted on the octagon shaped topside. The common shaft of both motor and crank shaft has two slide bearings, and is attached to the pistons with a connecting rod attached to the piston with a wrist pin. For the lubrication a centrifuge oil pump transports oil from the crank case into the enclosed bearings and the cylinder lubrication, where some of the oil is transported with and later separated from the main flow. [1] The gas enters into the crank case through a centrally located suction duct, where it also acts as cooling for the motor. The pressure of the gas is governed by valves for each cylinder.

		Value/Range
Height x Width x Length	[mm]	500 x 440 x 830
Weight	[kg]	286
Volume flow rate	[m^3/h]	10-90
Displacement	[cm^3]	380
Max power consumption	[kW]	100
Revolutions per minute	[rpm]	800 - 4000
Frequency range	[Hz]	53-267

Table 2: Compressor data

2.3 ENERGY LOSS ANALYSIS

The main objective of the new development and further testing of the SINTEF / Obrist compressor is to produce a compressor that can handle both higher flow and higher pressures needed for industrial CO_2 cooling applications. A successful result is not only depending of how well it works in general and if it is operating within standards and limits for the industrial marked, but if it is efficient and economic on a long term basis, which is depending on an overall efficiency factor calculated from energy losses in the compressor.

1 Parts of the lubrication system is still in a patent evaluation.

A total efficiency is defined as the total effect from the respective loss factors, and the main losses include the following terms:

1. Motor and VSD loss
2. Volumetric loss
3. Valve loss
4. Lubrication and bearing loss
5. Heat loss

2.4 MOTOR AND VSD LOSS

A high performance motor has a highly positive effect on the total compression application, where it counts for the rate of which it transforms electricity to torque in the shaft. In the current compressors application, a permanent magnet motor was used, which, compared to comparable reciprocating compressors, gives a more efficient application. Here the speed of the motor is equal to the rotating magnetic field speed, and to variate the speed of the compressor a Danfoss Da131F4867 [8] frequency converter was provided with an efficiency provided by the vendor. The electricity consumption was also measured before and after the frequency converter.

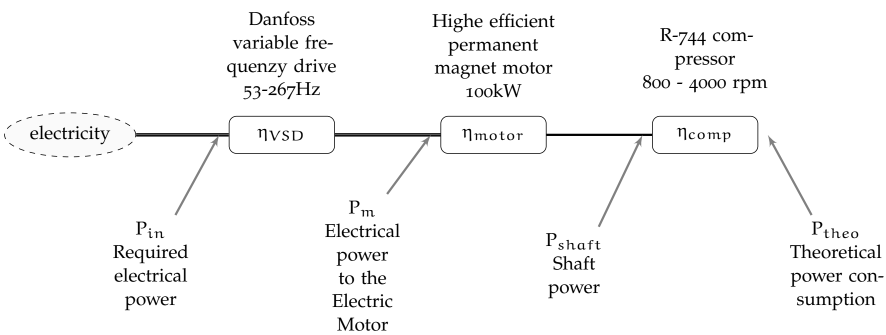

Figure 5: The compressor - motor - VSD arrangement showing four levels

Figure 5 shows the set-up of the variable speed drive system in the compression circuit. Losses in couplings between the VSD and motor are here not considered. The losses in the motor result in heating of the wirings, which are cooled by the inlet suction gas. Thus an decrease in motor efficiency will affect the super heat, and a further reduction in compressor efficiency. The efficiency of the motor varies as the frequency and load changes, the plot in figure 6 is a general variation for frequency converters and high performance motors published[4].

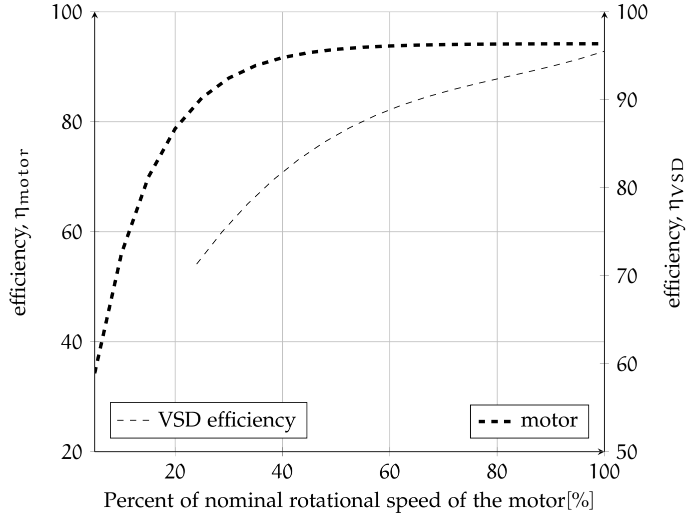

Figure 6: Typical efficiencies for high-efficient motors and VSD as a function of % nominal speed, *ASHRAE Journal, December 1999*

The curve for η_{motor}, motor efficiency, is the curve for high-efficiency motors presented in the *1996 ASHRAE Hand book-HVAC Systems and Equipment*[4]. The curves apply for motors with a relatively high effect (typically >25 hp). The motor efficiency decrease significantly for a part load below 25%, while at above 50% it is almost constant.
The electrical power requirement is influenced by efficiencies in motor, VSD and compressor. Therefore the required electrical power consumption of the VSD-system is

$$P_{in} = \frac{P_{theoretical}}{\eta_{VSD}\eta_{motor}\eta_{compressor}} \tag{9}$$

Where η_{VSD} is the efficiency of the frequency converter, which variates according to nominal speed of the motor, as seen in figure 6, and extends from 20% - 100% speed ratio, where the efficiency is slightly below 100% at full nominal speed.
The electrical power feed to the motor:

$$P_m = \frac{P_{shaft}}{\eta_{motor}} \tag{10}$$

The shaft power is a function of what consumption there is need for in the compression, where the theoretical power needed are depending on mass flow rate and pressure ratio in the compression cycles.
The theoretical power consumption is:

$$P_{theo} = \dot{m}(h_{s_{suct},p_{disch}} - h_{T_{suct},p_{suct}}) \tag{11}$$

For the main part losses in the VSD-system were provided by the manufacturer, and arranged by given set-up.

2.5 LUBRICATION SYSTEM

The characteristic high operation pressure in a CO_2 application may force high force loads on bearings and frictional conjunctions in the compressor. All of these are at all-time supplied with lubricant and a layer of lubrication oil is present at all time. An absence of oil will lead to high frictional forces and a reliable supply system is an important feature of the compressor and one of the key parts of which a general improvement has been done in the newly developed compressor. On that basis, there are three main parts where the frictional losses take place and a constant oil feed is of importance[18]

- Between the piston and the cylinder
- Crankshaft journal bearings
- Connecting-rod big end journal bearings

The oil feed is performed by an internal shaft driven oil pump. It is a centrifugal pump and draws oil from an oil sump at the bottom of the crankcase through a filter placed prior to the oil pump.

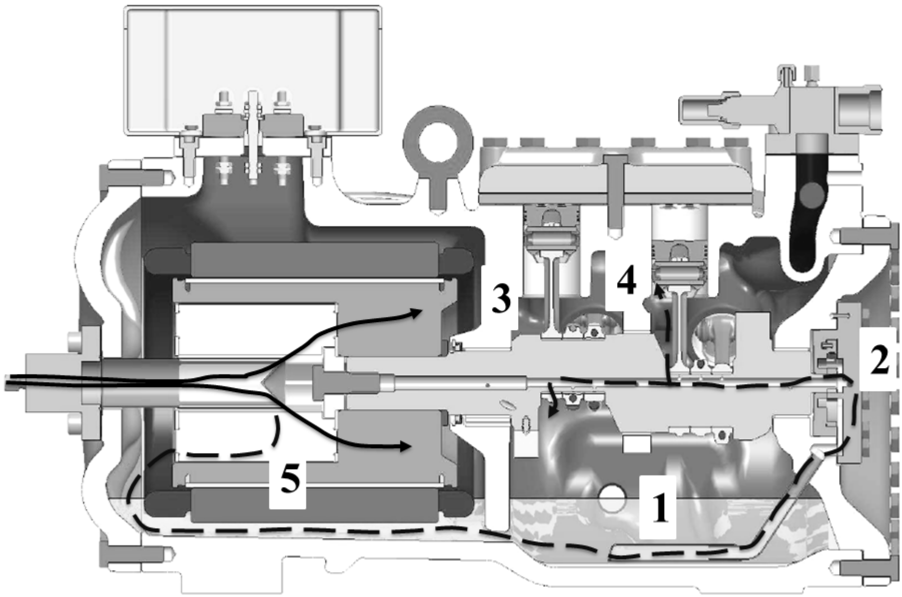

Figure 7: The sketched oil flow for lubricant in the compressor unit. Constant lines indicates the main gas flow, whilst the black dashed lines indicates the oil flow

From the filter, at point 1 in figure 7, oil is led under pressure to the crankshaft (point 2), and the main bearings are lubricated through drilled passages in the crankshaft and connection rod(point 3) to lubricate the crank-pin bearings, cross-head pin bushing, and the cross-head slide. A pressure gauge is fitted in the compressor housing after the filter, and the oil temperature inside the oil sump is also monitored at all time. Oil is sprayed into the cylinder at point 4 from a small feed line to maintain an oil film between the piston ring and the cylinder, and unavoidable, from here some of the oil is transported along with the main gas stream. An external oil separator is mounted on the main gas stream. The effectiveness of the separator depends partly on the amount of oil in the gas stream out of the compressor, but at equilibrium conditions most of the oil from the gas is transported back to the crankcase. This flow is also measured with a mass flow meter, and controlled by a level switch on the crank house. The total oil flow is rather complex, and a calculation of the losses in the flow is mostly done by a computational fluid dynamics (CFD) analysis. Even if CFD has shown not to be reliable in many applications, it is an approximation of the real case, an analyzis doen by Obrist engineering showed a pressure difference between the motor and the compressor housing, causing oil to flow in the direction of the main gas flow. This was a problem met in the initial tests where the pressure build up in the oil sump caused the oil to flow in the direction of the cylinder and main gas stream. Further on the external oil separator could not handle all the oil in the main stream, and the whole R-744 circuit was flooded with lubrication oil, resulting in efficiencies below what was expected. One solution was to add a plastic ring in the area where the pressure difference between oil and gas was biggest between the motor and motor housing.

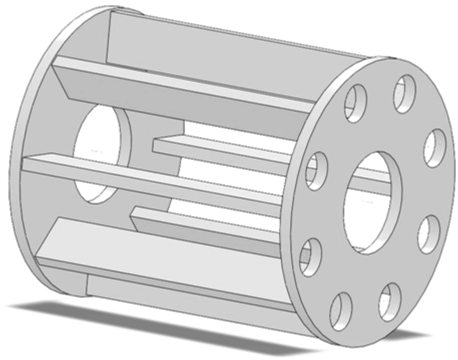

Figure 8: The oil droplet separation unit in the suction gas

An important factor in this system is the centrifugal oil removal in the inlet gas at point 5. This is where parts of the design is newly developed, and in general it is working as an additional oil separator, before the gas is fed in to the cylinders. There is a "hamster wheel" in the inlet, shown in figure 8 connected to the shaft from the motor and spinning in the same speed as the compressor. Its purpose is to remove oil droplets from the suction stream and redirect them in the flow path shown in figure 7. This will decrease the mass flow, as well as increase the volumetric flow, hence increase the efficiency of the compression.

2.6 VALVE LOSS

Two types of valves were planned used in the compressor, one standard plate valve and one custom made poppet valve. At all initial tests the plate valve was used, but in the future experiments it will be replaced by a ring valve made custom by Obrist Engineering, which is, on basis of simulations done, expected to raise the performance of the compression.

For a valve the crucial elements are to

- open at the right time
- close at the right time
- open at the right speed
- close at the right speed

They are opening and closing one time each for every rotation on the shaft, and have to work under extreme conditions both in temperature changes, pressure differences and frictional forces. Therefore, the valves are a critical point in the compressing process representing a great deal of the total energy loss in the compressor. They are responding on the system pressure, which is controlling the opening and closing of the valves on both discharge and inlet. When the pressure in the cylinder is higher than the pressure on the high pressure side (condenser/gas cooler side) which is set by the throttling valves, the valve opens and gas is let out (point 4 in fig. 4). However, there is some resistance in the valve as well, and the pressure in the cylinder builds up somewhat over the system pressure before the valve opens and the pressure in the cylinder is decreasing.

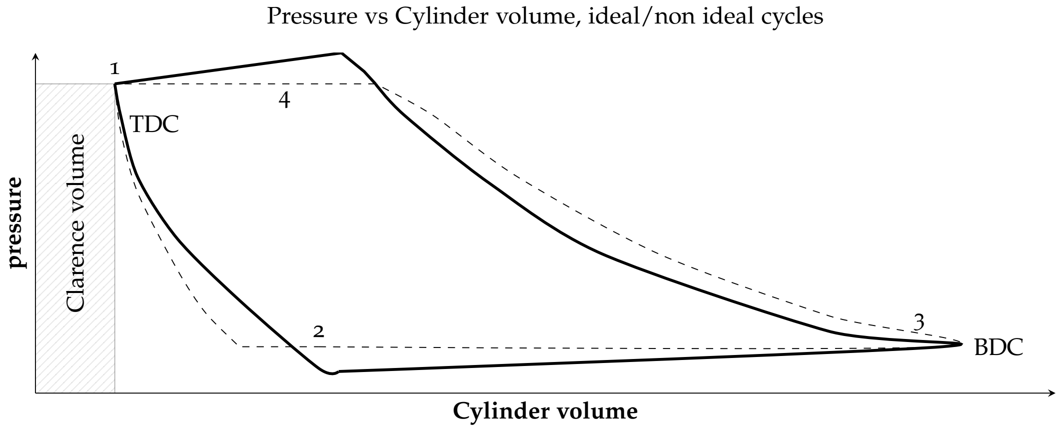

Figure 9: The pressure volume diagram shows a compression cycles as ideal and non ideal, with TDC (top dead center) and BDC (bottom dead center)

Figure 9 displays the cycles in a pressure versus cylinder volume diagram, and it shows that the pressure build-up is well above the system pressure. The cylinder pressure has to overcome several factors, and initially, as the valve is closed, it is firmly set against the seat and the sealing is intact. As the pressure rises, it initially lifts off the seat slowly, and accelerates rapidly as the resisting forces are overcome. In general the forces have three main outsprings[17]:

- Cylinder pressure is exposed to the entire surface area of the sealing element, and the inertia in the valve material has to be overcome.
- The so called sticking effect is due to an oil film between the seat and the valve orifice which, because of surface tension in the fluid, will "hold on to" the valve until a required force is met. Discharge and suction has sticktion in the valve, and in the suction it is seen in figure 9 as a pressure decrease when the valve should open, and a delay in the opening process compared to the ideal one. The main influencing factor is the oil viscosity, which is also changing with the temperature in the cylinder.

- The valves are loaded with a spring to secure a fast closing of the valves in both suction and closing. The spring force has to be overcome, which is also a force to overcome in the discharge and inlet process.

These forces cause the cylinder pressure to build up above the system pressure, causing more more energy to be used, compares to an ideal cycle were no extra resistance is met. More work has to be done to overcome the energy used in resistance in the valve opening which influences both thermodynamic and volumetric efficiencies.

In a real case the valve will open like shown in figure 10 and cause a fluctuation in the gas velocity as the gas is discharged. Then, as the discharge valve opens, the cylinder pressure is higher than the discharge pressure because of the resisting forces, and the sealing element is accelerated towards the spring load and impacts against the guard. Here the valve is considered fully open, and at this stage the gas pressure in the cylinder causes the velocity through the valve to be extremely high. Further on, this high velocity in the flow will cause the pressure in the channel to drop, and the valve will be forced to close the passage causing the pressure to rise above the discharge pressure again. In figure 10 the opening of the valve is shown as a function of the crank angle, and it is seen that the valve is not fully open in more than parts of the whole process.[14] This valve resistance also causes a throttling effect as the gas passes, point 1 and 3 is moved in vertical direction to the left and the points for compression and expansion no longer start on the same vertical line, and in figure 9 point 2 is placed to the left of point 4.

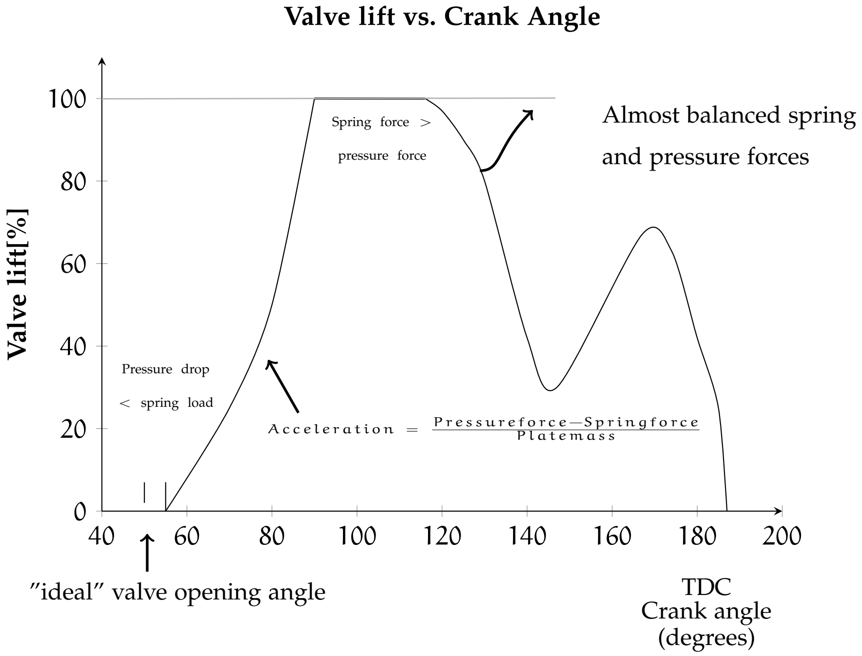

Figure 10: The Valve lift displayed as a function of the crank angle, where a typical actual opening in a plate valve is shown

Also as the valve opening takes place, the valve opens after an ideal point, and the acceleration due to pressure build-up makes the valve hit the guard in a relatively high speed, causing temperature increase and lowering the efficiency of the compression. At closing the valve closes relatively rapid, before cylinder pressure builds up. It is noted that the forces met by the pressure is given from $F = p_{cyl}A_{valve}$, and once this force is higher than the acceleration forces, spring force and system pressure the valve opens again. When the cylinder has reached TDC it returns into suction there pressure will decrease, and the valve closes. Also here it is too slow, and closes after TDC, and some of the gas from the discharge will be sucked into the cylinder, having effects on the volumetric efficiency.
The area of the valve affects the lift and the losses in the process, whereas a small valve area calls for a high velocity in the gas, and big area yields a lower velocity. However, big valve areas needs more space which increases the clearance volume and calls for a greater inertia and higher pressure build-up. The pressure drop increases with the square of the velocity of the gas, mainly due to loss of kinetic energy caused by friction through the valves.[9]

The same effect are also appearing at the suction inlet. The piston is one step ahead of the valve, and a study of figure 9 reveals that the pressure increase in point 4 is lower in the actual process, than in the ideal. This is because the valve is not fully closed when the piston reaches BDC, and travels from suction to compression, and some of the gas inside the cylinder will return through the inlet valve, and cause a suction loss in the process. This together with the losses in the discharge is a major concern for the volumetric efficiency.

There is no simple way to calculate the described valve dynamics and simulate them, since the valve movements are quite complex. In the Obrist /SINTEF compressor, a pressure transmitter was fitted in one of the cylinders, measuring the pressure variations as the piston travels from point 1-4. From this the pressure loss in the cylinder was possible to be measured, which in part also will be indirectly proportional to the valve losses in the process.

From a p-V diagram it is also possible to calculate the work done, from equation 5 the input energy are easily adaptable from an indicator diagram. Thus, from a pressure indicator inside one cylinder it is possible to quantify a value for the indicated work in the cycles, $P_indicated$ [W].

2.7 VOLUMETRIC LOSS

Clearance between the piston and the cylinder head are causing big negative effects on the volumetric efficiency in the compressor. On the discharge stroke a small amount of gas remains in the clearance between the piston and cylinder head. The gas is here pressurized and when the piston starts its return stroke, this clearance gas at discharge pressure must expand to intake pressure in order for the inlet valves to open. Thus, no air enters the cylinder for that portion of stroke, which in turn reduces the intake volume by that amount. The volume of this amount of lost gas in the suction stroke, varies with the compression ratio. Thus it follows that the volumetric efficiency, and the actual capacity of the compressor, varies with the compressor ratio.

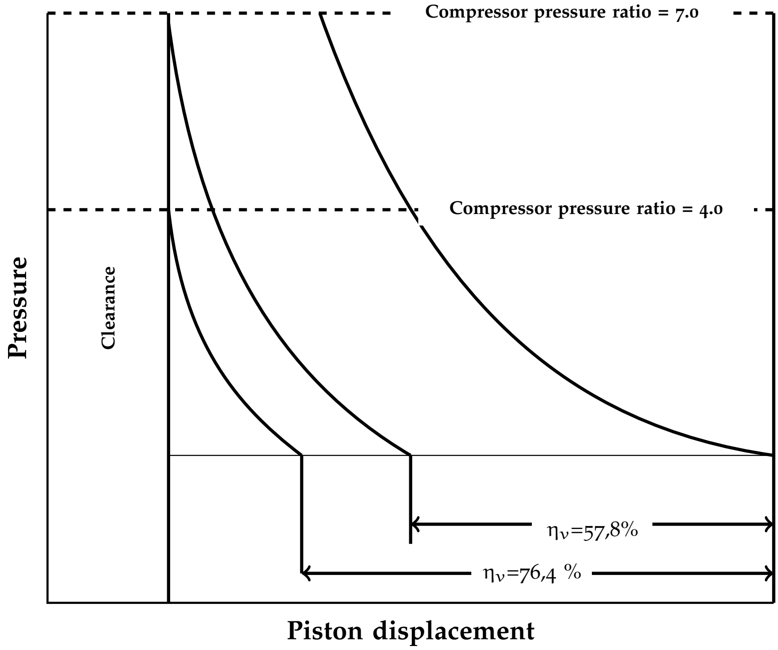

Figure 11: Effect of different pressure ratios on the volumetric efficiency of a given cylinder

As seen in figure 11 the pressure ratio has an effect on the volumetric flow, since an increase in pressure ratio causes the expansion line to draw to the right and a smaller percentage of the total stroke length is effective. The pressurized gas also affects the total work done in the cylinder, since it is compressed and expanded instead of been delivered as compressed gas.

Pressures in a R-744 circuit is rather high, and the ratio of pressure in the compressor is smaller than in a system using synthetic fluids. A relatively higher volumetric efficiency could therefore be expected in the Obrist / SINTEF compressor.

Leakage between the piston ring and the cylinder allows gas from the compression chamber to escape past the piston into the other end of the cylinder. This causes the capacity to reduce due to hot leakage gas heats up incoming gas into the cylinder. Also at discharge stroke gas is let past the piston rings because of the pressure difference in front of and below the piston. As seen from figure 3 the velocity of the piston is at the slowest as the pressure is highest, and the gas has time to leak past the piston ring, thus the ring leakage is highest at discharge. In assembly of the piston rings, they need to be cut and expanded to fit the piston. This leaves a small gap on the ring, which are the cause of relatively high gas leakage. In the Obrist / SINTEF compressor this was a concern, and a ring with better sealing was used after initial test.

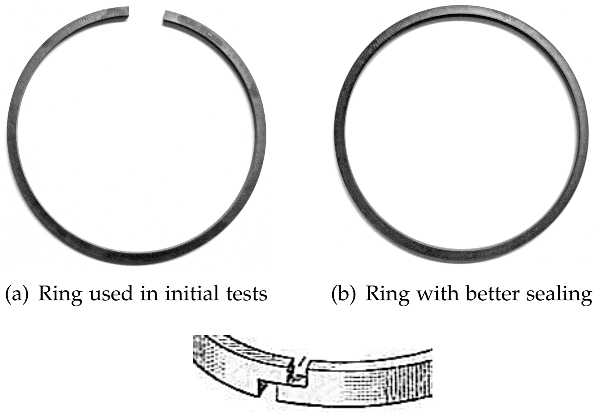

(a) Ring used in initial tests (b) Ring with better sealing

(c) Sealing in the permanent pistonring

Figure 12: Picture a) and b) are pictures of the used piston rings, and c) is the ends used on the permanent piston ring in picture b)

Figure 12 a) displays the ring that was used in the initial tests, showing a worsening effect on the volumetric efficiency due to the small gap between the endings. This construction is necessary when installing the rings, but the gap can be concealed, as shown in figure 12 b) where the endings are jointed together as shown in figure 12 c), where they are fitted to create a more intact sealing surrounding the piston.

As the piston goes from suction to compression there is a delay in the valve which causes the air inside the cylinder to reverse through the inlet valve. This valve slip can obviously occur in both suction and discharge, but is usually much less in the intake valve compared to the discharge valve. The motion of the piston in figure 3 reveals that the acceleration of the piston also is at its highest at 0 and 90 degrees, but this is favourable in terms of reducing valve slip. Minimum slippage will occur in a responsive valve, which has a minimum inertia so that the moving element can easily be controller by air flow. The theoretical volumetric efficiency is a function of the maximum stroke length, cylinder volume and the measured volumetric flow:

$$\eta_v = \frac{\text{Theoretic suction volume} \times \text{RPM}/60}{\text{Measured volum flow}} \tag{12}$$

It follows from this that every decrease in suction volume will affect the theoretical volumetric efficiency, and all the above factors have a negative impact.

However, and increase in temperature which increase the volume and the volumetric efficiency, will decrease the mass which from equation 8 will decrease the isentropic efficiency. Therefore a favourable temperature in the suction is as low as possible.

2.8 INTERNAL HEAT EXCHANGE

Heat generated by the dynamic parts in the compressor is the main source of heat exchange to the ambient. The motor parts are cooled by the gas flow, as shown in figure 8 (a), hence warmer when it flows out of the motor than at the measured suction temperature. As the flow travels through the valve and narrow passages, the frictional losses ads additional heat to the flow. This added superheat affects the performance of the compression cycle, and in a p-H diagram the point for compression will move to the right.

As from the equation 8 the ideal compression follows the line for constant entropy, the heat losses are neglected and the point h_2s is placed at an "ideal" temperature. The actual temperature however is presumably to the right of this point, because of temperature increase due to the compression.

Now both the actual points for discharge h_{disch}, and the inlet h_{suckt} is moved to the left of what is expected because of heat differences in the flow. For an approximation of the heat exchange in the cycle the following can be used.

Theoretical compression work:

$$\dot{W} = \dot{m} dh \tag{13}$$

Thus the enthalpies are

$$h_{suct} = h_{disch} - \frac{\dot{W}}{\dot{m}} \tag{14}$$

$$h_{disch} = \frac{\dot{W}}{\dot{m}} - h_{suct} \tag{15}$$

Both the work input $\dot{W}$ to the compressor and the pressures p_{suct} and P_{disch} are measured, which gives the possibility to calculate a plausible actual temperature at the inlet. The heat loss in the compression is then the difference between the measured heat from pressure and temperature, and given from the work required to do the compression.

$$q_{loss} = h_{disch} - h_{\dot{W}} \tag{16}$$

This is not the total truth, as discussed in chapter 2, there are, unwillingly, a certain possible oil flow in the gas stream. And the mass flow $\dot{m}$ is the sum of

$\dot{m}_{R-744}$ and $\dot{m}_{oil}$ thus the heat per mass from $\frac{\dot{W}}{\dot{m}}$ is both oil and R-744, whilst the heat per mass($h(T,p)$) given from pressure and temperature is for R-744 only. A more reliable approach is to calculate the specific heat in the suction by implementing also the specific heat for all the containing oil left in the discharge gas. From this it is also possible to calculate a heat influence due to oil in the gas and the differences in specific heat in oil compared to superheated gas.

The specific heat for gas with oil:

$$h = h(T,p)_{R-744} + cp_{oil}T \tag{17}$$

Actual heat difference:

$$q_{loss} = \frac{\dot{W}}{\dot{m}} + h(T,p)_{suct} \cdot (1 - OCR) + cp_{oil}T \cdot OCR - h(T,p)_{disch} \tag{18}$$

	OCR	Oil Circulation Rate in the system
Where	Cp	Specific heat capacity
	q	Specific heat

If it is assumed a constant specific heat duty for the oil, the heat difference between measured and calculated specific heat will be linear between 1 and 5 % oil in the suction gas.

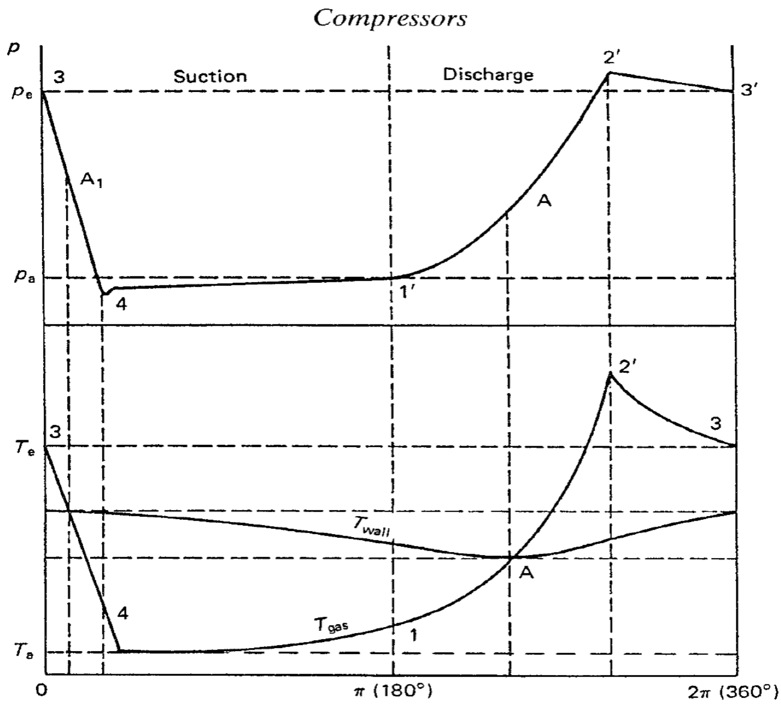

Figure 13: Temperature and pressure variation in a complete compression cycle

In the cycle there is heat exchange between the gas and the walls of the cylinder through a compression cycle. Figure 13(from [9] shows the changes in gas and wall temperature as a complete revolution in the vapour compression is being done, along with the pressure variations in the cylinder. At the start the cylinder walls will have a higher temperature than the gas, and the temperature will increase to point A. Afterwards the gas will reject heat to the cylinder walls, and as the pressure increases to the point where the valve opens, there will be a big drain of energy from the gas to the surrounding cylinder walls, and as the discharge valve opens the temperature inside the cylinder will decrease to point 3. From this the net heat loss travels through the cylinder wall to the ambient. The compressed gas will have a top just at point 2' at the same point as the pressure has a peak before discharge. here the cylinder walls are warmed up, thus energy from the gas is drained.

3 THE TEST RIG

The test plant was built in order to conduct experiments on high capacity components like compressors, heat exchangers, expansion- and work recovery devices in a real refrigeration cycle using R-744 as refrigerant. The maximum power input are 100kW to the compressor, and the plant is able to work in real system performance from evaporation temperatures around triple point of R-744 to maximum discharge temperature of 130 bars. The plant is developed by SINTEF in cooperation with Obrist engineering where it was built, and eventually it will be transported in to the laboratories at SINTEF and NTNU in Trondheim. Besides a closed system using R-744 it has an additional supporting system using ethynol-glycol-water to reject and recover heat from the R-744 system. The heat exchanger applications are replaceable, and topic of later experiments.

3.1 DESCRIPTION OF THE TEST PLANT

Figure 14 shows the container which the rig is implemented in and an air cooler with variable speed fitted in the rear of the container. The measurements are 1,6 mx 1,2m x 2,53m, the air cooler adds additional 0.25m to the total length. Along with a water cooled heat exchanger the air cooler is rejecting the heat done by the compressor which cannot be conserved in the supporting glycol-water system.

(a) View from the outside of the container

(b) View of the inside, with the VSD on the right and the green cables for the cylinder pressure transmitters out from the compressor on the floor

Figure 14

The rig is built as flexible as possible, and all of the key applications in the R-744 refrigerant circuit are replaceable or has the opportunity to make use of additional equipment as expansion or work recovery devices desired for future experiments. The system is set to work at a maximum discharge pressure at 130 bar with temperatures in ranges of -50 - 180 °C in the R-477 cycle and the maximum electrical power input to the compressor is in the range of 100kW,
For safety reasons the rig was controlled by a 3. party company specialized in quality assurances of weldings using x-ray, also it has been pressurized up to 160 bar and leakage tested.
The rig was built to be flexible for future experiments, and in testing of compressors it is possible to bypass some of the heat exchangers, as shown in figure 15, and reject the heat generated by the compressor in the air cooled gas cooler only. At higher ambient temperatures it is possible to connect the water cooling as well. From figure 15 following components are recognized:

Were:
1: R-744 compressor
2: Air cooled gas cooler
3: Water cooled gas cooler
4: Gas cooler/condenser a and b
5: Internal heat exchanger
6: Evaporator a and b
7: Expansion valve
8: Separator
9: Oil separator

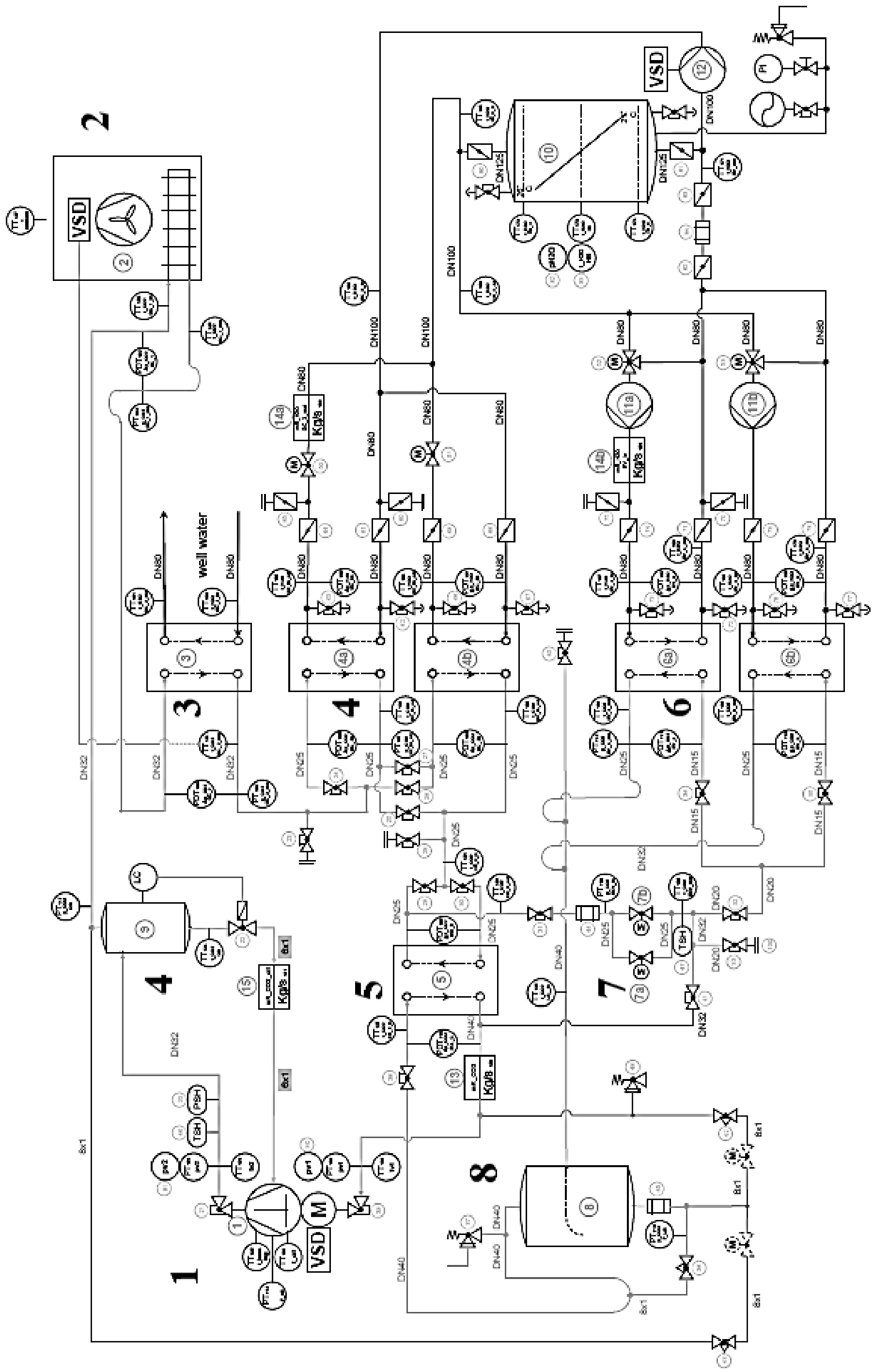

Figure 15: Principal drawing of the test rig facility incorporating the pipe work, vessels, heat exchanger and supporting system

In general the rig consists of two independent closed systems, one using R-744 as refrigerant getting compressed in the gas phase, and cooled either in critical or sub-critical conditions. As a supporting system the ethylene system worked both as heat sink and heat source at constant temperature. In experiments with the compressor it was not required to use the supporting systems, and the ethylene water systems were not in operation during the test.

3.2 DESCRIPTION OF THE REFRIGERATION CIRCUIT

After compression the R-744 went in to an oil separator (9), where most of the oil was separated from the working fluid and fed back to the compressor lubrication system. From the oil separation and back to the compressor there was mounted an on/off valve responding to the oil level in the oil separator. At high compressor speeds this caused the throttling valve to shut on and off very rapid, causing a inconsistent flow.
Then the gas was led through the air cooler (2) mounted on the outside of the container. The only purpose of this gas cooler was to reject heat from the compression. At lower ambient temperatures this cooler was able to reject all the heat generated from the compressor and at higher ambient temperatures there was an additional system using water as coolant (3). In experiments inside the lab it might be preferable to use the water cooled system, to avoid too high temperatures in the lab facilities.
Downstream of the water cooler there were mounted two plate heat exchangers (4) between the two systems, where 4b was bypassed. In future experiments it is possible to run these exchangers both in parallel and series for possible performance evaluations. In addition there is made room in the test rig to replace them with other applications, or mount additional equipment downstream or upstream.
The throttling valves (7) were placed downstream of the internal heat exchanger (5) which was bypassed. By adjusting the opening in the two throttling valves the system pressure was set. And in order to fine tune it to the appropriate pressure the pressure reduction application was a set of two valves, where one had a smaller pressure range, and was used to control small pressure variations.
A set of plate heat exchangers(6) was installed downstream of the heat exchangers to transfer rejected heat from glycol to R-744, but for compressor experiments exchanger both these, the gas-liquid separator(8) and the internal heat exchanger(5) low pressure side were bypassed.

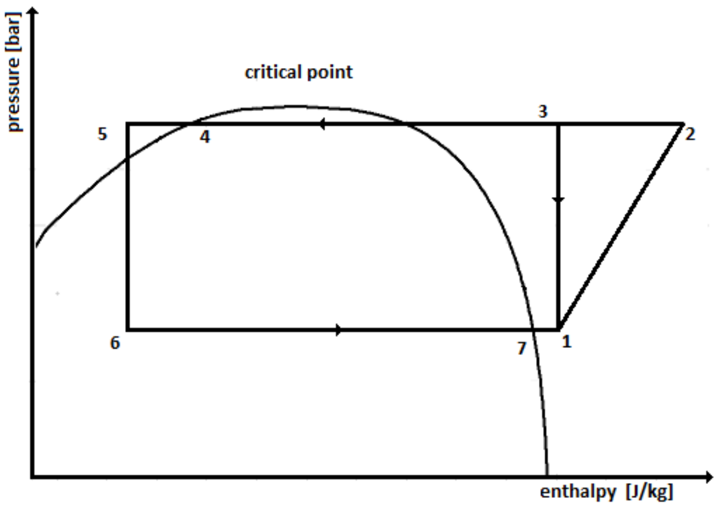

Figure 16: Drawing of the refrigeration cycles in log p-h chart

In point 1 the gas conditions are at low pressure and low temperature. Thereby the gas is compressed "isotropically" from point 1 to the discharge at point 2. The compressed gas is cooled in two gas coolers using water or air until it reaches a point 3 where the heat from the compression is removed and no longer in the system. The gas is then cooled in heat exchangers 4a and 4b where heat is rejected to the supporting system using a glycol/water mixture. When the mixture of gas and vapor reaches the saturation line at point 4 it is sub-cooled in an internal heat exchanger until it reaches a point 5 where it is throttled in two throttling valves until it reaches suction pressure. The gas is heated in exchangers 6a and 6b from the system using a glycol/water mixture and recovers the heat from point 3-4. When the liquid/gas mixture is reaching saturation line at point 7 it is superheated to a point 1 where it is fully in gas phase and at the inlet of the compressor.

In the cycles running to evaluate the compressor the gas the fluid was throttled from point 3 at high pressure to suction pressure at point 1. Bypassing the heat exchangers working with glycol/water mixture and using only the air and water coolers to remove heat generated in the compression stage.

The experimental results were logged using Labview, and the measured data was directly implemented in to a calculation sheet where measurements of mean quantities uncertainties and experimental results was calculated. The general calculation method is adapted from today's standards.

Table 3 summarizes the measurement devices used in the refrigeration rig. For the thermocouples there are two different types; PT100 which is resistance thermometer, and a K-type thermometer. The PT100 is calibration tolerance according to DIN EN 60751 Class A and the K-type uses tolerance according to DIN EN 60584-2, Class 1.

Sensors	Measured variable	Measuring device	Calibration range	Calibrated accuracy
14	Temperature (°C)	K-type thermocouple	-40-145	±0.5
18	Temperature (°C)	PT100 Resistance thermometer	0-140	±0.03
13	Pressure (Bar)	Pressure gauge	0-160	±1.2
11	Pressure (Bar)	Pressure gauge	0-80	±0.7
1	Refrigerant mass flow rate (kg/s)	Coriolis mass flow meter	0.0–1.4	±0.1% of reading
1	Lubricating oil (m^3/h)	Coriolis volume flow meter	0-4	±0.25% of reading
1	Power consumption (kW)	Digital wattmeter	0-100	±0.5% of reading
1	Compressor revolution speed (rpm)	Analog signal from the inverter drive	0-4000	±1.3% of reading

Table 3: The installed transducers in the full test rig

3.3 UNCERTAINTY

There is an international standard consisting of general rules for evaluating and expressing uncertainty in measurements that is intended to be applicable in scientific measurements. The rules are developed by an international organization, after the highest authority in meteorology in France, the Comitè International des Poids et Measures(CIPM), requested the Bureau International des Pods et Measures (BIPM) to address the problem together with the national standards laboratories and to make a recommendation. The BIPM made a document covering issues regarding general measurements, and sent it to 32 national meteorology laboratories known to have an interest in the subject as well as five international organizations. Almost all believed that it was an important issue to address and by 1979 the responses were received with a conclusion that it was important for all international institutions to have a common acceptance regarding a procedure for expressing measurements uncertainty and for combining individual uncertainty components into a single total uncertainty. This was attended by 11 national standards laboratories, and the recommendation INC-1(1980) was developed. The working group's recommendation is a brief outline, rather than a detailed description, and the task of making a detailed guide was given to the Organization for Standardization (ISO). Within ISO many organizations were appointed, especially within meteorology, and the result is *Evaluation of measurement data - Guide to the expression of uncertainty in measurements* JCGM 100:2008. In the calculations within the test rig all uncertainty results are calculated from this guide, as seen in appendix C. [2]

3.4 EXPERIMENTAL SETUP

The rig was placed outside the buildings of Obrist Engineering in Lustenau Austria. There was attached a power cable from the local power grid, and an external computer screen on the outside of the rig set up. When the tests were performed the doors on the rig were shut, and the speed and temperatures in the cycle were

adjusted manually from a computer on the outside.
The set points for investigation was considered with background in a cooling application on a fishing vessel, and three pressure ratios were set with an interval from 800 rpm - 3800 rpm. This was decided on the basis of time consumption, whereas there was only 3 days available for conducting the experiments. Also the logging period for each set point was reduced to a minimum, in order to reach as many points as possible.

Constant Parameters		**Variable Parameter**				
		Values				Units
p_{disch}=65	bar	800	1000	1500	2000	RPM
p_{suct}=30	bar	2500	3000	3500	3800	
t_{super}=10	°C					
p_{disch}=110	bar	800	1000	1500	2000	RPM
p_{suct}=30	bar	2500	3000	3500	3800	
t_{super}=10	°C					
p_{disch}=80	bar	800	1000	1500	2000	RPM
p_{suct}=20	bar	2500	3000	3500	3800	
t_{super}=10	°C					

Table 4: Test program matrixes for the R-744 compressor, planed by Obrist Engineering

The experiments were run in a superheated area only, and only the air cooler was used in terms of rejecting the heat from the compressor. One full cycle experiment was executed for the first time, but not for other means than to adapt the calculation sheet for future experiments.

4 EXPERIMENTAL RESULTS

This chapter presents the results from the compressor experiments. The tests were executed with the help of Obrist engineering and their team in Lustenau Austria. All tests are presented with basis in the superheated cycle as described in Chapter 3 where the gas is in superheated area at all time. Volumetric and isentropic efficiency were the values calculated to reveal the overall efficiencies and the volumetric compression efficiency. The tests results were thoroughly supervised, and when the system was in equilibrium it was logged into an excel sheet with one measurement each second. There were mounted two pressure devises for measuring the cylinder gas pressure, and two sets of measurements were performed, one before and on after, to check that the transducers inside the cylinder suction and discharge chamber did not influence on the performance of the compressor. Measurements were logged at 3 different pressure ratios with varying speed, from 800 rpm to 3800 rpm. However, the power supply to the rig was limited to 94kW due to lacks in local power supply.

The following efficiencies are presented:

1. isentropic (is)
2. volumetric (vol)

In addition the following relations are also presented:

1. oil circulation rate (ocr)
2. frequency converter (vsd)

Also indicator diagrams for the gas pressures in the cylinder are presented. As for the accuracy in the calculations and measurements, these are presented for the isentropic and volumetric efficiency as well as for the suction and discharge temperatures. The full overview of calculated uncertainties and actual measured values are attached in Appendix C.

4.1 THE ISENTROPIC EFFICIENCY

The overall efficiency as well as the volumetric efficiency is the most defining measurement for the compressor and how it is performing. The isentropic efficiency accounts for losses in both the motor and compressor, motor and compressor, as described in chapter 2. In the calculations the following was therefore used:

$$\eta_{is} = \frac{P_{is}}{P_{el}} 100 = \frac{m_{oil+R-744} \Delta h_{is}}{P_{el}} 100 \tag{19}$$

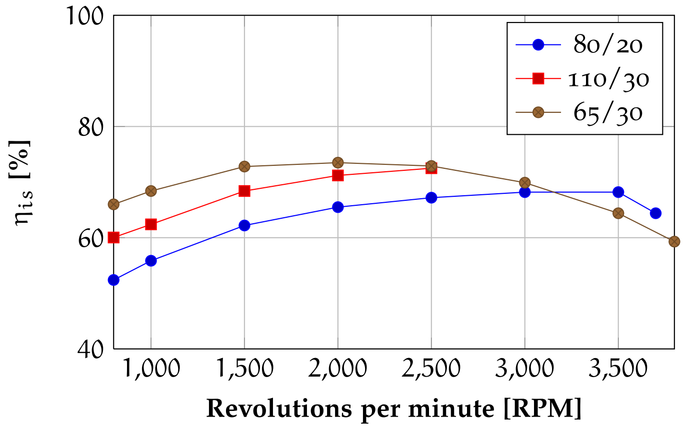

Figure 17: Isentropic efficiency with variation in rpm with a constant superheat at 10K

Figure 17 displays 3 different pressure ratios where the speed of the motor is the only varying parameter. The superheat in the suction was held at 10K for all of the different pressure ratios. The highest pressure ratio was at 4, and with a suction pressure at 20 bar and a discharge pressure at 80 bar, the temperatures were stable at -10 °C and 125 °C, respectively. For pressure ratios at 110/30 and 65/30 the suction and discharge temperatures were held at 4°C and 5°C for the suction and 125°C and 75°C for the discharge side, respectively.

The discharge temperature varied with 1-2 degrees °C for each of the different set-points, see table 8

Figure 17 indicates that the overall efficiency for pressure ratios between 2 and 4 is at its peak at motor speeds between 2000 and 3000 revolutions per minute. Also earlier initial test results has indicated a peak performance in the area of 2500 rpm. Further on, the line for pressure ratio of 110/30 bar(—■—) ends at 2500 rpm, which was due to power consumption above 94kW at motor speed < 3000 rpm causing the system to shut down. This was the case also for pressure ratio 80/20, where the maximum motor speed was set to 3700 rpm. For pressure ratio 65/30 the maximum motor speed was set to 3800 rpm. Points for high speed and high pressure ratio has to be run on a later stage as the rig has been transported to Norway and at NTNUs labs in Trondheim where sufficient power supply is on place.

Further on the line for 80/20(—●—) in figure 17 show a slightly better efficiency at motor speeds above 3250 rpm in comparison to pressure ratio at 30/65 bar which shows a more strongly decreasing trend at higher rpm. It is also indicated that the top point for the highest pressure ratio is between 3000 and 3500 rpm. In the measurements the peak for 20/80 bar is at 3000 rpm with an overall efficiency at 68.2%. Maximum calculated efficiency value for 110/30 and 30/65 is at 71.4% and 72.8%, respectively.

RPM	Pressure ratios followed by η_{is} and $\delta\eta_{is}$						
	80/20		110/30		65/30		
800	52.40	$\pm$ 0.59	60.4	$\pm$ 0.52	66.0	$\pm$ 0.87	%
1000	51.86	$\pm$ 0.68	62.4	$\pm$ 0.47	68.4	$\pm$ 0.78	%
1500	61.5	$\pm$ 0.90	68.4	$\pm$ 0.42	72.8	$\pm$ 0.64	%
2000	65.5	$\pm$ 0.40	71.2	$\pm$ 0.39	73.5	$\pm$ 0.56	%
2500	67.2	$\pm$ 0.37	72.5	$\pm$ 0.37	72.9	$\pm$ 0.51	%
3000	68.2	$\pm$ 0.35	-	-	69.9	$\pm$ 0.46	%
3500	67.2	$\pm$ 0.35	-	-	64.4	$\pm$ 0.41	%
3700	64.4	$\pm$ 0.30	-	-	-	-	%
3800	-	-	-	-	59.3	$\pm$0.36	%

Table 5: The calculated isentropic efficiency with calculated uncertainties as the percentage value of deviation

The uncertainties in the calculated efficiency values are viewed in table 8 for all the different pressure ratios and motor speeds, and listed as the value of deviation $\delta\eta_{is}$. The uncertainties are at a maximum of ±0.56% of the total, which for the maximum efficiency given by —●— in figure 17 yields 72.94% at minimum and 74.06% at maximum.

4.2 VOLUMETRIC EFFICIENCY

The volumetric efficiency is viewed in figure 18 for the same pressure ratios. As expected the highest pressure ratio causes the highest volumetric loss and has a maximum volumetric efficiency at 69.1% for motor speed at 3000 rpm. From equation 12 the following are used for volumetric efficiency.

$$\eta_{vol} = \frac{\dot{m}_{tot}}{\rho_{R-744} V_s \omega} \tag{20}$$

For pressure ratio at 65/30 bar(—●—) the volumetric efficiency stays above 80% from 1500 to 3500 rpm, and has a peak point at 2500 rpm where the volumetric efficiency is at 83.1%. For all the pressure ratios it is an indication that the highest volumetric efficiency is between 2500 and 3000 rpm, whereas the gradient shows to be steeper at slower rpm compared to motor speeds above 2000 rpm. The oil circulation rate (OCR) has been a concern in the compressor, which strongly affects the volumetric efficiency. In initial tests the oil circulation showed to vary between 5% and 1.5% of the total mass flow in the circuit at 2500 rpm and pressure ratio of 80/32 bar for different oil levels[1]. The replacement of the

1 Graph in appendix D

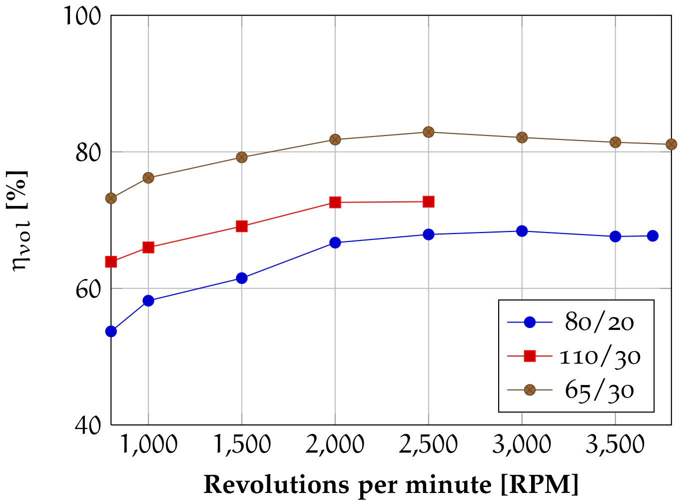

Figure 18: Volumetric efficiency at varying rpm

piston rings, and an additional ring between the motor and compressor, as described in chapter Chapter 2 was done and the measurements resulted as shown figure 19.

As figure 19 shows, the maximum OCR in in the discharge stream are at 1.46% at 80/20 bar pressure ratio and 3500 rpm. There are indications that that shows an increasing OCR for a pressure ratio of 110/30 bar, where the gradient is relatively high compared to the two other ratios, and until the maximum power consumption at 2500 rpm the OCR increases from 0.07% for 1500 rpm to 1.21% at the top. A more stable trend can be noticed for the ratio of 65/30 bar, where the gradient is relatively low, and seems to decrease and stabilize at higher speeds.

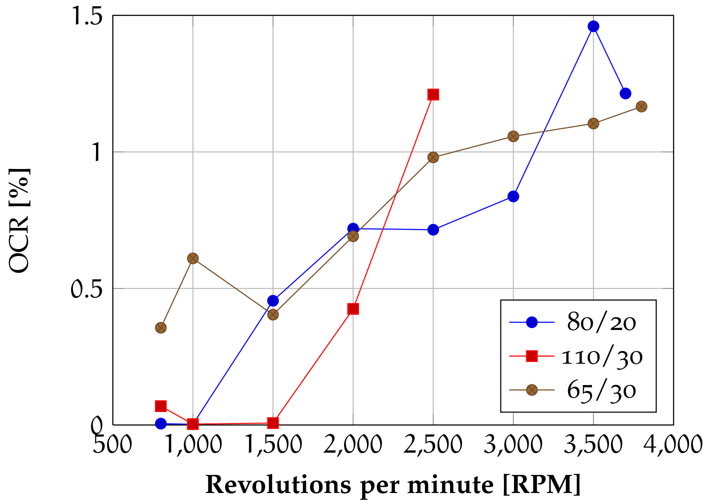

Figure 19: The oil circulation rate for 3 different pressure ratios

RPM	Pressure ratios followed by η_{vol} and $\delta\eta_{vol}$						
	80/20		110/30		65/30		
800	53.7	± 0.19	63.9	± 0.68	73.2	± 0.40	%
1000	58.2	± 0.19	66.0	± 0.28	76.2	± 0.40	%
1500	62.2	± 0.15	69.1	± 0.26	79.2	± 0.36	%
2000	66.7	± 0.17	72.6	± 0.39	81.8	± 0.43	%
2500	67.9	± 0.62	72.7	± 0.68	82.9	± 0.46	%
3000	68.4	± 0.45	-	-	82.1	± 0.35	%
3500	67.6	± 0.62	-	-	81.4	± 0.29	%
3700	67.7	± 0.55	-	-	-	-	%
3800	-	-	-	-	81.1	±0.38	%

Table 6: The calculated volumetric efficiency with calculated uncertainties as the percentage value of deviation

The accuracy of calculated volumetric efficiencies show to be quite high, as shown in table 6. Here the maximum deviation is calculated to $\delta\eta_{vol}$=0.68%.

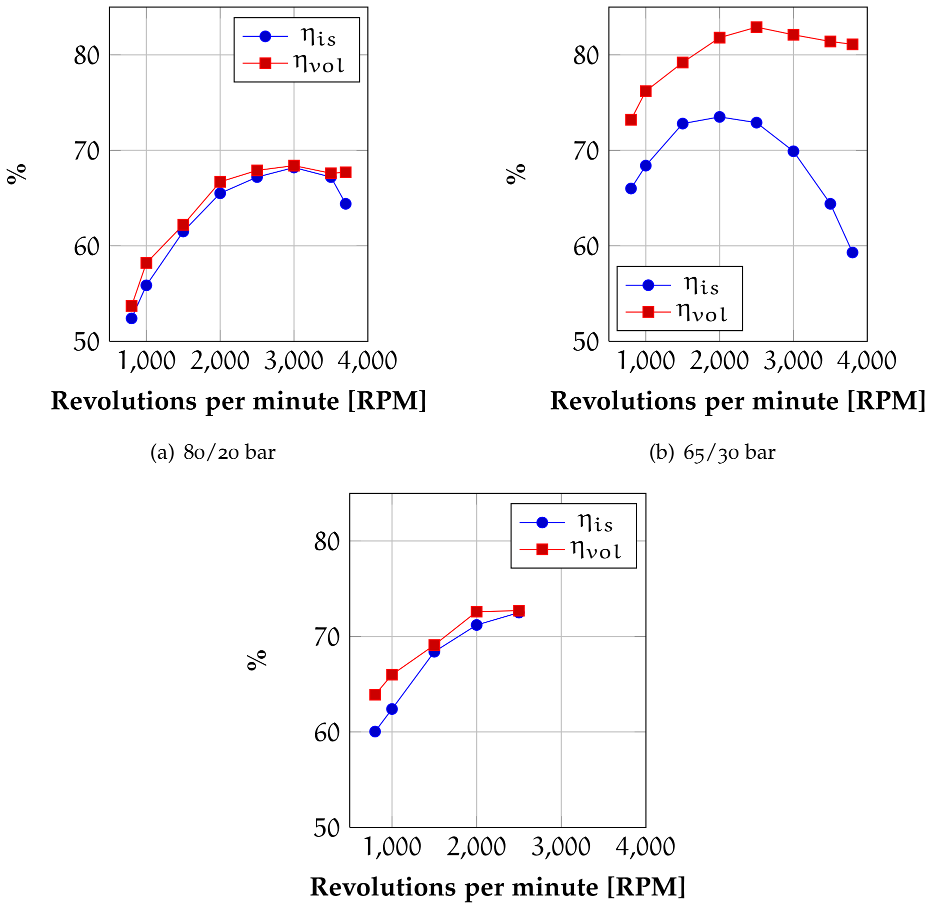

(a) 80/20 bar

(b) 65/30 bar

(c) 110/30 bar

Figure 20: Compariosn of volumetric and isentropic efficiencies.

4.2.1 *Indicator diagram*

The cylinder pressure was measured with dynamic pressure transducers at a rate of 1.665×10^{-5} seconds, in two cylinders. For a motor speed of 800 revolutions per minute this yields 4503 measurements for each revolution which takes 0.075 seconds, and the indicator diagrams are plotted for one full cycle.

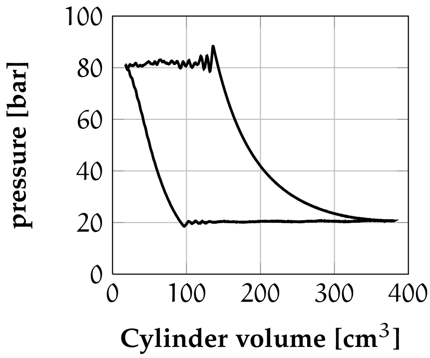

(a) 800rpm 80/20 bar

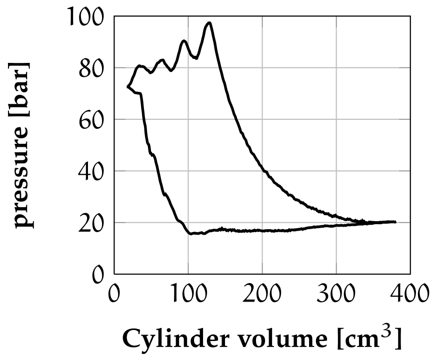

(b) 3700 rpm 80/20 bar

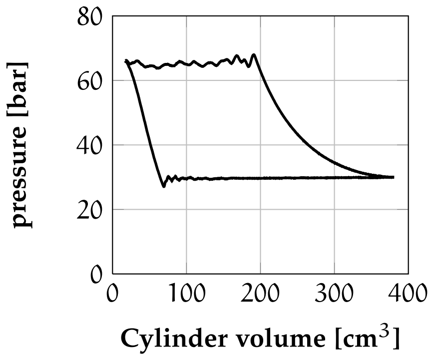

(c) 800 rpm 65/30 bar

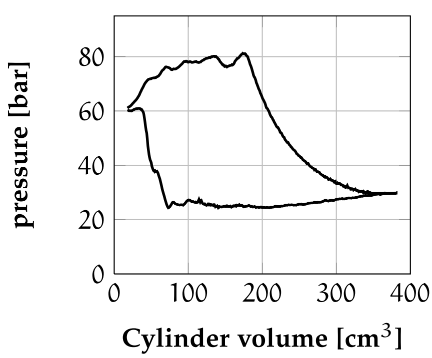

(d) 3800 rpm 65/30 bar

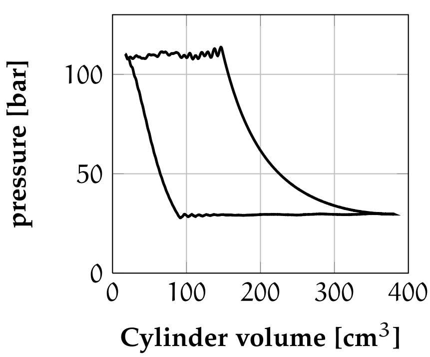

(e) 800 rpm 110/30 bar

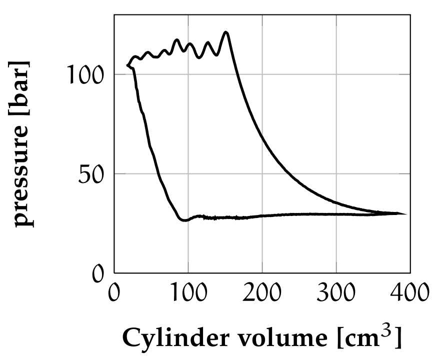

(f) 2500 rpm 110/30 bar

Figure 21: Measured indicator diagram with the suction- and discharge chamber pressures at varying motor speed and pressure ratios

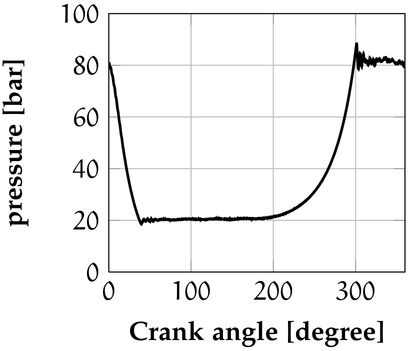

(a) 800rpm 80/20 bar

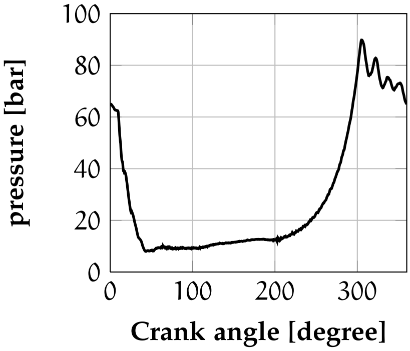

(b) 3700rpm 80/20 bar

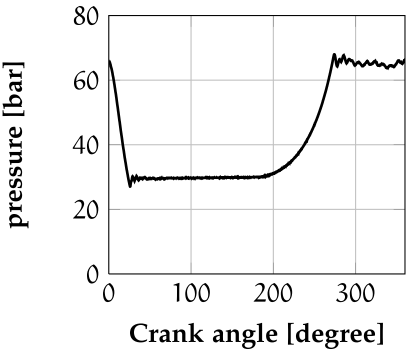

(c) 800 rpm 65/30 bar

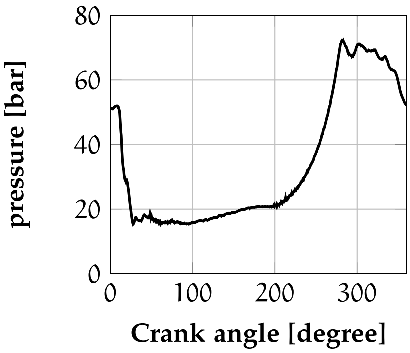

(d) 3800 rpm 65/30 bar

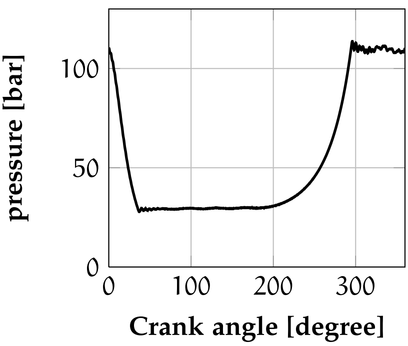

(e) 800 rpm 110/30 bar

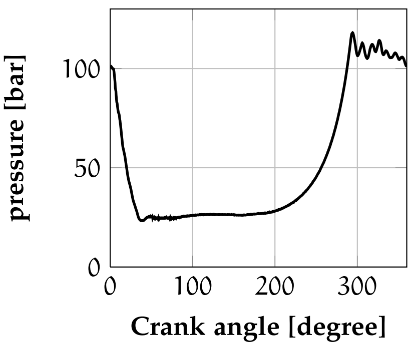

(f) 2500 rpm 110/30 bar

Figure 22: Measured suction- and discharge chamber pressures versus crank angle at varying motor speed and pressure ratios.

Figure 21 shows the indicator diagrams for the maximum and minimum motor speed for each of the pressure ratios, where the left side has 800 rpm and the right side shows the maximum speed for the respective pressure ratio. The clearance volume is at 4.5% which for the total cylinder volume yields 17.1 cm^3 as the total clearance volume. In the measurements there were no indicator or output device showing when the piston was at TDC or BDC, and for the plotting of the diagram it was necessary to guess on where the top and bottom of the cylinder was in the measured results, which in turn, can be source of some inaccuracy in the diagrams.
The highest motor speeds had between 900-1000 measurements for each round, which is noticeable in the diagrams (b) and (d) where the speed were 3700 and 3800 rpm. Still the indication is that the high speed diagrams show a tendency to late closure and opening of suction and discharge valves.

The peak at the point where the discharge valve opens shows a higher cylinder pressure than the discharge pressure, as expected. Also the peak at the bottom when the suction valve opened was expected due to cylinder pressure below the suction pressure. At BDC the tendency is a slow closing of the suction valve, causing the line to follow a near constant pressure before the valve shuts and the pressure builds up.

There are some fluctuation of the pressure in the discharge, shown as a variation in pressure on the high pressure side of the diagram. However this is most symptomatic in the beginning, and gradually diminishes as the piston is closing up to the TDC. Some fluctuations are also seen at the suction as the suction valve opens, but it is not in the same amount as on the discharge. As the piston is going in return from the TDC the pressure is decreasing, but at the very top of the stroke some small symptoms of late closure can be noticed even for speeds at 800 rpm.

On higher speeds it seems that the fluctuation on the discharge has decreased, it is still lasting throughout the discharge, with a peak also here in the beginning as the valve opens. However, the impact is greater causing higher peaks. Compared to a slower speeds it is more evident that the pressure lies on a near constant line as the piston leaves TDC. This is also seen in the BDC, where the pressure increase is delayed. As the suction valve opens, the fluctuation is no longer seen as noticeable in the high speed, and the pressure looks more or less linear until TDC is reached.
In 22 the suction and discharge pressure was plotted in against the crank angle, and it is easier to see the difference in fluctuation in the discharge area for the high and low speeds. The impact is much greater as the speed is higher, and especially where the pressure ratio was at 80/20 bar with a motor speed at 3700, the impact of the fluctuation was really noticeable. Also at motor speed of 3800 the uneven line in the suction area was distinctive and shows a fluctuation and pressure drop in the suction chamber.

4.2.2 *Temperature variation*

Temperature variation in the discharge gas in the different pressure ratios are displayed in figure 23.

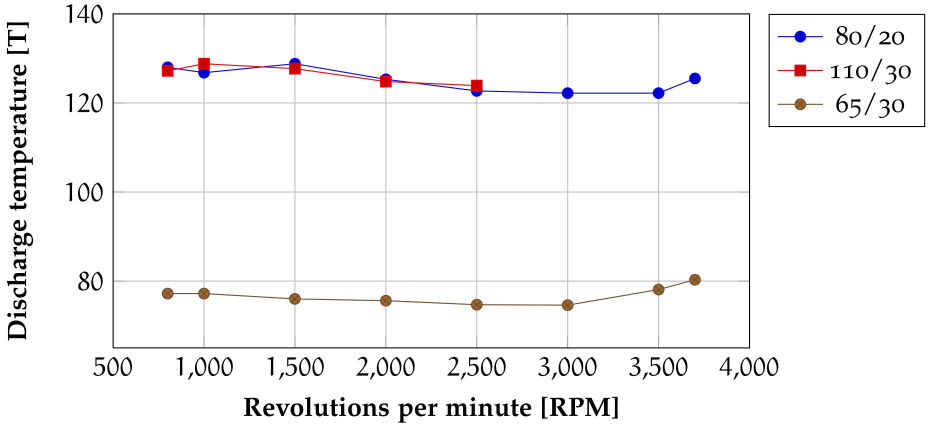

Figure 23: Variation in the discharge temperature at different pressure ratios for variation in motor speed

As for the highest discharge pressures the temperature was at 128.0°C and 128.8°C for 80 and 110 bar, respectively. For 65 bar discharge pressure the temperature was at 80.3°C. There is a pressure difference at 30 bar between the two discharge pressures with highest discharge temperatures, however, since the pressure ratio of 80/20 is higher, the discharge temperatures follows near to the same line.

4.3 FREQUENCY CONVERTER

For a pressure ratio at 65/30 and a motor speed at 3800, the inlet power consumption to the frequency converter was at 92.67kW, whilst the power out of the converter was at 86.14kW, hence there was efficiency at acceptable 93%. However this efficiency showed to be inconsistent, and as figure 24 shows, the frequency converter efficiency varied between 85.3% at the lowest and 93% at the highest.

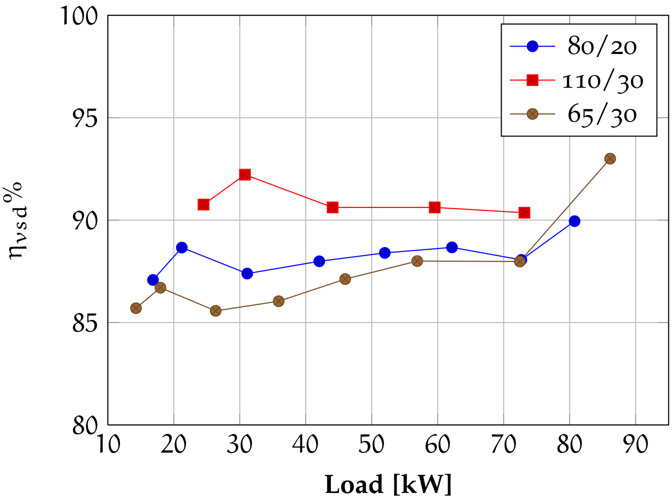

Figure 24: Efficiency for the danfoss frequency converter for variation in the motor load

Figure 24 also shows that the efficiency is increasing as the load from the motor increases, and from 72 - 86 kW in load the efficiency rises with 5% for a pressure ratio of 65/30 bar. For all of the measurements there are a local top point at 1000 rpm, before it decrease when the motor speed is at 1500 rpm. Here it has, for all three pressure ratios, its lowest efficiency, at 90.62%, 87.39% and 85.57%. The maximum input power to the converter was 92.62kW, at 65/30 bar.

5 DISCUSSION

All the results which are presented in Chapter 5 were executed at Obrists facilities over a time period of 3 days, and the executed tests were therefore very roughly picked out with respect to represent the span of the compressor which it can work in. Later executions will doubtfully work with different pressure ratios and also higher motor speeds, but the presented results give a rough estimate of what the compressor is capable for. The main objective with the experiments was to determine how the compressor was performing under certain conditions. In this matter the most interesting results are how energy economic it was, thereby the isentropic efficiency along with the volumetric efficiency is of most interest.

5.1 ISENTROPIC EFFICIENCY

Obirst engineering has done a series of experiments of some "on the shelf" compressors available to the marked today, to have some reference points regarding which efficiencies are acceptable in such a test campaign. Figure 25 shows the values for two different commercially available compressors running at 1500 rpm, 80 bar discharge pressure 10K superheat and varying compressor ratio plotted against the Obrist / SINTEF compressor running with the same conditions with motor speeds from 1000 to 2500 rpm.

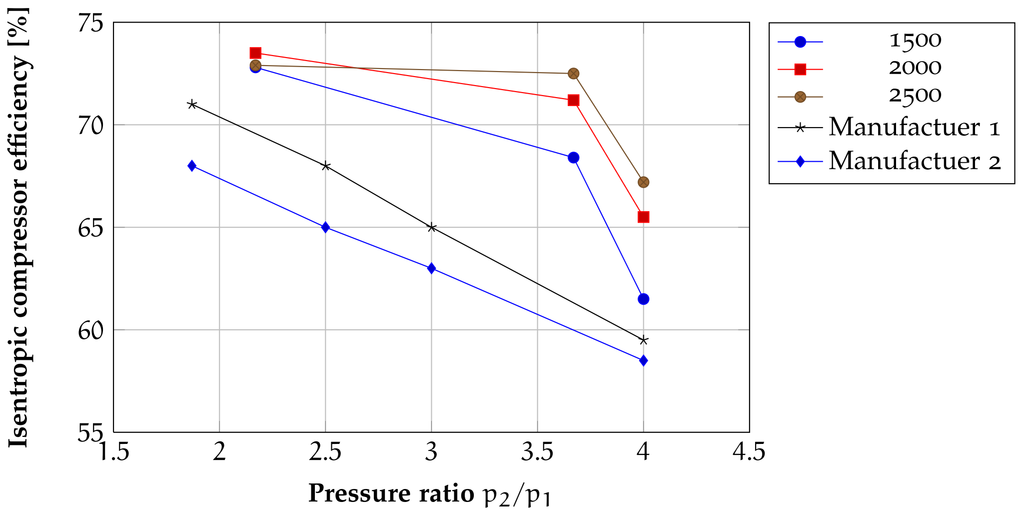

Figure 25: Comparison of efficiencies with 2 different on the shelf compressors available on the marked today, running at 1500 rpm with discharge pressure of 80 bar and 10K superheat

The test results show promising results in comparison with the given compressors, where the results from chapter 4 shows to be satisfying in view of energy efficiency. These data are also presented at the Gustav Lorenzen Conference On Natural Refrigerants in June 2012, where it was emphasized that much of the improvement in efficiency was due to the use of a permanent magnet motor[8]. However, as the reference lines has a near linear negative trend against higher rpm, the Obrist / SINTEF compressor shows to be more stable, at pressure ratios up to 4, which implies a relatively robust compressor for handling pressures and speeds within a pressure and flow interval, which is of great use in an industry cooling application. Further on, improvements in the compressor arrangement are still to be expected, and the presented test results reveal some indications on the general performance of the compression cycle.

For the isentropic efficiency the trend is a steep negative gradient as the rotational speed increase, and figure 17 shows a descending line for both 80/20 bar as well as 65/30 bar. This trend is more visible in figure 20 (b), where the steepness is near dramatic from 2500 to 3700 rpm. For justification purposes it is predictive to compare the p-V diagrams on the right with the same diagrams on the left in figure 21, where it is evident that there is a high increase in fluctuation and pressure build-up for the high rotational speeds. The work lost from this fluctuation is defined by $\int dp dV$, and every build-up and fluctuation in pressure will cause excessive work for the compression cycle.

5.2 VOLUMETRIC EFFICIENCY

Volumetric losses greatly influences the capacity and energy efficiency, and as expected the volumetric efficiency is strongly dependent on the pressure ratio, which is evident from figure 18 where the best volumetric efficiency is present at pressure ratio of 65/30 bar. In addition, as the speed of the motor increase the volumetric efficiency flattens out for all of the three pressure ratios.

A reason for the increasing losses at higher pressure ratios could be the clearance volume of 4.5%, which is relatively small, but for a compressor this size the actual volume of 17.1cm^3 is quite high, which in turn affects the volumetric efficiency as seen in figure 11. Also in figure 18 it is strongly indicated that a high difference between suction and discharge pressure affects the volumetric efficiency negatively. As the rotational speed increase, the curves for volumetric efficiency also flatten out, and seem to stay at a more efficient working point. One possible reason for this was discussed in chapeter 2 where it was argued that the efficiency of the motor increase as the load increase, until a certain point. Thus the heat loss in the motor decrease and the contribution from the motor to add extra super heat to the suction gas is less dominating, which in turn affects the volumetric efficiency.
An additional effect to the volumetric efficiency can be shown in figure 20 (a) which shows the difference between volumetric and istentropic efficiency for pressure ratio of 80/20 bar. Here the trend is that the difference between the two values are relatively small, compared to the same graph for 65/30 bar. One reason for this is most likely that the pressure difference from suction and discharge is at 60 bars for 80/20, whilst the difference for 65/30 is 35 bars. Thus the gas leakage from high pressure side to low pressure side of the piston is more likely to occur at high pressure ratios. There has been a change of piston rings in the compressor, as discussed in chapter 2, but from the test results it is plausible that the leaking trend is still of concern, in particular for high pressure ratios. An amplifying effect could also be the high discharge temperature causing the specific gas volume to decrease, and the gas to slip past the piston rings more easy.

5.2.1 *Valve loss*

The total indicated word, $P_{indicated}$, for high rpm are much higher than for low rpm. From figure 25 this is evident.

It is seen a larger pressure build-up in the high speed ranges, than in a low speed range. In the suction this is not as critical as in the suction. Main reason for this may be a too small valve area, and from the looks of figure B.32(a) it is seen that the valve is kept open for a longer period, with less fluctuation, which can be caused by small passage area for the discharge gas. With a higher valve

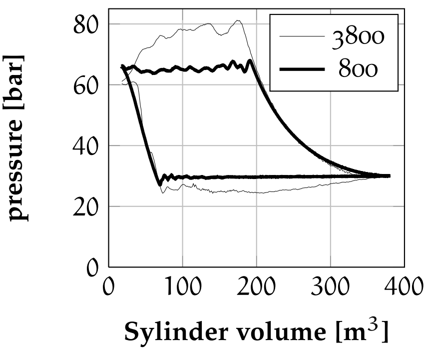

(a) 65/30 bar

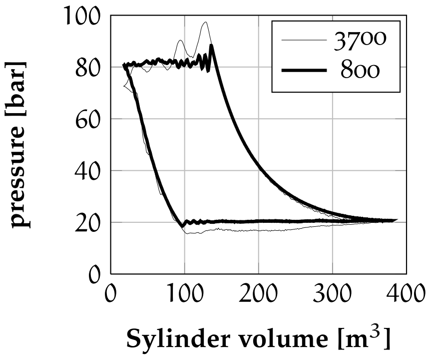

(b) 80/20 bar

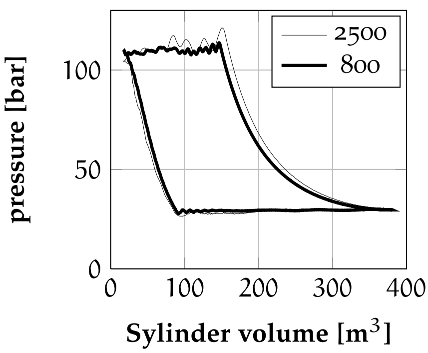

(c) 110/30 bar

Figure 26: Plot of indicator diagram in the same figures for 3 different pressure ratios

area, more room in the passage would have caused for smaller pressure in the cylinder discharge port. It is also seen that the compression line is near isentropic for all 3 of the plots. Discharge is not big losses in any of the plots, however this is also decreasing at lower speeds.

5.2.2 *Oil Circulation Rate*

In earlier tests there has been a high value of oil circulation rate in the system, these test results however, indicates an oil reduction in the main flow, and a peak point of 1.5% at the highest pressure ratio. Though, it also shows a decrease on OCR at speeds from 3500 to 3700 rpm. It should be noted that the oil flow from the oil separator was not constant, but rather a product of an on/off valve responding to the oil level in the separator and it is very plausible that a test campaign with longer log intervals would have shown some different results. i. e. a running test of 10 minutes would give a more reliable result with concern to calculate an average value in the oil flow.

80/20 BAR, 1000 RPM	VALUE	DEVIATION
Total mass flow R-744	653 kg/h %	± 0.30%
Total measured oil flow	0.027 kg/h	± 68.10%
Oil circulation rate	0.0042%	68.07%

Table 7: Uncertainty results for pressrue ratio of 4 and 1000 rpm[1]

Table 7 shows the accuracy of oil flow measurement and the calculated OCR value, and it is evident that the results are not reliable in a scientific aspect. A possible solution to get reliable results from the oil measurements would be to add a flow regulator on the line, and disable the on/off valve. In addition it would have to be added a series of level emergency stops in LabView to avoid insufficiency of oil in the compressor. As for now, the oil flow is directed in to the crankcase with a copper tube and connected with a quick coupling. A fast solution to install a flow regulator is therefore to add the valve at the end of the tube, and redirect the oil through a new tube in to the compressor. The regulation of flow in this case would have to be done manually by the operator.

5.2.3 *Improvement in the oil separation*

Even though the results may seem inaccurate, earlier test results show that it might be a too high value of oil in the main mass flow.[2] Some alternative solutions were therefore proposed to SIETF and OB as methods for increasing the

2 Appendix D

droplets removal in the main suction gas stream. Two improvements were presented:

1. Improve the flow pattern in the suction by adding descending traces in the motor, forcing the gas to leave in a backwards direction due to centrifugal forces.
2. Replace the "hamster wheel" with a method, currently under investigation at NTNU Trondheim[3], showing great potential in the oil and gas industry for removing droplets in natural gas flows.

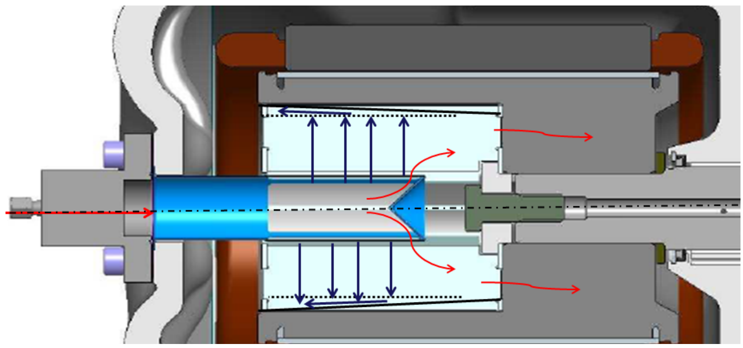

Figure 27: Draft sketch of the first proposal for improvement of the oil droplets removal in the suction gas

Proposal nr 1 is viewed in figure 27 as a sketch, and shows that the walls are descending backwards, instead of being parallel to the direction of the gas flow. This will cause the oil droplets which are sent against the wall from the hamster wheel to be forced in a backwards direction by the centrifugal force. Also the proposal is sketched with an extra drum penetrated with several holes (like in a washing machine) fitted with a clearance to the wall. Its purpose is to keep flowing gas from being contaminated with oil and bring it further and in to the suction chamber. The second proposal is a combination of the proposal nr. 1, and a replacement of the hamster wheel. The idea is to use an arrangement that has been tested at NTNU Trondheim and proved very promising results for droplets removal in the oil and gas industry.

3 INNSEP, http://folk.ntnu.no/cadorao/

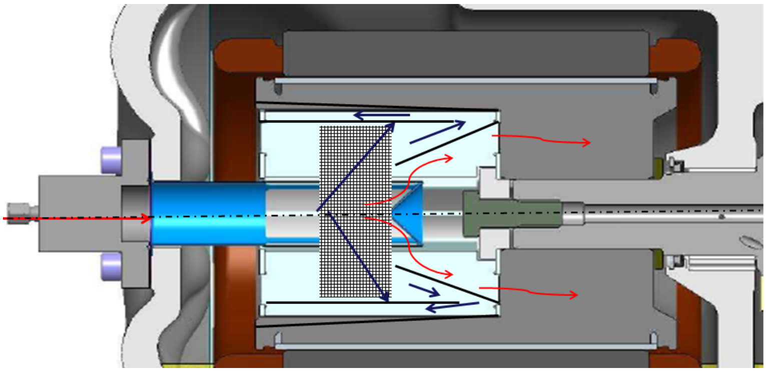

Figure 28: Draft sketch of the second proposal for improvement of the oil droplets removal in the suction gas

In figure 28 there is placed a rotating wire mesh in the inlet section. The thought is that the rotation of the mesh causes the oil droplets to be thrown to the edges, which also are spinning and further that the oil is forced backwards and further to the oil sump. In the proposal there was also added a splitting construction meant to force the oil and gas on either sides, whereas the gas is shown with red lines and the oil is sketched with blue lines.
The wire mesh was thought to be rotating, either by attaching it to the shaft of the motor, or by implementing a propeller in the gas flow which, by the help of the gas stream, rotates at a slower speed than the motor.

Wire mesh is currently a field of study at NTNU Trondheim, and has shown great potential. It can be made of several materials, catch droplets in all different sizes and experiments has shown that it is up to 100% effective in droplets removal.

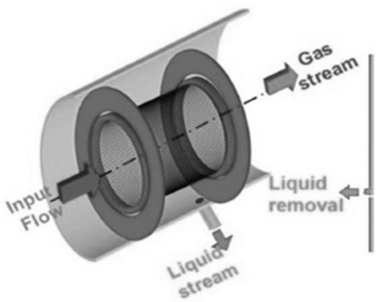

Figure 29: Sketch of the wire mesh functionality, where contaminated gas is at the inlet section of a rotational mesh

Figure 29 is given in a presentation from Innsep [4], and is a sketch of the functionality of the mesh is viewed. The experiments conducted has resulted in near 100% efficiency at the highest speed at 20 Hz, which yields 1200 rpm[5].

5.3 FREQUENCY CONVERTER

The reason for measurements of the frequency converter efficiency was to qualify the variable speed drive (Danfoss Da31F4867), and its performance. It was delivered by Danfoss with guarantees of a stable efficiency at 95%. This was, however, not the case.[6]

For the compressor as a commercial product it is crucial to maximize the efficiency also of the VSD in order to sell a high efficient compression package. Here the Danfoss package shows a tendency to increase in efficiency at higher loads, as argued in figure 5, thus there might be some adjustment possibilities in the settings. A further evaluation of the drive can be taken in to consideration, possibly in cooperation with Danfoss.

4 http://folk.ntnu.no/cadorao/
5 From personal contact with INNSEP
6 Personal discussion with Roman Laesser

6 CONCLUSION

An analysis of piston compressor losses and a view on which factors that are of interest to evaluate in a testing campaign for reciprocating compressors has been conducted. The rig made by Obrist Engineering in Austria is fitted with possibilities to test compressors up to 100kW electrical power and 400kW cooling capacity, and has multifunctional testing possibilities. The first test results for a 100kW 6 cylinder newly developed piston compressor have been presented and discussed.

6.1 OVERALL EFFICIENCY

The test campaign showed overall compressor efficiencies up to 73.5%, and at a wide range of motor revolution speeds it showed a relatively high efficiency. I.e for lower pressure ratios the compressor shows a really favourable trend, and at pressure ratio at 65/30, the overall efficiency stays above 70% from 1500 to 3000 rpm. In comparison with an on the shelf compressor the newly developed SINTEF/OE compressor is showing great potential, and within a cooling application it will have the ability to deliver high pressures and high flows at a higher efficiency than what is experienced today. For a fishing vessel, where also weight is an issue, its capabilities will be of interest in the marked. Also typically in cooling applications in supermarkets, where the effect is quite high the compressor will be a good replacement for smaller compressors used to day.

6.2 VOLUMETRIC EFFICIENCY

Some factors regarding losses have been pointed out, and at high pressure ratios there are indications that there is a gas leakage past the piston rings. In addition the clearance volume of 17.1cm^3 is quite high, and causes a negative trend for the volumetric efficiency. This despite that the clearance volume is not particularly big, with its 4.5%. It is the sheer size of the cylinder that causes the high value of clearance volume.

6.3 OIL CIRCULATION

The oil circulation rate (OCR) is shown, but since the accuracy of the measured value is low due to the valve arrangement with an on/off valve responding to the filling level in the oil separator, some more experiments should be done before a conclusion is drawn. It is possible to implement a flow regulator, which controls the flow and keeps it constant.

If further experiments show a high grade of oil in the gas flow, it is possible to look into alternative solutions in the oil droplets separation unit. Two possible methods are presented as sketches, where one focuses on making the wall arrangement nonlinear to the flow direction, and the other focuses on changing the hamster wheel with a high efficient rotating wire mesh.

6.4 FREQUENCY CONVERTER

The frequency converter has shown a too low efficiency compared to promise from the vendor. This issue can be solved in a dialogue with Danfoss, or by replacing it. Further commercializing the compressor package should be presented with a VSD working under its maximum potential.

7 FURTHER WORK

This chapter serve as a point wise summary of advices for further work within the experimental investigation of the compressor, as well as the test rig.

EXPERIMENTAL INVESTIGATION OF THE COMPRESSOR

1. It was argued that the oil flow in the rig was not optimal with regards to measuring the accurate flow. A further study with longer time intervals are recommended.
2. If the studies in point 1 show a too high OCR value, a study of new possibilities for removing oil droplets in the inlet gas stream can be taken in to consideration. As for the wire mesh it has never been tested in the required high velocities earlier, and this can be a topic of interest. Also the backwards descending flow passage in the motor can be a topic of further study.
3. For further testing of higher motor speeds, a reliable high power source capable of delivering 100kW is needed.
4. The new valve system custom made by Obrist Engineering is an exciting feature, and will in future experiments be of great interest.
5. In these experiments heat loss was to be measured roughly with a thermo camera. This was how ever not possible to conduct due to a missing camera in the labs of NTNU. For future work a investigation on where the camera is will be necessary before heat loss can be made visible.
6. The compressor has 6 cylinders, and with the uniform shape it has there should not be a big impact on the overall performance from pulsations, but for future experiments this is also a topic of interest. Both analytical and experimental.
7. The test data from the operations described in chapter Chapter 4 was a result of too little time, and the set points were not logged for more than 50-100 sec, with 1 measurement each second. For continuing experiment, a longer time interval i. e.15 seconds and longer test period ,i. e.10 min, can be an advantage in terms of see if the system is stable.

THE TEST RIG

1. These test results have in main part been conducted in a superheated area only, and the test facility and calculation sheet have been adapted to this experiments and works very good. However, the rig is quite complex and several cycles are possible to run. One test result has been collected from a full cycle test, which also showed satisfactory results, but the adoption of

the calculation sheet for several cycles will need more work. For multiple long term test campaigns running in parallel a sheet where the switch between different cycles is easily done would be an advantage. The best solution here will most likely be to use a macro.

2. There has been written a report on documenting the calculations, but the sheet has e massive extent, and calculations of performance data and uncertainties makes room for minor errors in the calculations. Therefore a thoroughly quality insurance and a documentation of the calculations when the sheet is more complete would be of interest for everyone using it for different kinds of test in the rig.

Part III

APPENDIX

A
TEST RESULTS AND UNCERTAINTIES

RPM		80/20		110/30		65/30		[bar]
800	T_{suct}	-10.1	± 0.12	5.5	± 0.13	5.2	± 0.05	°C
	T_{disch}	128.0	± 0.09	127.2	± 0.07	77.2	± 0.05	°C
1000	T_{suct}	-10.8	± 0.18	6.5	± 0.04	5.0	± 0.03	°C
	T_{disch}	126.8	± 0.04	128.8	±0.10	77.2	± 0.03	°C
1500	T_{suct}	-10.1	± 0.05	5.1	± 0.07	5.7	± 0.02	°C
	T_{disch}	128.8	± 0.04	127.7	±0.06	76.0	± 0.06	°C
2000	T_{suct}	-9.9	± 0.01	4.7	± 0.01	5.3	± 0.07	°C
	T_{disch}	125.3	± 0.04	124.8	±0.05	75.6	± 0.07	°C
2500	T_{suct}	-10.6	± 0.02	3.5	± 0.06	5.0	± 0.04	°C
	T_{disch}	122.7	± 0.05	123.9	±0.08	74.7	± 0.04	°C
3000	T_{suct}	-10.4	± 0.03	-	-	4.4	± 0.01	°C
	T_{disch}	122.2	± 0.05	-	-	74.6	± 0.03	°C
3500	T_{suct}	-10.4	± 0.03	-	-	4.4	± 0.01	°C
	T_{disch}	122.2	± 0.05	-	-	78.1	± 0.03	°C
3700	T_{suct}	-9.3	± 0.02	-	-	-	-	°C
	T_{disch}	125.5	± 0.04	-	-	-	-	°C
3800	T_{suct}	-10.4	± 0.03	-	-	4.5	± 0.05	°C
	T_{disch}	122.2	± 0.05	-	-	80.3	±0.05	°C

Table 8: Uncertainty in the results with 3 different pressure ratios

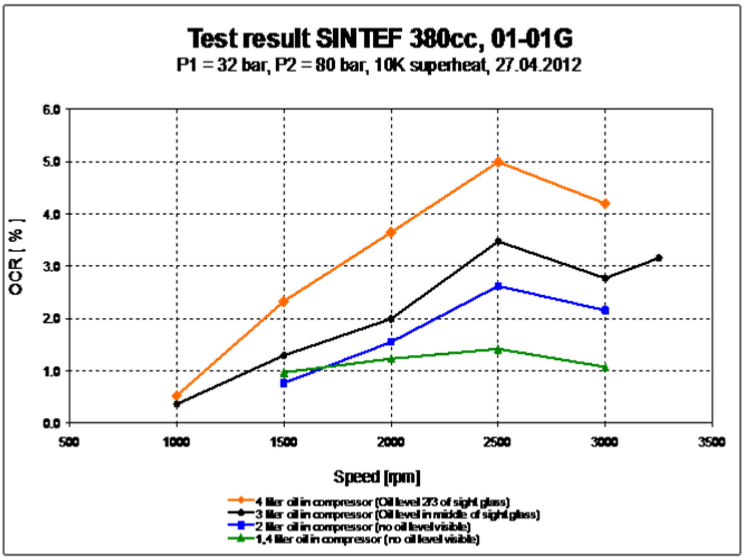

Experiments from Obrist, done as initial to see the performance of the oil flow:

Experiment no: 4
Date: 22.05.2012
Operator: Obrist/Roman
Mode: comp.test 800 rpm
Measured points 84

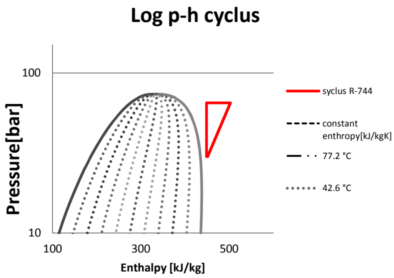

Components		Description
Compressor		Piston compressor
Gascooler/condenser		Air fan
Gasscooler condenser		Water to sink
Gascooler/condenser	4a/b	Heat to glycol
Internal heat exhanger		
Evaporator	6a/b	R-774/glycol
Separator		
Oil separator		

System performance

				Total Deviation	Total uncertainty	Comment
COP	-		1.0	± 0.02	1.90 %	
Compressor Speed		[rpm]	800	± 1.60	0.2 %	
Mass flow R744		[kg/h]	987	± 2.04	0.2 %	
Mass flow water/ethyleneglycol		[kg/h]	0.0	± 0.00	15.0 %	
Ambient temperature		[°C]	20.3	± 0.07	0.4 %	
Supply power		[kW]	16.7	± 0.03	0.2 %	
Power consumtion compressor		[kW]	14.3	± 0.18	1.2 %	
Danfoss VSD efficiency			85.51 %	± 0.01	1.26 %	
Volumetric efficiency			73.2 %	± 0.40 %	0.54 %	
Isentropic efficiency			66.0 %	± 0.87 %	1.32 %	
Oil cirkulation rate (OCR)			0.3568 %	± 0.873 %	117.81 %	Uncertainty high due to on/off valve
Heat rejection		[kW]	14.7	± 0.06	0.4 %	
Cooling capasity		[kW]	0.0	± 0.00	0.0 %	
Pressure, evaporator, inlet		[bar]	62.7	± 0.16	0.3 %	
				0.00		
Pressure, throttle valve,in		[bar]	65.2	± 0.16	0.3 %	
Temperature, throttle valve, in		[°C]	42.6	± 0.06	0.1 %	
Temperature, throttle valve out		[°C]	-1.3	± 0.03	2.0 %	

Compressor

			Total Deviation	Total uncertainty	Comment
Inlet suction pressure	[bar]	30.1	± 0.08	0.3 %	
Inlet temperature	[°C]	5.3	± 0.05	1.0 %	
Inlet super heat	[K]	10.7	± 0.05	0.5 %	
Outlet pressure	[bar]	65.1	± 0.16	0.3 %	
Outlet temperature	[°C]	77.2	± 0.05	0.07 %	
Pressure ratio	[-]	2.2	± 0.008	0.4 %	
Lubricant return mass flow rate:	[kg/h]	3.5	± 4.18	118.2 %	on/off valve
Temperature, lubricant return:	[°C]	48.6	± 0.70	1.4 %	
Compressor Speed	[rpm]	800	± 1.60	0.2 %	
Torque	[Nm]	171	± 2.16	1.3 %	
Power consumption	[kW]	14.3	± 0.18	1.2 %	
Massflow R-744	[kg/h]	987	± 2.04	0.2 %	
Specific volume (suction line)	[m3/kg]	0.01	± 0.00	0.2 %	
Density CO2 (suction line)	[kg/m3]	74.1	± 0.12	0.2 %	
Volumetric efficiency	[%]	73.2 %	± 0.40 %	0.54 %	
Isentropic efficiency	[%]	66.0 %	± 0.87 %	1.32 %	

Experiment no: 4
Date: 22.05.2012
Operator: Obrist/Roman
Mode: comp.test 3800 rpm
Measured points 26

Components		**Description**
Compressor		Piston compressor
Gascooler/condenser		Air fan
Gasscooler condenser		Water to sink
Gascooler/condenser	4a/b	Heat to glycol
Internal heat exhanger		
Evaporator	6a/b	R-774/glycol
Separator		
Oil separator		

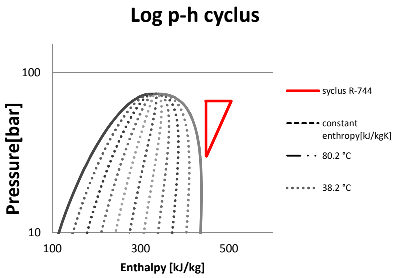

System performance

			Total Deviation	Total uncertainty	Comment
COP	-	1.0	± 0.01	0.81 %	
Compressor Speed	[rpm]	3800	± 7.60	0.2 %	
Mass flow R744	[kg/h]	5202	± 10.88	0.2 %	
Mass flow water/ethyleneglycol	[kg/h]	0.0	± 0.00	35.9 %	
Ambient temperature	[°C]	26.8	± 0.50	1.9 %	
Supply power	[kW]	92.4	± 0.49	0.5 %	
Power consumtion compressor	[kW]	86.2	± 0.40	0.5 %	
Danfoss VSD efficiency		93.28 %	± 0.00	0.42 %	
Volumetric efficiency		81.1 %	± 0.39 %	0.49 %	
Isentropic efficiency		59.2 %	± 0.36 %	0.60 %	
Oil cirkulation rate (OCR)		1.1645 %	± 0.357 %	31.41 %	Uncertainty high due to on/off valve
Heat rejection	[kW]	82.2	± 0.34	0.4 %	
Cooling capasity	[kW]	0.0	± 0.00	0.0 %	
Pressure, evaporator, inlet	[bar]	61.9	± 0.16	0.3 %	
			0.00		
Pressure, throttle valve,in	[bar]	60.6	± 0.15	0.3 %	
Temperature, throttle valve, in	[°C]	38.2	± 0.02	0.1 %	
Temperature, throttle valve out	[°C]	-1.3	± 0.03	2.0 %	

Compressor

			Total Deviation	Total uncertainty	Comment
Inlet suction pressure	[bar]	30.2	± 0.08	0.3 %	
Inlet temperature	[°C]	4.5	± 0.05	1.0 %	
Inlet super heat	[K]	9.8	± 0.05	0.5 %	
Outlet pressure	[bar]	66.5	± 0.17	0.3 %	
Outlet temperature	[°C]	80.2	± 0.04	0.06 %	
Pressure ratio	[-]	2.2	± 0.008	0.4 %	
Lubricant return mass flow rate:	[kg/h]	61.3	± 19.48	31.8 %	on/off valve
Temperature, lubricant return:	[°C]	72.4	± 0.11	0.2 %	
Compressor Speed	[rpm]	3800	± 7.60	0.2 %	
Torque	[Nm]	217	± 1.10	0.5 %	
Power consumption	[kW]	86.2	± 0.40	0.5 %	
Massflow R-744	[kg/h]	5202	± 10.88	0.2 %	
Specific volume (suction line)	[m3/kg]	0.01	± 0.00	0.2 %	
Density CO2 (suction line)	[kg/m3]	74.9	± 0.13	0.2 %	
Volumetric efficiency	[%]	81.1 %	± 0.39 %	0.49 %	
Isentropic efficiency	[%]	59.2 %	± 0.36 %	0.60 %	

Experiment no:	4
Date:	22.05.2012
Operator:	Obrist/Roman
Mode:	comp.test 800 rpm
Measured points	25

Components		**Description**
Compressor		Piston compressor
Gascooler/condenser		Air fan
Gasscooler condenser		Water to sink
Gascooler/condenser	4a/b	Heat to glycol
Internal heat exhanger		
Evaporator	6a/b	R-774/glycol
Separator		
Oil separator		

Log p-h cyclus

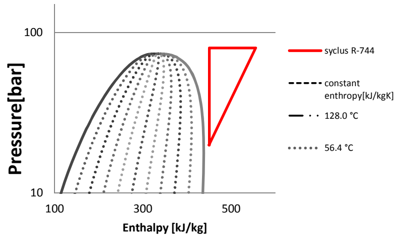

System performance

				Total Deviation	Total uncertainty	Comment
COP	-		0.8	± 0.01	1.64 %	
Compressor Speed		*[rpm]*	800	± 1.60	0.2 %	
Mass flow R744		*[kg/h]*	475	± 1.47	0.3 %	
Mass flow water/ethyleneglycol		*[kg/h]*	0.0	± 0.00	40.1 %	
Ambient temperature		*[°C]*	18.8	± 0.04	0.2 %	
Supply power		*[kW]*	19.4	± 0.04	0.2 %	
Power consumtion compressor		*[kW]*	16.9	± 0.18	1.1 %	
Danfoss VSD efficiency			87.08 %	± 0.01	1.11 %	
Volumetric efficiency			53.7 %	± 0.20 %	0.36 %	
Isentropic efficiency			52.4 %	± 0.59 %	1.12 %	
Oil cirkulation rate (OCR)			0.0051 %	± 0.585 %	79.34 %	Uncertainty high due to on/off valve
Heat rejection		*[kW]*	13.8	± 0.07	0.5 %	
Cooling capasity		*[kW]*	0.0	± 0.00	0.0 %	
Pressure, evaporator, inlet		*[bar]*	55.1	± 0.14 0.00	0.3 %	
Pressure, throttle valve,in		*[bar]*	80.6	± 0.21	0.3 %	
Temperature, throttle valve, in		*[°C]*	56.4	± 0.15	0.3 %	
Temperature, throttle valve out		*[°C]*	-1.3	± 0.02	1.9 %	

Compressor

			Total Deviation	Total uncertainty	Comment
Inlet suction pressure	*[bar]*	19.9	± 0.05	0.3 %	
Inlet temperature	*[°C]*	-10.1	± -0.12	1.2 %	
Inlet super heat	*[K]*	9.6	± 0.12	1.3 %	
Outlet pressure	*[bar]*	80.1	± 0.21	0.3 %	
Outlet temperature	*[°C]*	128.0	± 0.09	0.07 %	
Pressure ratio	*[-]*	4.0	± 0.015	0.4 %	
Lubricant return mass flow rate:	*[kg/h]*	0.0	± 0.02	79.3 %	on/off valve
Temperature, lubricant return:	*[°C]*	22.2	± 0.00	0.0 %	
Compressor Speed	*[rpm]*	800	± 1.60	0.2 %	
Torque	*[Nm]*	201	± 2.23	1.1 %	
Power consumption	*[kW]*	16.9	± 0.18	1.1 %	
Massflow R-744	*[kg/h]*	475	± 1.47	0.3 %	
Specific volume (suction line)	*[m3/kg]*	0.02	± 0.00	0.1 %	
Density CO2 (suction line)	*[kg/m3]*	48.4	± 0.06	0.1 %	
Volumetric efficiency	*[%]*	53.7 %	± 0.20 %	0.36 %	
Isentropic efficiency	*[%]*	52.4 %	± 0.59 %	1.12 %	

Experiment no: 4
Date: 22.05.2012
Operator: Obrist/Roman
Mode: comp.test 3700 rpm
Measured points 34

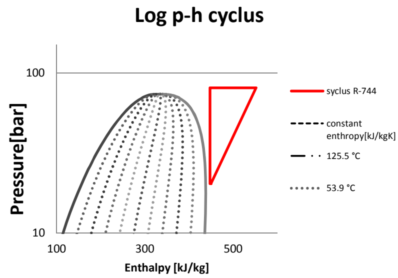

Components		Description
Compressor		Piston compressor
Gascooler/condenser		Air fan
Gasscooler condenser		Water to sink
Gascooler/condenser	4a/b	Heat to glycol
Internal heat exhanger		
Evaporator	6a/b	R-774/glycol
Separator		
Oil separator		

System performance

			Total Deviation	Total uncertainty	Comment
COP	-	1.0	± 0.01	0.70 %	
Compressor Speed	[rpm]	3700	± 7.40	0.2 %	
Mass flow R744	[kg/h]	2797	± 6.02	0.2 %	
Mass flow water/ethyleneglycol	[kg/h]	0.0	± 0.00	25.2 %	
Ambient temperature	[°C]	26.2	± 0.41	1.6 %	
Supply power	[kW]	89.8	± 0.63	0.7 %	
Power consumtion compressor	[kW]	80.8	± 0.39	0.5 %	
Danfoss VSD efficiency		89.96 %	± 0.00	0.43 %	
Volumetric efficiency		67.7 %	± 0.55 %	0.81 %	
Isentropic efficiency		64.4 %	± 0.30 %	0.46 %	
Oil cirkulation rate (OCR)		1.2743 %	± 0.295 %	59.07 %	Uncertainty high due to on/off valve
Heat rejection	[kW]	81.5	± 0.34	0.4 %	
Cooling capasity	[kW]	0.0	± 0.00	0.0 %	
Pressure, evaporator, inlet	[bar]	58.2	± 0.15	0.3 %	
			0.00		
Pressure, throttle valve,in	[bar]	79.5	± 0.20	0.3 %	
Temperature, throttle valve, in	[°C]	53.9	± 0.07	0.1 %	
Temperature, throttle valve out	[°C]	-1.3	± 0.03	2.0 %	

Compressor

			Total Deviation	Total uncertainty	Comment
Inlet suction pressure	[bar]	20.4	± 0.05	0.3 %	
Inlet temperature	[°C]	-9.3	± -0.02	0.3 %	
Inlet super heat	[K]	9.6	± 0.02	0.2 %	
Outlet pressure	[bar]	80.7	± 0.20	0.3 %	
Outlet temperature	[°C]	125.5	± 0.04	0.03 %	
Pressure ratio	[-]	4.0	± 0.014	0.4 %	
Lubricant return mass flow rate:	[kg/h]	36.1	± 21.60	59.8 %	on/off valve
Temperature, lubricant return:	[°C]	104.8	± 0.39	0.4 %	
Compressor Speed	[rpm]	3700	± 7.40	0.2 %	
Torque	[Nm]	208	± 1.10	0.5 %	
Power consumption	[kW]	80.8	± 0.39	0.5 %	
Massflow R-744	[kg/h]	2797	± 6.02	0.2 %	
Specific volume (suction line)	[m3/kg]	0.02	± 0.00	0.1 %	
Density CO2 (suction line)	[kg/m3]	49.6	± 0.05	0.1 %	
Volumetric efficiency	[%]	67.7 %	± 0.55 %	0.81 %	
Isentropic efficiency	[%]	64.4 %	± 0.30 %	0.46 %	

Experiment no: 4
Date: 22.05.2012
Operator: Obrist/Roman
Mode: comp.test 800 rpm
Measured points 53

Log p-h cyclus

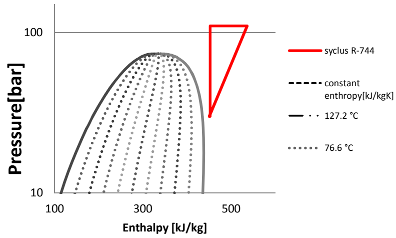

Components		**Description**
Compressor		Piston compressor
Gascooler/condenser		Air fan
Gasscooler condenser		Water to sink
Gascooler/condenser	4a/b	Heat to glycol
Internal heat exhanger		
Evaporator	6a/b	R-774/glycol
Separator		
Oil separator		

System performance

				Total Deviation	Total uncertainty	Comment
COP	-		0.8	± 0.01	1.31 %	
Compressor Speed		[rpm]	800	± 1.60	0.2 %	
Mass flow R744		[kg/h]	848	± 2.92	0.3 %	
Mass flow water/ethyleneglycol		[kg/h]	0.0	± 0.00	20.4 %	
Ambient temperature		[°C]	19.7	± 0.01	0.0 %	
Supply power		[kW]	27.0	± 0.06	0.2 %	
Power consumtion compressor		[kW]	24.5	± 0.20	0.8 %	
Danfoss VSD efficiency			90.75 %	± 0.01	0.84 %	
Volumetric efficiency			63.3 %	± 0.46 %	0.72 %	
Isentropic efficiency			59.9 %	± 0.52 %	0.86 %	
Oil cirkulation rate (OCR)			0.0008 %	± 0.518 %	418.98 %	Uncertainty high due to on/off valve
Heat rejection		[kW]	19.9	± 0.21	1.1 %	
Cooling capasity		[kW]	3.0	± 0.03	0.9 %	
Pressure, evaporator, inlet		[bar]	30.8	± 0.08 0.00	0.3 %	
Pressure, throttle valve,in		[bar]	110.2	± 0.29	0.3 %	
Temperature, throttle valve, in		[°C]	76.6	± 0.05	0.1 %	
Temperature, throttle valve out		[°C]	-1.3	± 0.03	2.0 %	

Compressor

			Total Deviation	Total uncertainty	Comment
Inlet suction pressure	[bar]	30.0	± 0.09	0.3 %	
Inlet temperature	[°C]	5.3	± 0.12	2.4 %	
Inlet super heat	[K]	10.9	± 0.12	1.1 %	
Outlet pressure	[bar]	109.9	± 0.31	0.3 %	
Outlet temperature	[°C]	127.2	± 0.08	0.06 %	
Pressure ratio	[-]	3.7	± 0.016	0.4 %	
Lubricant return mass flow rate:	[kg/h]	0.0	± 0.03	419.0 %	on/off valve
Temperature, lubricant return:	[°C]	25.8	± 0.03	0.1 %	
Compressor Speed	[rpm]	800	± 1.60	0.2 %	
Torque	[Nm]	293	± 2.45	0.8 %	
Power consumption	[kW]	24.5	± 0.20	0.8 %	
Massflow R-744	[kg/h]	848	± 2.92	0.3 %	
Specific volume (suction line)	[m3/kg]	0.01	± 0.00	0.4 %	
Density CO2 (suction line)	[kg/m3]	73.8	± 0.32	0.4 %	
Volumetric efficiency	[%]	63.3 %	± 0.46 %	0.72 %	
Isentropic efficiency	[%]	59.9 %	± 0.52 %	0.86 %	

Experiment no: 4
Date: 22.05.2012
Operator: Obrist/Roman
Mode: comp.test 2500 rpm
Measured points 34

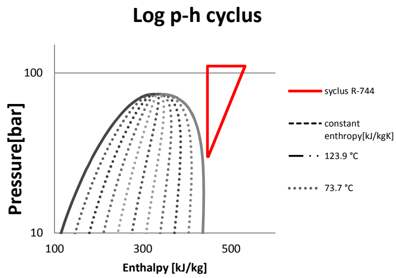

Components		**Description**
Compressor		Piston compressor
Gascooler/condenser		Air fan
Gasscooler condenser		Water to sink
Gascooler/condenser	4a/b	Heat to glycol
Internal heat exhanger		
Evaporator	6a/b	R-774/glycol
Separator		
Oil separator		

System performance

			Total Deviation	Total uncertainty	Comment
COP	-	1.0	± 0.01	0.80 %	
Compressor Speed	[rpm]	2500	± 5.00	0.2 %	
Mass flow R744	[kg/h]	3065	± 6.25	0.2 %	
Mass flow water/ethyleneglycol	[kg/h]	0.0	± 0.00	22.6 %	
Ambient temperature	[°C]	19.2	± 0.03	0.1 %	
Supply power	[kW]	80.9	± 0.16	0.2 %	
Power consumtion compressor	[kW]	73.1	± 0.33	0.4 %	
Danfoss VSD efficiency		90.33 %	± 0.00	0.45 %	
Volumetric efficiency		72.7 %	± 0.69 %	0.95 %	
Isentropic efficiency		72.5 %	± 0.37 %	0.51 %	
Oil cirkulation rate (OCR)		1.4147 %	± 0.366 %	58.37 %	Uncertainty high due to on/off valve
Heat rejection	[kW]	72.3	± 0.77	1.1 %	
Cooling capasity	[kW]	12.7	± 0.10	0.8 %	
Pressure, evaporator, inlet	[bar]	33.1	± 0.08 0.00	0.3 %	
Pressure, throttle valve,in	[bar]	109.8	± 0.28	0.3 %	
Temperature, throttle valve, in	[°C]	73.7	± 0.05	0.1 %	
Temperature, throttle valve out	[°C]	-1.3	± 0.03	2.0 %	

Compressor

			Total Deviation	Total uncertainty	Comment
Inlet suction pressure	[bar]	30.0	± 0.08	0.3 %	
Inlet temperature	[°C]	3.4	± 0.06	1.7 %	
Inlet super heat	[K]	9.0	± 0.06	0.7 %	
Outlet pressure	[bar]	110.7	± 0.28	0.3 %	
Outlet temperature	[°C]	123.9	± 0.07	0.06 %	
Pressure ratio	[-]	3.7	± 0.013	0.4 %	
Lubricant return mass flow rate:	[kg/h]	44.0	± 26.04	59.2 %	on/off valve
Temperature, lubricant return:	[°C]	103.9	± 0.38	0.4 %	
Compressor Speed	[rpm]	2500	± 5.00	0.2 %	
Torque	[Nm]	279	± 1.37	0.5 %	
Power consumption	[kW]	73.1	± 0.33	0.4 %	
Massflow R-744	[kg/h]	3065	± 6.25	0.2 %	
Specific volume (suction line)	[m3/kg]	0.01	± 0.00	0.3 %	
Density CO2 (suction line)	[kg/m3]	75.1	± 0.21	0.3 %	
Volumetric efficiency	[%]	72.7 %	± 0.69 %	0.95 %	
Isentropic efficiency	[%]	72.5 %	± 0.37 %	0.51 %	

Experiment no:	4
Date:	24.05.2012
Operator:	Obrist/Roman
Mode:	comp.test 1500 rpm
Measured points	30

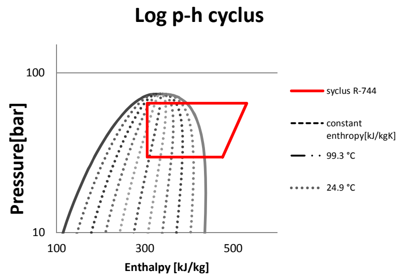

Components		**Description**
Compressor		Piston compressor
Gascooler/condenser		Air fan
Gasscooler condenser		Water to sink
Gascooler/condenser	4a/b	Heat to glycol
Internal heat exhanger		
Evaporator	6a/b	R-774/glycol
Separator		
Oil separator		

System performance

			Total Deviation	Total uncertainty	Comment
COP	-	4.1	± 0.05	1.30 %	
Compressor Speed	[rpm]	1500	± 3.00	0.2 %	
Mass flow R744	[kg/h]	1708	± 3.94	0.2 %	
Mass flow water/ethyleneglycol	[kg/h]	33.3	± 0.07	0.2 %	
Ambient temperature	[°C]	20.0	± 0.08	0.4 %	
Supply power	[kW]	30.5	± 0.17	0.6 %	
Power consumtion compressor	[kW]	26.1	± 0.26	1.0 %	
Danfoss VSD efficiency		85.54 %	± 0.01	0.80 %	
Volumetric efficiency		79.0 %	± 0.23 %	0.29 %	
Isentropic efficiency		73.9 %	± 0.62 %	0.84 %	
Oil cirkulation rate (OCR)		0.0031 %	± 0.618 %	31.57 %	Uncertainty high due to on/off valve
Heat rejection	[kW]	107.1	± 1.35	1.3 %	
Cooling capasity	[kW]	76.4	± 0.19	0.2 %	
Pressure, evaporator, inlet	[bar]	32.5	± 0.08	0.3 %	
			0.00		
Pressure, throttle valve,in	[bar]	64.3	± 0.35	0.5 %	
Temperature, throttle valve, in	[°C]	24.9	± 0.22	0.9 %	
Temperature, throttle valve out	[°C]	-1.3	± 0.03	2.1 %	

Compressor

			Total Deviation	Total uncertainty	Comment
Inlet suction pressure	[bar]	29.7	± 0.08	0.3 %	
Inlet temperature	[°C]	25.1	± 0.14	0.6 %	
Inlet super heat	[K]	31.1	± 0.14	0.4 %	
Outlet pressure	[bar]	64.6	± 0.34	0.5 %	
Outlet temperature	[°C]	99.3	± 0.36	0.36 %	
Pressure ratio	[-]	2.2	± 0.013	0.6 %	
Lubricant return mass flow rate:	[kg/h]	0.1	± 0.02	31.6 %	on/off valve
Temperature, lubricant return:	[°C]	39.4	± 0.10	0.3 %	
Compressor Speed	[rpm]	1500	± 3.00	0.2 %	
Torque	[Nm]	166	± 1.66	1.0 %	
Power consumption	[kW]	26.1	± 0.26	1.0 %	
Massflow R-744	[kg/h]	1708	± 3.94	0.2 %	
Specific volume (suction line)	[m3/kg]	0.02	± 0.00	0.1 %	
Density CO2 (suction line)	[kg/m3]	63.3	± 0.07	0.1 %	
Volumetric efficiency	[%]	79.0 %	± 0.23 %	0.29 %	
Isentropic efficiency	[%]	73.9 %	± 0.62 %	0.84 %	

Aircooler						
Gascooler TAG 2			**Total Deviation**		**Total uncertainty**	**Comment**
Spesific heat difference	*kJ/kg*	59.3	±	0.56	0.9 %	
Capacity	*[kW]*	28.1	±	0.27	1.0 %	
Temperature difference R-744	*°C*	43.4	±	0.10	0.2 %	
Mass flow air	*kg/h*	-				
Effect	*%*		±			
Pressure drop	*bar*	0.1	±	0.00	2.8 %	
Mass flow R744	*kg/h*	1708	±	3.94	0.2 %	
Inlet temperature		96.2	±			
Outlet temperature		52.87				
			±			
			±			

Watercooler						
Gascooler TAG 3			±			
Spesific heat difference	*kJ/kg*	2.0		0.71	36.1 %	
Cooling capasity	*kW*	0.9	±		0.0 %	
Mass flow water	*Kg/h*		±			
Temperature differenca R-744	*°C*	1.3		0.13	9.7 %	
Pressure drop	*bar*	0.0		0.00	4.3 %	
Mass flow R-744	*kg/h*	1708	±	3.94	0.2 %	
Temperature difference water	*°C*	1.6		0.09	5.3 %	

Gascooler 4a						
R744 side			**Total Deviation**		**Total uncertainty**	**Comment**
Inlet temperature	*°C*	51.6	±	0.11	0.2 %	
Outlet temperature	*°C*	25.0	±	0.21	0.9 %	
Spesific heat difference	*kJ/kg*	0.15	±	0.00	1.0 %	
Temperature difference	*°C*	26.6	±	0.24	0.9 %	
Mass flow R744	*Kg/h*	1708	±	3.94	0.2 %	
Cooling capasity	*kW*	71.5	±	0.74	1.0 %	
Pressure drop	*bar*	0.07	±	0.00	4.9 %	
Glycol side						
Spesific heat difference	*kJ/kg*	0.08	±	0.67	860.9 %	
Temperature difference	*°C*	22.2	±	0.19	0.9 %	
Mass flow glycol	*Kg/h*	2892	±	0.87	0.0 %	
Cooling capasity	*kW*	62.58	±	0.15	0.2 %	
Pressure drop	*Pa*	0.00	±	0.00	2.5 %	

Gascooler 4b

R744 side				
Inlte temperature	°C	51.6	±	0.9 %
Outlet temperature	°C	25.3	±	0.6 %
Spesific heat difference	kJ/kg	69.2	±	119.9 %
Temperature difference	°C	26.3	±	0.7 %
Mass flow R744	kg/h	1708	±	0.2 %
Cooling capacity	kW	0.00	±	119.9 %
Pressure drop	Bar	0.02	±	10.8 %
Glycol side				
Spesific heat difference	kJ/kg	37.7	±	685.5 %
Temperature difference	°C	10.9	±	0.7 %
Mass flow glycol	Kg/h	1446	±	0.1 %
Cooling capacity	kW	109110	±	0.2 %
Pressure drop	bar	0.01	±	12.2 %

IHX

HP side			Total Deviation		Total uncertainty	Comment
Spesific heat difference	kJ/kg	30.2	±	2.01	6.6 %	
Temperature difference	°C	0.1	±	0.30	400.7 %	
Mass flow R744	kg/h	1708	±	3.94	0.2 %	
Cooling capacity	kW	14.3	±	0.95	6.6 %	
Pressure loss	bar	1.8	±	0.00	0.1 %	
			±			
LP side						
Spesific heat difference	kJ/kg	72.1	±	80.39	111.6 %	
Temperature difference	°C	30.3	±	0.14	0.5 %	
Mass flow R744	Kg/h	1708	±	3.94	0.2 %	
Cooling capacity	kW	0.0	±	0.00	0.0 %	
Pressure loss	bar	0.20	±	0.00	0.5 %	
Superheat IHX inlet	[°C]	-10.3				

Evaporator 6a

R744 side			Total Deviation		Total uncertainty	Comment
Pressure inlet	bar	32.5	±	0.08	0.25 %	
Temperature difference	°C	-4.1	±	0.00	0.0 %	
Mass flow R744	kg/h	1708	±	3.94	0.2 %	
Heat difference R744	kJ/kg	161	±	0.09	0.1 %	
Cooling capacity	kW	76.42	±	0.04	0.1 %	
Pressure drop	bar	2.03	±	0.03	1.3 %	
Glycol side						
Spesific heat difference	kJ/kg	3.72	±	143	3839.9 %	
Temperature difference	°C	1.11	±	0.05	4.8 %	
Mass flow glycol	Kg/h	33	±	0.07	0.2 %	
Cooling capacity	kW	0.03	±	6074	17629505.0 %	
Pressure drop	bar	1.69	±	0.01	0.5 %	

Evaporator 6b

R744 side					
Pressure inlet	bar	32.5	±	0.08	0.25 %
Spesific heat to R744	kJ/kg	10.6	±	0.16	1.5 %
Temperature difference	°C	19.1	±	0.03	0.2 %
Mass flow R744	kg/h	1708	±	3.9	0.2 %
Cooling capacity	kW	0.0	±	0.00	1.2 %
Pressure drop	bar	0.03	±	0.00	6.1 %
Glycol side					
Spesific heat out	kJ/kg	23.2	±	193.5	834.4 %
Temperature difference	°C	6.7	±	0.07	1.0 %
Mass flow glycol	Kg/h	33	±	0.07	0.2 %
Cooling capacity	kW	0.8	±	7.64	988.6 %
Pressure drop	bar	0.01	±	0.00	11.7 %

B HIGH EFFICIENT 100KW R-744 COMPRESSOR

B.1 ABSTRACT

For experiment purposes the losses in the reciprocating cycle were evaluated, where the overall isentropic efficiency is most defining for the energy efficiency, and also the defining value for the entirety of all losses in the compressor unit.

The test campaign was conducted in different test series, where the test points were set by Obrist Engineering with background in a cooling application on a fishing vessel. 3 series were set, where a fixed pressure ratio of 65/30 bar, 110/30 bar and 80/20 bar was tested in experiments with varying motor speed from 800 - 3800 rpm and a constant superheat at 10K. As the executions showed, some of the test points were not able to be tested, because of lack of power supply in the local power grid, and the maximum input power was set to 94kW.
Test results revealed a relatively high overall efficiency with values at 73.5% for a pressure ratio of 65/30 bar. Also for the two other pressure ratios the efficiency showed to be satisfying in comparison with on the shelf compressors commercially available to day. However, the test campaign revealed a high volumetric loss in high pressure ranges, which partly can be substantiated with a relatively high clearance volume due to the shear size of the cylinder. In addition, $P_{indicated}$ for low speeds versus high speeds shows a possible too small valve area at discharge for the highest speeds.

B.2 INTRODUCTION

CO_2 is a natural refrigerant and is well suitable in many cooling applications. It has been used within the refrigeration industry from the 1900s, but got replaced as the synthetic refrigerants got introduced. In 1990 these fluids were proved damaging to the ozone layer and got replaced by a new series of synthetic fluids, which later have shown to be harmful to the global climate and therefore bound with restrictions from the governments. In the early 1990s at Norwegian University of Science and Technology(NTNU), professor Gustav Lorentzen introduced the transcritical refrigeration process and reintroduced CO_2 as a refrigerant with favourable properties.
Now the use of CO_2 in heat pump applications is wide spread, and competitive alternatives within most markets are presented. However, there are still areas of improvement, and at the laboratories of SINTEF and NTNU a rig is being installed meant to do experiments on high effect CO_2 cooling systems, with a cooling capacity of 400kW and a compressor capacity of el 100kW. Currently the

rig is placed in Lustenau Austria at Obrist Engineerings facility where a 100kW high efficient semi hermetic 6 cylinder single stage piston compressor is being tested. This compressor is a new development and a result of a cooperation between SINTEF and Obrist Engineering. The background for this development was the lack of single stage compressors able to deliver flow rates in the range of 10 to $90m^3/h$.

B.3 DESCRIPTION OF THE TEST PLANT

The rig was implemented in to a container, with measurements 1,6 mx 1,2m x 2,53m. An air cooler adds additional 0.25m to the total length. Along with a water cooled heat exchanger the air cooler is rejecting the heat done by the compressor which cannot be conserved in the supporting glycol-water system.

The rig is built as flexible as possible, and all of the key applications in the R-744 refrigerant circuit are replaceable or has the opportunity to make use of additional equipment as expansion or work recovery devices desired for future experiments. The system is set to work at a maximum discharge pressure at 130 bar with temperatures in ranges of -50 - 180 °C in the R-477 cycle and the maximum electrical power input to the compressor is in the range of 100kW,
For safety reasons the rig was controlled by a 3. party company specialized in quality assurances of weldings using x-ray, also it has been pressurized up to 160 bar and leakage tested.
The rig was built to be flexible for future experiments, and in testing of compressors it is possible to bypass some of the heat exchangers, as shown in figure 30, and reject the heat generated by the compressor in the air cooled gas cooler only. At higher ambient temperatures it is possible to connect the water cooling as well. From figure 15 following components are recognized:

Were:	1: R-744 compressor	7: Expansion valve
	2: Air cooled gas cooler	8: Separator
	3: Water cooled gas cooler	9: Oil separator
	4: Gas cooler/condenser a and b	
	5: Internal heat exchanger	
	6: Evaporator a and b	

In general the rig consists of two independent closed systems, one using R-744 as refrigerant getting compressed in the gas phase, and cooled either in critical or sub-critical conditions. As a supporting system the ethylene system worked both as heat sink and heat source at constant temperature. In experiments with the compressor it was not required to use the supporting systems, and the ethylene water systems were not in operation during the test.

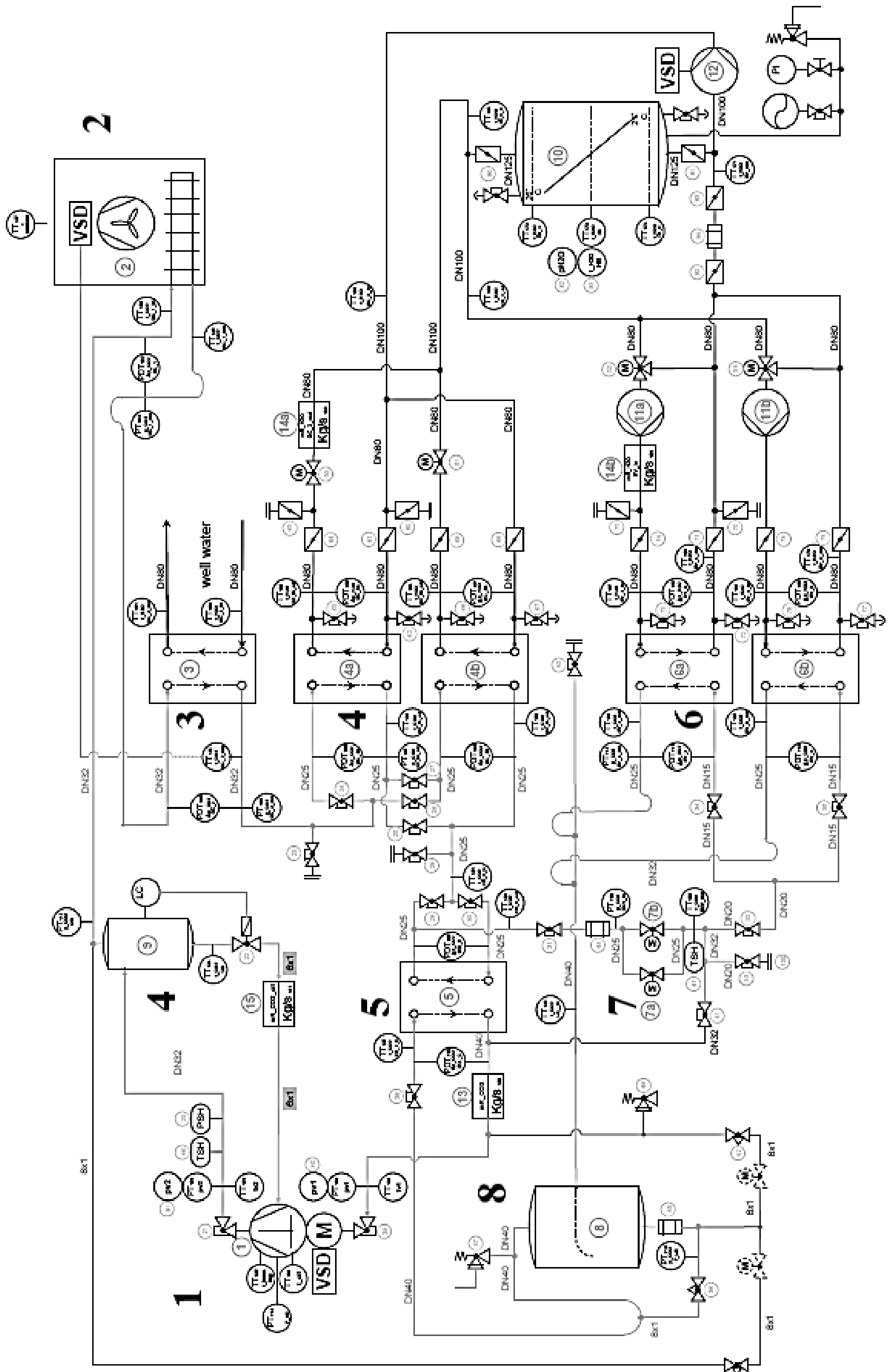

Figure 30: Principal drawing of the test rig facility incorporating the pipe work, vessels, heat exchanger and supporting system

B.3.1 *Compressor build-up*

The housing is made from cast iron which cowers on both ends witch are reinforced with ribs on the inside. The housing has ribs on the outside for better cooling, and is also mounted with 6 cylinders bolted on the octagon shaped topside. The common shaft of both motor and crank shaft has two slide bearings, and is attached to the pistons with a connecting rod attached to the piston with a wrist pin. For the lubrication a centrifuge oil pump transports oil from the crank case into the enclosed bearings and the cylinder lubrication, where some of the oil is transported with and later separated from the main flow. The gas enters into the crank case through a centrally located suction duct, where it also acts as cooling for the motor. The pressure of the gas is governed by valves suction- and discharge valves for each cylinder.

		Value/Range
Height x Width x Length	[mm]	500 x 440 x 830
Weight	[kg]	286
Volume flow rate	[m^3/h]	10-90
Displacement	[cm^3]	380
Max power consumption	[kW]	100
Revolutions per minute	[rpm]	800 - 4000
Frequency range	[Hz]	53-267

Table 9: Compressor data

B.3.2 *Description of the refrigeration circuit*

After compression the R-744 went in to an oil separator (9), where most of the oil was separated from the working fluid and fed back to the compressor lubrication system. From the oil separation and back to the compressor there was mounted an on/off valve responding to the oil level in the oil separator.
Then the gas was led through the air cooler (2) mounted on the outside of the container. The only purpose of this gas cooler was to reject heat from the compression. At lower ambient temperatures this cooler was able to reject all the heat generated from the compressor and at higher ambient temperatures there was an additional system using water as coolant (3).
Downstream of the water cooler there were mounted two plate heat exchangers (4) between the two systems, where 4b was bypassed. In future experiments it

is possible to run these exchangers both in parallel and series for possible performance evaluations. In addition there is made room in the test rig to replace them with other applications, or mount additional equipment downstream or upstream.
The throttling valves (7) were placed downstream of the internal heat exchanger (5) which was bypassed. By adjusting the opening in the two throttling valves the system pressure was set. And in order to fine tune it to the appropriate pressure the pressure reduction application was a set of two valves, where one had a smaller pressure range, and was used to control small pressure variations.
A set of plate heat exchangers(6) was installed downstream of the heat exchangers to transfer rejected heat from glycol to R-744, but for compressor experiments exchanger both these, the gas-liquid separator(8) and the internal heat exchanger(5) low pressure side were bypassed.

Table 10 summarizes the measurement devices used in the refrigeration rig. For the thermocouples there are two different types; PT100 which is resistance thermometer, and a K-type thermometer. The PT100 is calibration tolerance according to DIN EN 60751 Class A and the K-type uses tolerance according to DIN EN 60584-2, Class 1.

Sensors	Measured variable	Measuring device	Calibration range	Calibrated accuracy
14	Temperature (°C)	K-type thermocouple	-40-145	±0.5
18	Temperature (°C)	PT100 Resistance thermometer	0-140	±0.03
13	Pressure (Bar)	Pressure gauge	0-160	±1.2
11	Pressure (Bar)	Pressure gauge	0-80	±0.7
1	Refrigerant mass flow rate (kg/s)	Coriolis mass flow meter	0.0–1.4	±0.1% of reading
1	Lubricating oil (m^3/h)	Coriolis volume flow meter	0-4	±0.25% of reading
1	Power consumption (kW)	Digital wattmeter	0-100	±0.5% of reading
1	Compressor revolution speed (rpm)	Analog signal from the inverter drive	0-4000	±1.3% of reading

Table 10: The installed transducers in the full test rig

B.4 RESULTS AND DISCUSSION

In the calculations the following relations were used:

$$\eta_{is} = \frac{P_{is}}{P_{el}} 100 = \frac{m_{oil+R-744} \Delta h_{is}}{P_{el}} 100 \tag{21}$$

$$\eta_{vol} = \frac{\dot{m}_{tot}}{\rho_{R-744} V_s \omega} \tag{22}$$

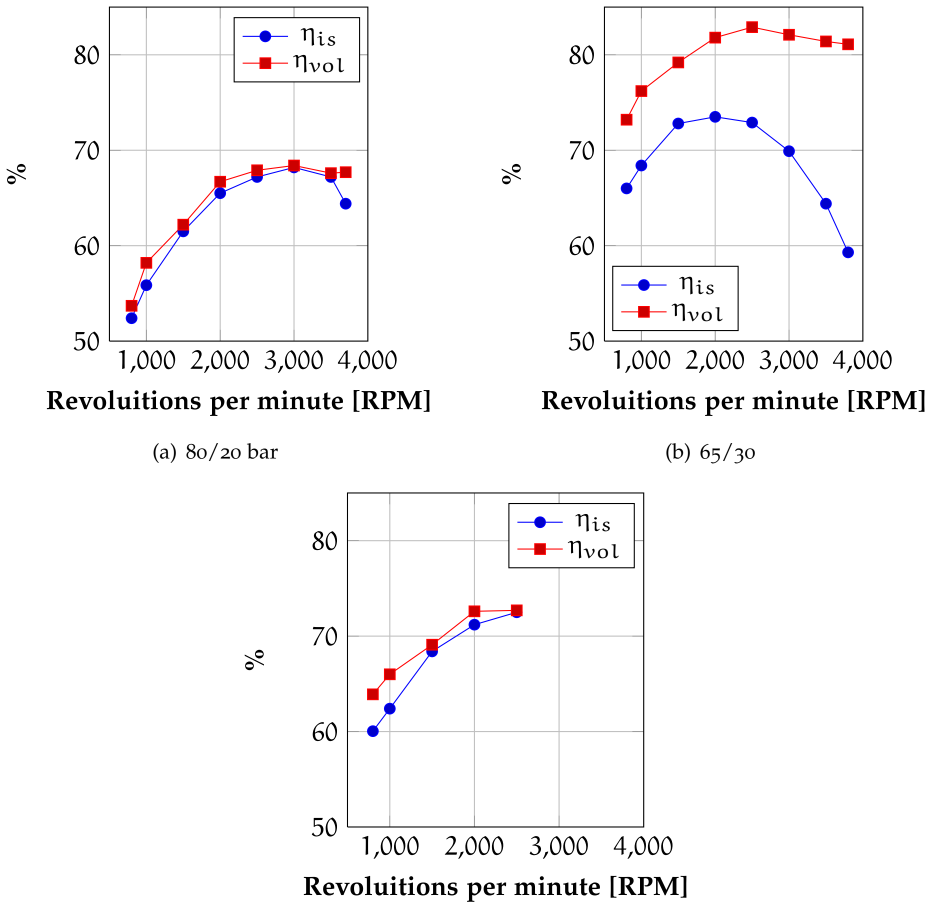

(a) 80/20 bar

(b) 65/30

(c) 110/30 bar

Figure 31: Compariosn of volumetric and isentropic efficiencies.

For the isentropic efficiency the trend is a steep negative gradient as the rotational speed increase, and figure 31 shows a descending line for both 80/20 bar as well as 65/30 bar. This trend is more visible in figure 31 (b), where the steepness is near dramatic from 2500 to 3700 rpm.

Volumetric losses greatly influences the capacity and energy efficiency, and as expected the volumetric efficiency is strongly dependent on the pressure ratio, which is evident from figure 31 where the best volumetric efficiency is present at pressure ratio of 65/30 bar. In addition, as the speed of the motor increase the volumetric efficiency flattens out for all of the three pressure ratios.

A reason for the increasing losses at higher pressure ratios could be the clearance volume of 4.5%, which is relatively small, but for a compressor this size the actual volume of $17.1 cm^3$ is quite high, which in turn affects the volumetric

efficiency. It is strongly indicated that a high difference between suction and discharge pressure affects the volumetric efficiency negatively. As the rotational speed increase, the curves for volumetric efficiency also flatten out, and seem to stay at a more efficient working point. One possible reason could be that the efficiency of the motor increase as the load increase, until a certain point. Thus the heat loss in the motor decrease and the contribution from the motor to add extra super heat to the suction gas is less dominating, which in turn affects the volumetric efficiency.
An additional effect to the volumetric efficiency can be shown in figure 31 (a) which shows the difference between volumetric and istentropic efficiency for pressure ratio of 80/20 bar. Here the trend is that the difference between the two values are relatively small, compared to the same graph for 65/30 bar. One reason for this is most likely that the pressure difference from suction and discharge is at 60 bars for 80/20, whilst the difference for 65/30 is 35 bar. Thus the gas leakage from high pressure side to low pressure side of the piston is more likely to occur at high pressure ratios. There has been a change of piston rings in the compressor, but from the test results it is plausible that the leaking trend is still of concern, in particular for high pressure ratios. An amplifying effect could also be the high discharge temperature causing the specific gas volume to decrease, and the gas to slip past the piston rings more easy.

The total indicated work, $P_{indicated}$, for high rpm are much higher than for low rpm. From figure 32 this is evident.

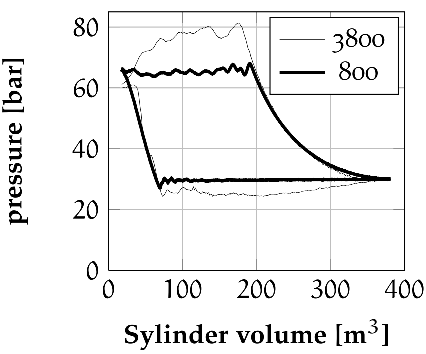

(a) 65/30 bar

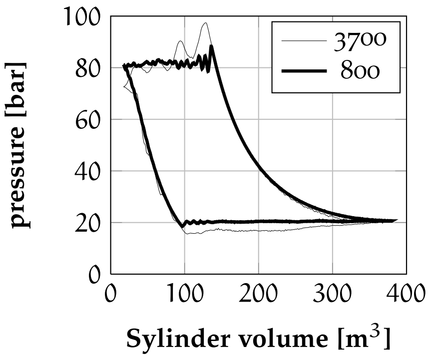

(b) 80/20 bar

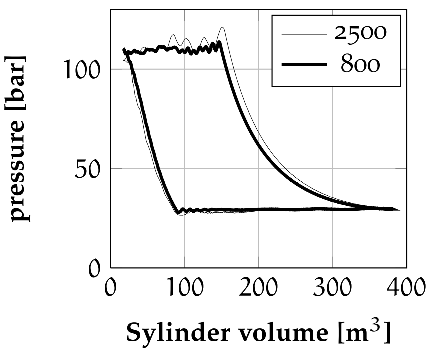

(c) 110/30 bar

Figure 32: Plot of indicator diagram in the same figures for 3 different pressure ratios

It is seen a larger pressure build-up in the high speed ranges, than in a low speed range. In the suction this is not as critical as in the suction. Main reason for this may be a too small valve area, and from the looks of figure 32 it is seen that the valve is kept open for a longer period, with less fluctuation, which can be caused by small passage area for the discharge gas. With a higher valve area, more room in the passage would have caused for smaller pressure in the cylinder discharge port. It is also seen that the compression line is near isentropic for all 3 of the plots. Discharge is not big losses in any of the plots, however this is also decreasing at lower speeds.

Obirst engineering has done a series of experiments of some "on the shelf" compressors available to the marked today, to have some reference points regarding which efficiencies are acceptable in such a test campaign. Figure 25 shows the values for two different commercially available compressors running at 1500 rpm, 80 bar discharge pressure 10K superheat and varying compressor ratio plotted against the Obrist / SINTEF compressor running with the same conditions with motor speeds from 1000 to 2500 rpm.

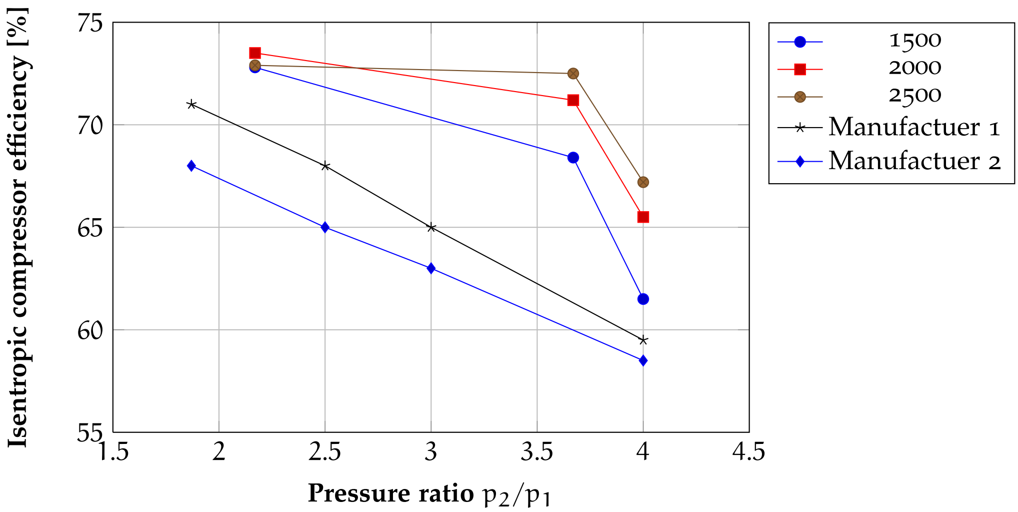

Figure 33: Comparison of efficiencies with 2 different on the shelf compressors available on the marked today, running at 1500 rpm with discharge pressure of 80 bar and 10K superheat

As the reference lines has a near linear negative trend against higher rpm, the Obrist / SINTEF compressor shows to be more stable, at pressure ratios up to 4, which implies a relatively robust compressor for handling pressures and speeds within a pressure and flow interval, which is of great use in an industry cooling application. Further on, improvements in the compressor arrangement are still to be expected, and the presented test results reveal some indications on the general performance of the compression cycle.

B.5 CONCLUSION

An analysis of piston compressor losses and a view on which factors that are of interest to evaluate in a testing campaign for reciprocating compressors has been conducted. The rig made by Obrist Engineering in Austria is fitted with possibilities to test compressors up to 100kW electrical power and 400kW cooling capacity, and has multifunctional testing possibilities. The first test results for a 100kW 6 cylinder newly developed piston compressor have been presented and discussed.

The test campaign showed overall compressor efficiencies up to 73.5%, and at a wide range of motor revolution speeds it showed a relatively high efficiency. I.e for lower pressure ratios the compressor shows a really favourable trend, and at pressure ratio at 65/30, the overall efficiency stays above 70% from 1500 to 3000 rpm. In comparison with an on the shelf compressor the newly developed SINTEF/OE compressor is showing great potential, and within a cooling application it will have the ability to deliver high pressures and high flows at a higher efficiency than what is experienced today. For a fishing vessel, where also weight is an issue, its capabilities will be of interest in the marked. Also typically in cooling applications in supermarkets, where the effect is quite high the compressor will be a good replacement for smaller compressors used to day.

C UNCERTAINTY

C.0.1 *Fixed error*

If we a ruler is thought of as a meter, we can measure a length, but since the ruler has the smallest value of $1mm$ there will always be an error of ± 0.5, and no matter how small the smallest units are, there will always be an uncertainty of ±0.5, and the true value will never be found. This means that all measuring devices have an uncertainty, no matter how expensive or well made. The best way to specify a uncertainty is to express an value for how much off the measurement is. This value given in experiments are given from $Error = x_{measured} - x_{true}$. From this one can claim a numerical value of the uncertainty as a $estimate$ of the error, not a guarantee of the accuracy, but a expected accuracy. If the accuracy is given to be 5%, the $Error = x_{measured} - x_{true}$ is $0.05x_{true}$.

Uncertainties are given from the producer of the measurement equipment in values of a certain deviation which is expected. The equipment was calibrated by Obrist to match these values and as for a fixed uncertainty these values are used in the calculations. Often this error will be given in percent of the measured value, given the subscript δ. Thus, if $X_i = the\, measured\, value$, the actual uncertainty is δX_i.

$$X_i = X_{i,measured} \pm \delta X_i \qquad (20:1) \tag{23}$$

X_i is the maximum or minimum value, and it is certain within a 95% confidence that the real value is within this interval. When using this in scientific experiments it is referred to as the $fixed$ error. δ will always be provided by the vendor.

C.0.2 *Random error*

Single sample measurements have a higher uncertainty compared to multi-sample measurements, were the quality of the measurements increase with several measurements. I.e: if a distance is measured with a ruler 15 independent times it is likely that there will be a small variation in the results. From the multiple measured data one can calculate a standard deviation from the mean of a sample N

$$\text{If} \quad \bar{x} = \frac{x_1 + x_2 + x_3 +, ..., +N}{N}$$

The deviation is the difference between the measured value and the mean value in a set of results.

$$\delta x_i = \overline{x}_i - x_i, \quad \text{for} i = 1, 2, \ldots, N$$

From this the standard deviation σbecomes

$$\sigma = \sqrt{\frac{\delta x_1^2 + \delta x_2^2 + \delta x_3^2 +, \ldots, +\delta x_N^2}{(N-1)}} \tag{24}$$

The standard uncertainty u in a result with multiple experiments is

$$u = \frac{\sigma}{\sqrt{N}} \tag{25}$$

This is the experimental standard deviation of the mean. In scientific result the confidence interval should be within 95%, and from the t-distribution, or students distribution where the degrees of freedom is

$$\nu = N - 1 \tag{26}$$

from table with students t-test $t \approx 2$, and the total uncertainty for a confidence interval at 95% is

$$cd \approx 2\sigma \tag{27}$$

In practical evaluations it means that minimum 19 of 20 measurements needs to be within $\overline{x} \pm \delta\overline{x}$

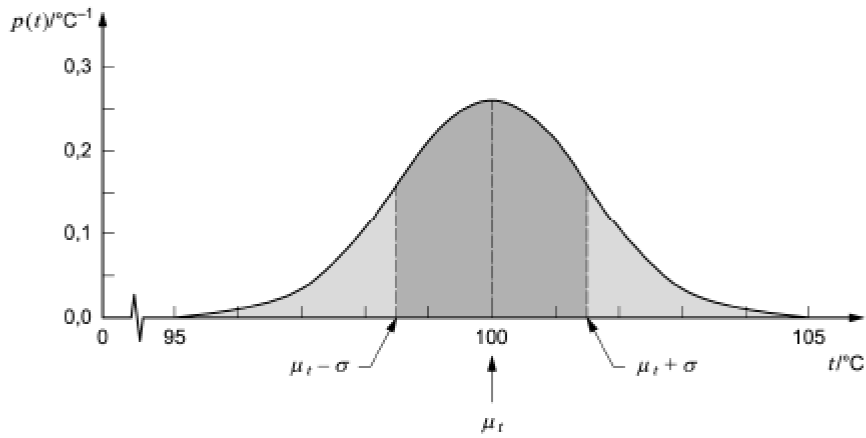

Figure 34: *Gaussian distribution*

The certainty of the results will increase as more examples are collected.

C.0.3 *Experimental use*

The test results was used to calculate $f = f(x, y, \ldots,)$ with its error results $\delta x, \delta y, \ldots$. From a single variable function $f(x)$, the deviation in f can be related to the deviation in x with

$$\delta f = \left(\frac{df}{dx}\right) \partial x \tag{28}$$

For $f = f(x, y)$ the deviation will be the square and the average:

$$\delta f = \sqrt{\left(\frac{dy}{dx}\right)^2 \delta x + \left(\frac{\partial x}{\partial y}\right)^2 \delta y} \tag{29}$$

To calculate the uncertainty in difference between two measured values, i.e. $f(\Delta x)$, the function will be calculated or measured values, $f(x_1, x_2)$, thus:

$$\delta \Delta x = \sqrt{\left(\frac{\partial \Delta x}{\partial x_1} \delta x_1\right)^2 + \left(\frac{\partial \Delta x}{\partial x_2} \delta x_2\right)^2} \tag{30}$$

The partial derivative will be

$$\frac{\partial \Delta x}{\partial x_1} = 1$$

$$\frac{\partial \Delta x}{\partial x_2} = -1$$

Thus:

$$\delta \Delta x = \sqrt{1^2 \cdot \delta x_1 + (-1)^2 \cdot \delta x_2} = \sqrt{\delta x_1 + \delta x_2} \tag{31}$$

To calculate the total error from both random and fixed they are squared:

$$\delta_{total} = \sqrt{\delta^2_{random} + \delta^2_{fixed}} \tag{32}$$

C.1 MEASUREMENTS OF ACTUAL QUANTITIES

The enthalpy, specific heat difference and the entropy was collected from data sets implemented in excel. However, the uncertainty was calculated using equation 29 for the two local variables in temperature and pressure.
Thus, the uncertainty of the enthalpy value is:

$$\delta h = \sqrt{\left(\frac{\partial h_i}{\partial T_i} \delta T_i\right)^2 + \left(\frac{\partial h_i}{\partial p_i} \delta p_i\right)^2} \tag{33}$$

Where the partial derivative terms can be calculated by:

$$\frac{\partial h_i}{\partial T_i} = C_p(T_i, p_i)$$

The spesific heat capacity cp is a direct function of the heat capacity given from the same local pressure and temperature. A small step in output values gives the possibility to calculate the gradient, thus the uncertainty in enthalpy was calculated by

$$\frac{\partial h_i}{\partial p_i} = \frac{h(T_i, p_i + \Delta p) - h(T_i, p_i)}{\Delta p} \tag{34}$$

The cooling capacity, $\dot{Q}$ of each heat exhanger is a function of enthalpy difference on inlet and outlet and mass flow, $f(\dot{Q}) = f(\Delta T, \Delta h)$.

$$f(\dot{Q}) = \dot{m}(\Delta h_{in} + \Delta h_{out}) \tag{35}$$

where the displayed value in excel is the absolute value.
The uncertainty in the cooling capacity is derived from equation 35:

$$\delta\dot{Q} = \sqrt{\left(\frac{\partial \dot{Q}_{out}}{\partial \dot{m}}\delta\dot{m}\right)^2 + \left(\frac{\partial \dot{Q_{out}}}{\partial h_2}\delta h_2\right)^2 + \left(\frac{\partial \dot{Q_{out}}}{\partial h_1}\delta h_1\right)^2}$$

with the derivations

$$\frac{\partial \dot{Q_{out}}}{\partial \dot{m}} = h_2 - h_1$$

$$\frac{\partial \dot{Q_{out}}}{\partial h_2} = \dot{m}$$

$$\frac{\partial \dot{Q_{out}}}{\partial h_1} = -\dot{m}$$

By implementing the partial derative terms in the total equation which is implemented in excel are

$$\delta\dot{Q} = \sqrt{((h_2 - h_1) \cdot \delta\dot{m})^2 + (\dot{m} \cdot \delta h_2)^2 + (-\dot{m} \cdot \delta h_1)^2} \tag{36}$$

The torque was calculated from the speed of the compressor.

$$\omega = \frac{Rev\pi}{30} \qquad [\frac{1}{s}]$$

$$T = \frac{P_{shaft}}{\omega} \qquad [Nm]$$

Thus the torque is

$$T_{shaft} = \frac{P_{shaft}30}{\pi Rev} \tag{37}$$

The uncertainties derived from equation 37 are from equation 29

$$\frac{\partial T}{\partial Rev} = -\frac{30P_{shaft}}{\pi Rev^2}$$

$$\frac{\partial T}{\partial P_{shaft}} = \frac{30}{\pi Rev}$$

$$\delta T = \sqrt{\left[\left(-\frac{30P_{shaft}}{\pi Rev^2}\right)\delta Rev\right]^2 + \left[\left(\frac{30}{\pi Rev}\right)\delta P_{shaft}\right]^2} \tag{38}$$

The volumetric efficiency is implemented from the actual displacement volume versus the volume actually working inside the cylinder at compression. Theoretical volumetric flow is a function of the speed of the compressor Rev and the cylinder volume V_s, thus the total theoretical volumetric flow is $\dot{V}_{theoretical} = V_s Rev$. The actual flow is given from RnLib where the specific volume is given from the function r_vgas_tp, as a function of temperature and pressure at the outlet of the compressor. The mass flow is assumed constant through the compressor and the actual volumetric flow $\dot{V}_{actual} = \dot{m}\nu_{specific}$, following that the volumetric efficiency is

$$\eta_\nu = \frac{2\dot{m}\nu_{specific}}{V_s Rev} \tag{39}$$

Isotropic efficiency is given from the equation 8 in an ideal process, but for the actual process it is calculated from the shaft power, W_{shaft}, and an ideal isotropic line where s_{const} which starts at the inlet of the compressor and is a function of the p_{inlet}, and T_{inlet}. The entropy was an output from RnLib from the function r_sgas_tp and since s=const in the ideal process the enthalpy $h_{2_{is}}$ is a function of the pressure p_{outlet} and the entropy from the inlet. The change in enthalpy is for an the ideal process is $\Delta h = h_{2_{is}} - h_1$. The change in enthalpy for the actual process is $W/\dot{m}$, and the isentropic efficiency η_{is} is given by

$$\eta_{is} = \frac{h_{2_{is}} - h_1}{W/\dot{m}}$$

Alternatively one can use the enthalpy $h_{2_{actual}}$ in the outlet as a function of p_{outlet} and T_{outlet}, from RnLib.

$$\eta_{is} = \frac{h_{2_{is}} - h_1}{h_{2_{actual}} - h_1}$$

[Source kap 6.8 michael j moran] The uncertainties for the η_ν and η_{is} are derived from the two equations and implemented as in equation 29

$$\frac{\partial \eta_\nu}{\partial h_{2_{is}}} = \frac{\dot{m}}{W_{shaft}}$$

$$\frac{\partial \eta_v}{\partial h_1} = -\frac{\dot{m}}{W_{shaft}}$$

$$\frac{\partial \eta_v}{\partial W_{shaft}} = \frac{\dot{m}(h_1 - h_{2_{is}})}{W_{shaft}^2}$$

D RISK ANALYSIS

Risikovurdering av feltaktivitet (Grovanalyse)

Enhet: Energibruk

Prosjektnummer: 16X898.01

Dato: 21-24.05.2012

Adresse for oppdraget: Rheinstrasse 26-27, A-6890 Lustenau, Austria, tel: +43 5577 6237054

Linjeleder:

Deltakere: Anders Ask 95976371 og Titus Langhof

Aktivitet	Mulig uønsket hendelse/belastning	Eksisterende barrierer/ risikoreduserende tiltak	➢ Menneske	➢ Ytre miljø	➢ Omdømme	➢ Økonomi/ materiell	Nye barrierer/ risikoreduserende tiltak (handlingsplan)	❖ Menneske	❖ Ytre miljø	❖ Omdømme	❖ Økonomi/ materiell	Ansv-arlig Frist	Status
Transport til og fra Værnes	Problem med taxi	Bruk av flybuss. Bruk av bilbelte	1A	1A	1A	1A							
Fly til og fra Zürich	Forsinket fly, mister connection flight	Ikke fly med KLM	1A	1A	1A	1A	Ha med et utskrift av elektronisk billet	1A	1A	1A	1A	Hver for seg	Ok
Leiebiltur til og fra OE	Dårlig bil	Bruk tog fra flyplassen til St. Margerten, og ble hentet fra OE.	1A	1A	1A	1A							
Være med testkjøring av kompressoren og riggen	Høy lyd, høy trykk, At man blir kald, siden riggen er plassert utendørs	Ha på hørselsvern og vernebriller. Ha med varme klær	1A	1A	1A	1A	Ha med eget verneutstyr, hørselsvern, briller og varmedress	1A	1A	1A	1A	Hver for seg	Ok
Spise lunsj / middag	Maten er dårlig	Bare spis kokt eller helstekt mat	2B	1A	1A	1A	Ta med matpakke	1A	1A	1A	1A	Hver for seg	Ok

➢ I dette feltet skal en sette sannsynlighet x konsekvens, f.eks. 1A (Gir risikoverdi med eksisterende barrierer).

❖ I dette feltet skal en sette sannsynlighet x konsekvens, f.eks. 1A (Angir den nye risikoverdi etter at de fast satte tiltak er gjennomført)

Sannsynlighet
1. Svært liten
2. Liten
3. Middels
4. Stor
5. Svært stor

Konsekvens
A. Svært liten
B. Liten
C. Moderat
D. Alvorlig
E. Svært alvorlig

Kan risikovurdere:
Menneske = Sannsynlighet & Konsekvens Menneske
Ytre miljø = Sannsynlighet & Konsekvens Ytre miljø
Økonomi/materiell = Sannsynlighet & Konsekvens Øk/matriell
Omdømme = Sannsynlighet & Konsekvens Omdømme

SINTEF

Risikovurdering av feltaktivitet (Grovanalyse)

Sannsynlighet vurderes etter følgende veiledende kriterier:

Svært liten 1	Liten 2	Middels 3	Stor 4	Svært stor 5
Sjeldnere enn en gang hvert 50. år.	Mellom en gang hvert 10. år og en gang hvert 50. år.	Mellom en gang hvert år og en gang hvert 10. år.	Mellom en gang hver måned og en gang hvert år.	Oftere enn hver måned.

Konsekvens vurderes etter følgende veiledende kriterier:

Gradering	Menneske	Ytre miljø	Øk/materiell	Omdømme
E Svært Alvorlig	Død	Varig skade. Brudd på lov, forskrifter eller egne krav/mål med svært alvorlige følger.	Drifts- eller aktivitetsstans >1 år. Tap > 5 mill.	Troverdighet og respekt betydelig og varig svekket
D Alvorlig	Alvorlig personskade. Mulig uførhet.	Alvorlig miljøskade. Lang restitusjonstid. Brudd på lov, forskrifter eller egne krav/mål med alvorlige følger.	Drifts- eller aktivitetsstans Fra ½ år opp til 1 år Tap < 5 mill.	Troverdighet og respekt betydelig svekket
C Moderat	Alvorlig personskade. Skade m/fravær	Større miljøskade kort restitusjonstid. Brudd på retningslinjer/prosedyre/tradisjon.	Drifts- eller aktivitetsstans Fra1 måned og opp til ½ år Tap < 1 mill.	Troverdighet og respekt svekket
B Liten	Skade som krever medisinsk behandling, men ikke nødvendigvis skade m/fravær	Mindre miljøskade. Indikasjoner på at retningslinjer/prosedyrer ikke følges i tilstrekkelig grad.	Drifts- eller aktivitetsstans fra 1 uke opp til 1 måned. Tap < ¼ mill.	Negativ påvirkning på troverdighet og respekt
A Svært liten	Skade som krever førstehjelp	Ubetydelig miljøpåvirkning. . Dårlig visuelt inntrykk i kortere tid. Forholdet er ikke knyttet til brudd på retningslinjer eller prosedyrer.	Drifts- eller aktivitetsstans < 1uke. Tap < 50.000 NOK	Liten påvirkning på troverdighet og respekt

Risikoverdi = Konsekvens & Sannsynlighet (f.eks. ”C4”)
Beregn risikoverdi for Menneske. Enheten vurderer selv om de i tillegg vil beregne risikoverdi for Ytre miljø, Økonomi/materiell og Omdømme. I så fall beregnes disse hver for seg.

Til kolonnen ”Kommentarer/status, forslag til forebyggende og korrigerende tiltak”:
Tiltak kan påvirke både sannsynlighet og konsekvens. Prioriter tiltak som kan forhindre at hendelsen inntreffer, dvs. sannsynlighetsreduserende tiltak foran skjerpet beredskap, dvs. konsekvensreduserende tiltak.

MATRISE FOR RISIKOVURDERINGER I SINTEF

KONSEKVENS						
	Svært alvorlig	E1	E2	E3	E4	E5
	Alvorlig	D1	D2	D3	D4	D5
	Moderat	C1	C2	C3	C4	C5
	Liten	B1	B2	B3	B4	B5
	Svært liten	A1	A2	A3	A4	A5
		Svært liten	Liten	Middels	Stor	Svært stor
		SANNSYNLIGHET				

Prinsipp over akseptkriterium. Forklaring av fargene som er brukt i risikomatrisen.

Farge	Beskrivelse
Rød	Uakseptabel risiko. Tiltak skal gjennomføres for å redusere risikoen.
Gul	Vurderingsområde. Tiltak skal vurderes.
Grønn	Akseptabel risiko. Tiltak kan vurderes ut fra andre hensyn.

SINTEF

Obrist Engineering GmbH
Rheinstrasse 26-27
A-6890 Lustenau
Austria

SINTEF
SINTEF Group Head Office

Postboks 4760 Sluppen
NO-7465 Trondheim
NORWAY

Location:
Strindvegen 4
7034 Trondheim

Telephone: +47 73593000
Direct line: +47 73593063
Telefax: +47 73593350

info@sintef.no
www.sintef.no
Enterprise /VAT No: NO 948 007 029 MVA

Your ref.	***Our ref.***	***Project No. / File code***	***Date***
F.Obrist	*A.Hafner*	*16X898*	*17.02.2012*

Dear Frank Obrist

ACCEPTANCE OF FIELDWORK SAFETY REGULATIONS

In accordance with your development contract for the high efficient R744 compressor and the related test facility, SINTEF shall carry out a visit a Lustenau during week 8. The leader of the visiting team will be Armin Hafner. Further details regarding the visit are agreed in the relevant mail correspondence.

Fieldwork safety regulations

- At SINTEF, the safety of our employees takes precedence over any considerations.
- Our employees shall not carry out tasks which they believe may endanger human life or health. The employees may, pursuant to the Norwegian Working Environment Act, and with the full support of SINTEF, refrain from carrying out such tasks. This means that SINTEF authorises the subjective discretion of the individual to make such decisions, and that SINTEF supports such decisions.
- SINTEF's employees shall adhere to the Norwegian Working Environment Act and SINTEF's own safety and work procedures, regardless of where the work is carried out. Exceptions to the foregoing will involve those situations in which local regulations may be more rigorous than ours. In such situations, the local regulations shall be adhered to.
- Work shall not be performed outside the hours stipulated in the working hours' provisions of the Norwegian Working Environment Act.
- In situations where SINTEF is one of several parties involved in the fieldwork, HSE-activities shall be coordinated by the principal party. SINTEF undertakes responsibility for HSE-related activities when we are the sole party participating in the fieldwork, regardless of the identity of the client.
- Prior to the commencement of the fieldwork assignment, our employees shall be briefed by the client's safety representative regarding current safety procedures as they apply at the fieldwork location.

We kindly request your acceptance of the terms of the aforementioned "Fieldwork safety regulations" We will commence the project when you confirm acceptance.

We also request that you inform us of any circumstances that demand special safety requirements at the fieldwork/survey location. We will ourselves carry out an assessment of the need for safety equipment/measures. Our safety and organisational requirements for this project are as follows: safety glasses and ear protection.

Yours sincerely
for SINTEF

Armin Hafner
Senior Research Scientist

On behalf of the client
SINTEF's safety regulations are accepted herewith

BIBLIOGRAPHY

[1] UNEP: 2010 Report of the refrigeration, air conditioning and heat pumps technical options commitee. 2010. – Forschungsbericht

[2] 100:2008, JCGM: Evaluation of measurment data - Guide to the expression of uncertainty in measurment. BIPM, IEC, IFFC, ILAC, ISO, IUPAC and OIML. (2008)

[3] Bensafi, Ahmed ; Thonon, Bernard: Transcritical R744 (CO2) heat pumps Technician's Manual. , Nr. Rapport 2414173

[4] Bernier, Michel A. ; Bourret, Bernard: Pumping Energy And Variable Frequency Drives ASHRAE. (1999)

[5] Bloch, Heinz P. ; Hoefner, John J.: Reciprocationg compressors, operation and maintainance. (1996)

[6] Cengel, Younus A. ; Boles, Michael A.: Thermodynamics, an engineering approach. (2007), S. chpt.6

[7] Fagerli, Bjorn E.: On the feasibility of compressong CO2 as working fluid in hermetic reciprocating compressors. (1997), October

[8] Hafner, Armin ; Neksaa, Petter: High Efficient 100kW R744 Compressor. (2012)

[9] Koelet, P.C: Industrial Refrigeration - Principles, Design And Applications ISBN 0-8247-8731-5. (1992)

[10] Moran, Michael J. ; Shapiro, Howard N.: Fundamentals of Engineering Thermodynamics. (2010), S. chpt. 5

[11] Neksaa, P. ; Walnum, H. T. ; Hafner, A.: CO2 - a refrigerant from the past with prospects of being one of the main refrigerants in the future. (2010), April

[12] Neksaa, Petter.: CO2 Heat pump Systems. In: *Internal Journal of Refrigeration*, (2000)

[13] Pettersen, A J. ander H. J. ander Hafner ; G., Skaugen ; Rekstad, H: Development of compact heat exchangers for CO2 air-conditioning systems. (1998), December

[14] Prasad, B.G. S.: Regeneraitve heat transfer in reciprocating compressors. (2003)

[15] Sanchez, D. ; Torella, E. ; Cabello, R. ; Liopis, R.: Fundamentals of the superheat associated to a semi hermetic compressor of a transcritical CO2 refrigerant plant. (2009)

[16] Tangen, Grethe ; Hemmingsen, Anne Karin T. ; Neksaa, Petter: CREATIV: Research based innovation for industry energy efficiency. (2010), December

[17] Technology, Hoerbiger C.: Valve Theory and Design. (2007)

[18] Yang, Bin ; Li, Liansheng ; Zhao, Yuanyang: Analysis of the Journal Bearing Performance in a CO2 Reciprocating Compressor. (2010)